Budapest Neutron Centre
Centre for Energy Research

Prompt-gamma activation analysis (and instrumental neutron activation analysis)

László Szentmiklósi

Central European Training School on Neutron Techniques, Budapest, Hungary

Budapest Neutron Centre, Budapest, Hungary
szentm@bnc.hu

Nuclear Analysis and Radiography Department
Centre for Energy Research, Budapest, Hungary
szentmiklosi.laszlo@ek-cer.hu

BNC Budapest Neutron Centre

BUDAPEST RESEARCH REACTOR 60 YEARS OF RESEARCH & INNOVATION

What is Activation Analysis (AA) by neutrons?

- Discovery of neutron
  - J. Chadwick, "The Existence of a Neutron" Proceedings of the Royal Society A: Mathematical, Physical and Engineering Sciences 136 (830): 692 (1932).
- Neutron Activation Analysis (NAA)
  - The application of neutron-induced radioactivity for element analysis
  - György Hevesy 1936 (Hf, radioactive tracing, Nobel prize 1943) Hevesy, Gy., Levi, H., 1936, Danske Videnskap. Selskab. Matematisk Fysiske Medd., 14, 5.
- Prompt Gamma Activation Analysis (PGAA)
  - The application of radiative neutron capture ((n,γ) reaction) for chemical analysis
  - first observed in 1934: $^{1}H(n,\gamma)^{2}H$ D.E. Lea, "Combination of proton and neutron", Nature 133, 24-24 (1934)
- First PGAA implementations
  - Isenhour, T.L., Morrison, G.H., 1966, Anal. Chem., 38, 162.
  - R. Henkelmann, H.J. Born, Angew. Chem. 81. 1969 (22) 921

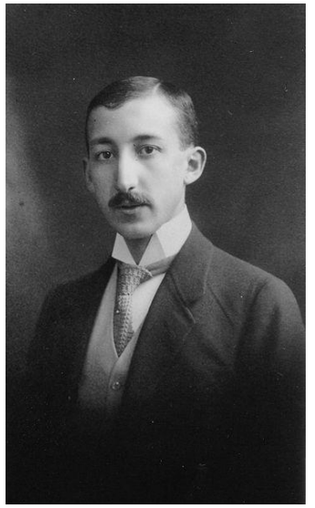

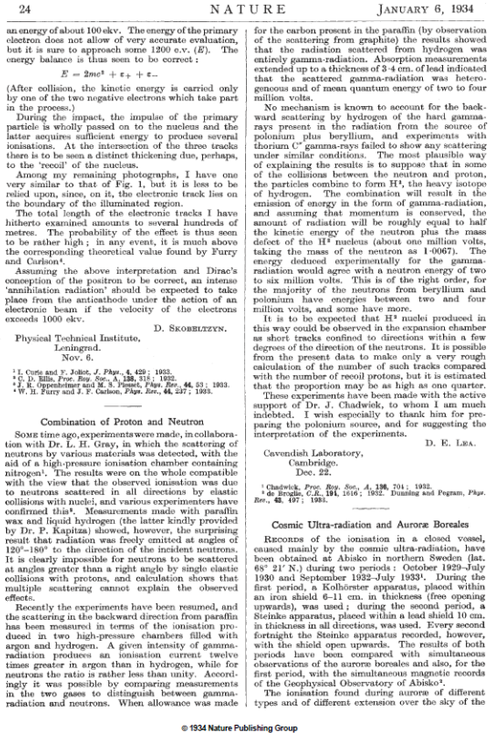

24 NATURE JANUARY 6, 1934

an energy of about 100 ekv. The energy of the primary electron does not allow of very accurate evaluation, but it is sure to approach some 1200 e.v. (E). The energy balance is thus seen to be correct:

$$E = 2mc^2 + \epsilon_+ + \epsilon_-$$

(After collision, the kinetic energy is carried only by one of the two negative electrons which take part in the process.)

During the impact, the impulse of the primary particle is wholly passed on to the nucleus and the latter acquires sufficient energy to produce several ionisations. At the intersection of the three tracks there is to be seen a distinct thickening due, perhaps, to the 'recoil' of the nucleus.

Among my remaining photographs, I have one very similar to that of Fig. 1, but it is less to be relied upon, since, on it, the electronic track lies on the boundary of the illuminated region.

The total length of the electronic tracks I have hitherto examined amounts to several hundreds of metres. The probability of the effect is thus seen to be rather high; in any event, it is much above the corresponding theoretical value found by Furry and Carlson[4].

Assuming the above interpretation and Dirac's conception of the positron to be correct, an intense 'annihilation radiation' should be expected to take place from the anticathode under the action of an electronic beam if the velocity of the electrons exceeds 1000 ekv.

D. SKOBELTZYN.

Physical Technical Institute,
Leningrad.
Nov. 6.

[1] I. Curie and F. Joliot, *J. Phys.*, **4**, 429; 1933.
[2] C. D. Ellis, *Proc. Roy. Soc.*, A, **138**, 318; 1932.
[3] J. R. Oppenheimer and M. S. Plesset, *Phys. Rev.*, **44**, 53; 1933.
[4] W. H. Furry and J. F. Carlson, *Phys. Rev.*, **44**, 237; 1933.

Combination of Proton and Neutron

SOME time ago, experiments were made, in collaboration with Dr. L. H. Gray, in which the scattering of neutrons by various materials was detected, with the aid of a high-pressure ionisation chamber containing nitrogen[1]. The results were on the whole compatible with the view that the observed ionisation was due to neutrons scattered in all directions by elastic collisions with nuclei, and various experimenters have confirmed this[2]. Measurements made with paraffin wax and liquid hydrogen (the latter kindly provided by Dr. P. Kapitza) showed, however, the surprising result that radiation was freely emitted at angles of 120°–180° to the direction of the incident neutrons. It is clearly impossible for neutrons to be scattered at angles greater than a right angle by single elastic collisions with protons, and calculation shows that multiple scattering cannot explain the observed effects.

Recently the experiments have been resumed, and the scattering in the backward direction from paraffin has been measured in terms of the ionisation produced in two high-pressure chambers filled with argon and hydrogen. A given intensity of gamma-radiation produces an ionisation current twelve times greater in argon than in hydrogen, while for neutrons the ratio is rather less than unity. Accordingly it was possible by comparing measurements in the two gases to distinguish between gamma-radiation and neutrons. When allowance was made for the carbon present in the paraffin (by observation of the scattering from graphite) the results showed that the radiation scattered from hydrogen was entirely gamma-radiation. Absorption measurements extended up to a thickness of 3·4 cm. of lead indicated that the scattered gamma-radiation was heterogeneous and of mean quantum energy of two to four million volts.

No mechanism is known to account for the backward scattering by hydrogen of the hard gamma-rays present in the radiation from the source of polonium plus beryllium, and experiments with thorium C″ gamma-rays failed to show any scattering under similar conditions. The most plausible way of explaining the results is to suppose that in some of the collisions between the neutron and proton, the particles combine to form H^3, the heavy isotope of hydrogen. The combination will result in the emission of energy in the form of gamma-radiation, and assuming that momentum is conserved, the amount of radiation will be roughly equal to half the kinetic energy of the neutron plus the mass defect of the H^3 nucleus (about one million volts, taking the mass of the neutron as 1·0067). The energy deduced experimentally for the gamma-radiation would agree with a neutron energy of two to six million volts. This is of the right order, for the majority of the neutrons from beryllium and polonium have energies between two and four million volts, and some have more.

It is to be expected that H^3 nuclei produced in this way could be observed in the expansion chamber as short tracks confined to directions within a few degrees of the direction of the neutrons. It is possible from the present data to make only a very rough calculation of the number of such tracks compared with the number of recoil protons, but it is estimated that the proportion may be as high as one quarter.

These experiments have been made with the active support of Dr. J. Chadwick, to whom I am much indebted. I wish especially to thank him for preparing the polonium source, and for suggesting the interpretation of the experiments.

D. E. LEA.

Cavendish Laboratory,
Cambridge.
Dec. 22.

[1] Chadwick, *Proc. Roy. Soc.*, *A*, **136**, 704; 1932.
[2] de Broglie, *C.R.*, **194**, 1616; 1932. Dunning and Pegram, *Phys. Rev.*, **43**, 497; 1933.

Cosmic Ultra-radiation and Auroræ Boreales

RECORDS of the ionisation in a closed vessel, caused mainly by the cosmic ultra-radiation, have been obtained at Abisko in northern Sweden (lat. 68° 21′ N.) during two periods: October 1929–July 1930 and September 1932–July 1933[1]. During the first period, a Kolhörster apparatus, placed within an iron shield 6–11 cm. in thickness (free opening upwards), was used; during the second period, a Steinke apparatus, placed within a lead shield 10 cm. in thickness in all directions, was used. Every second fortnight the Steinke apparatus recorded, however, with the shield open upwards. The results of both periods have been compared with simultaneous observations of the auroræ boreales and also, for the first period, with the simultaneous magnetic records of the Geophysical Observatory of Abisko[2].

The ionisation found during auroræ of different types and of different extension over the sky of the

Nuclear reactions

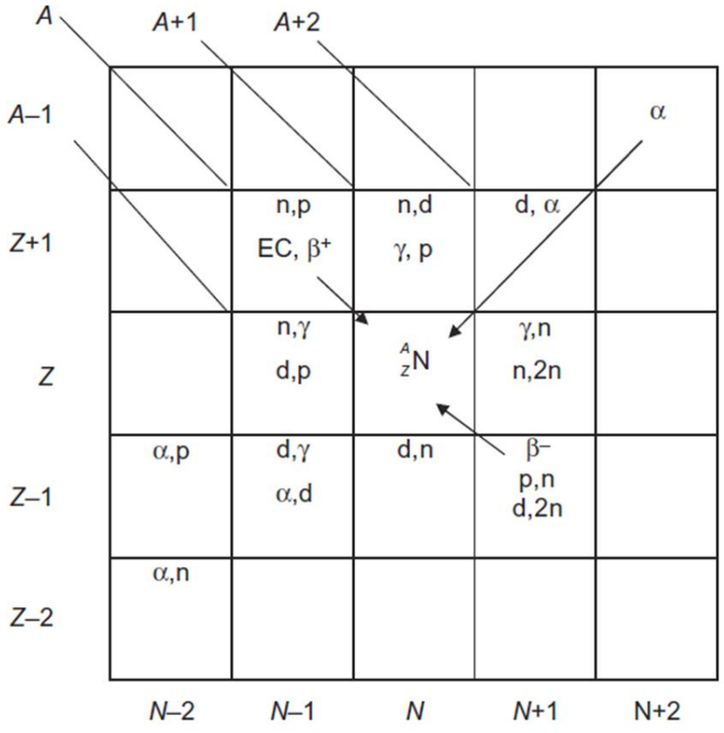

Figure 6.10 Summary of different options to produce a nuclide with Z atomic number and A mass number. It includes the formation of the nuclide by radioactive decays as well.

A(b,c)D = A + b → c + D (+ *Q*)

A – target nucleus

D – final nucleus

b - projectile

c – emitted particle

Q – reaction energy (+ exotherm, - endotherm)

IAEA Isotope Browser App

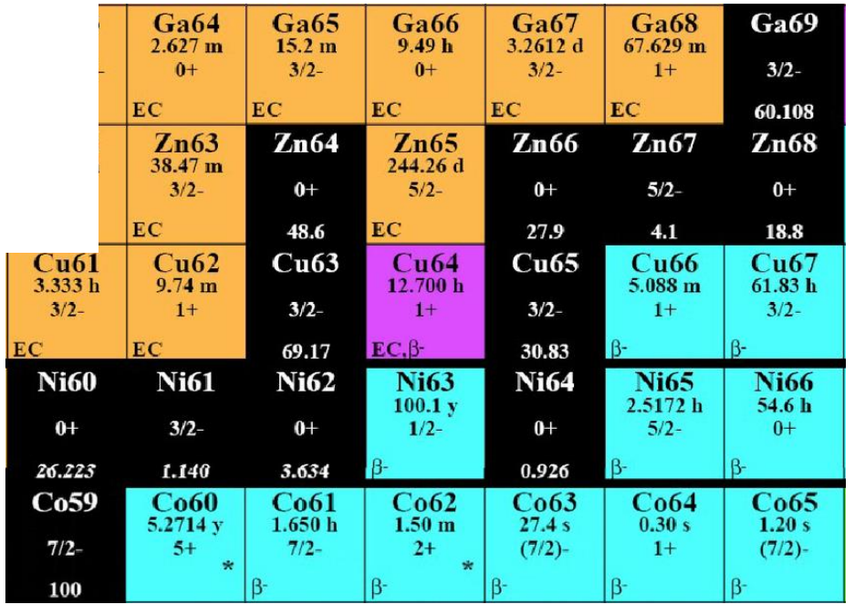

The radiative neutron capture - (n,γ) reaction

Neutrons interact with the condensed matter:

- Induce nuclear reactions (capture, fission)
- Scattering (elastic, inelastic)
- Reflection
- Unaffected neutrons pass through the sample

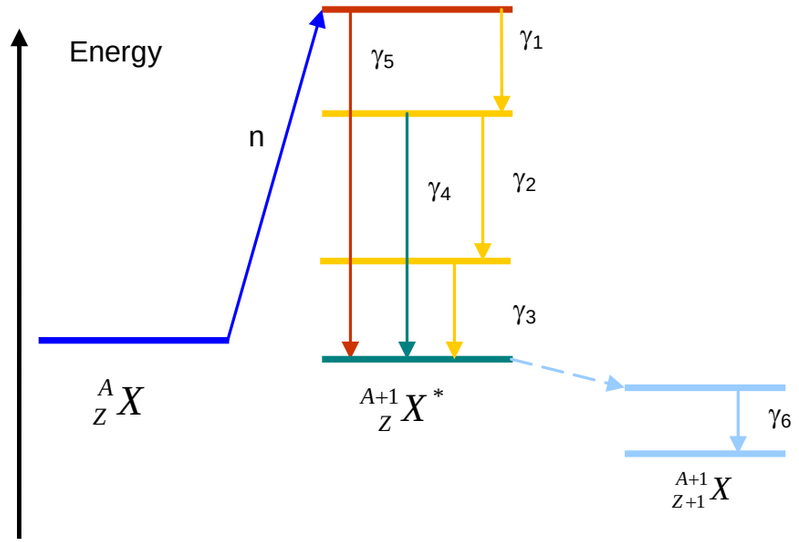

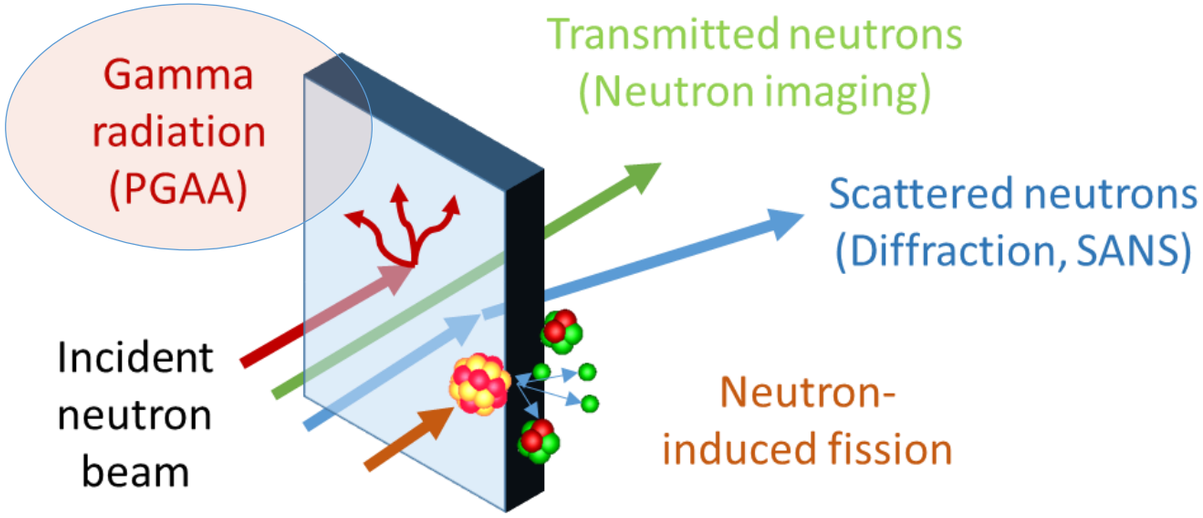

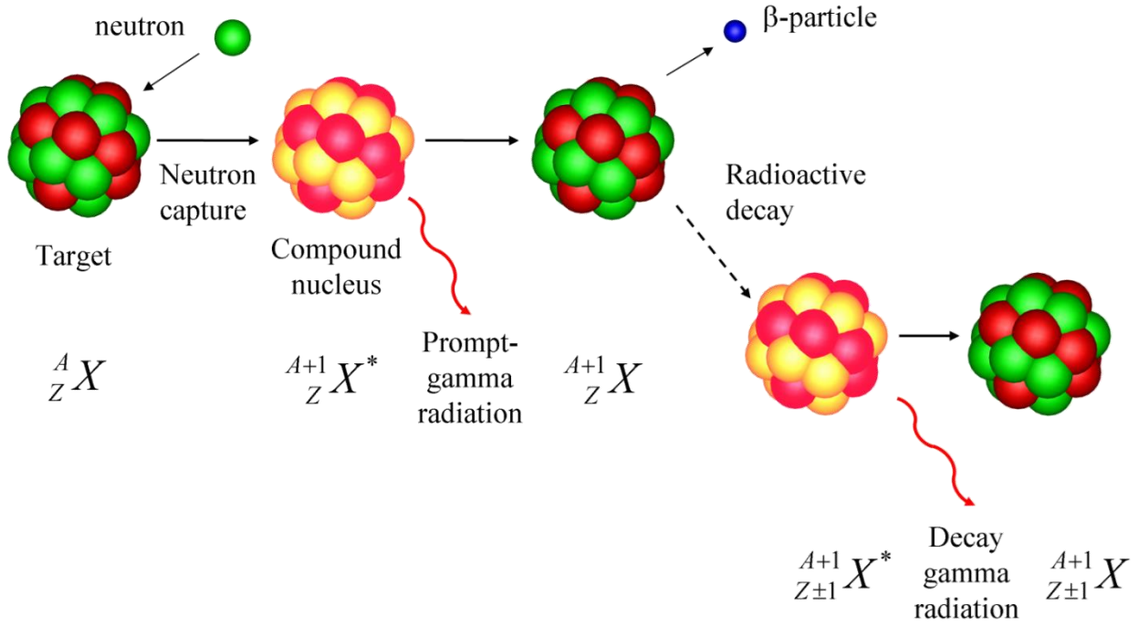

Level schemes - PGAA and NAA

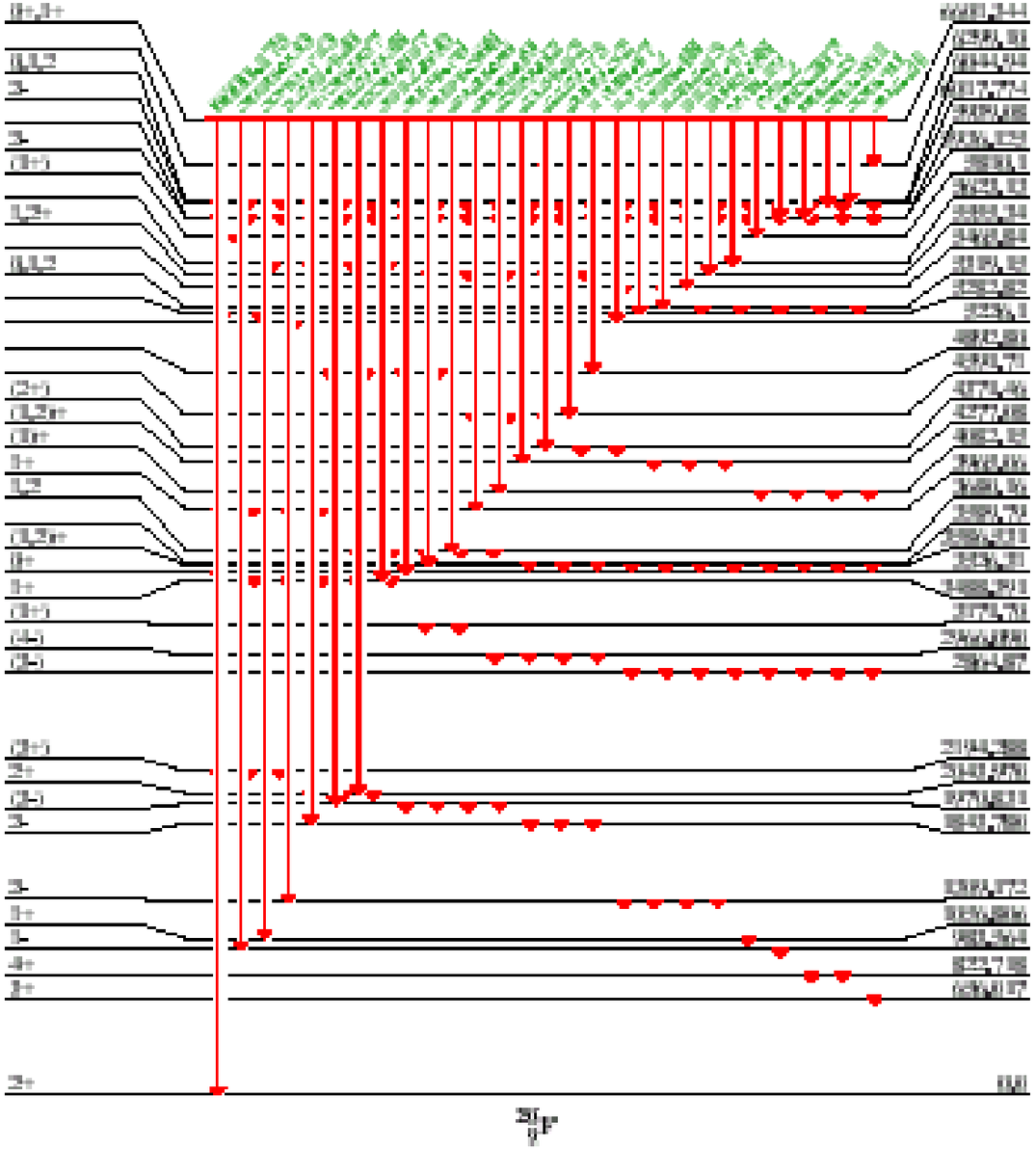

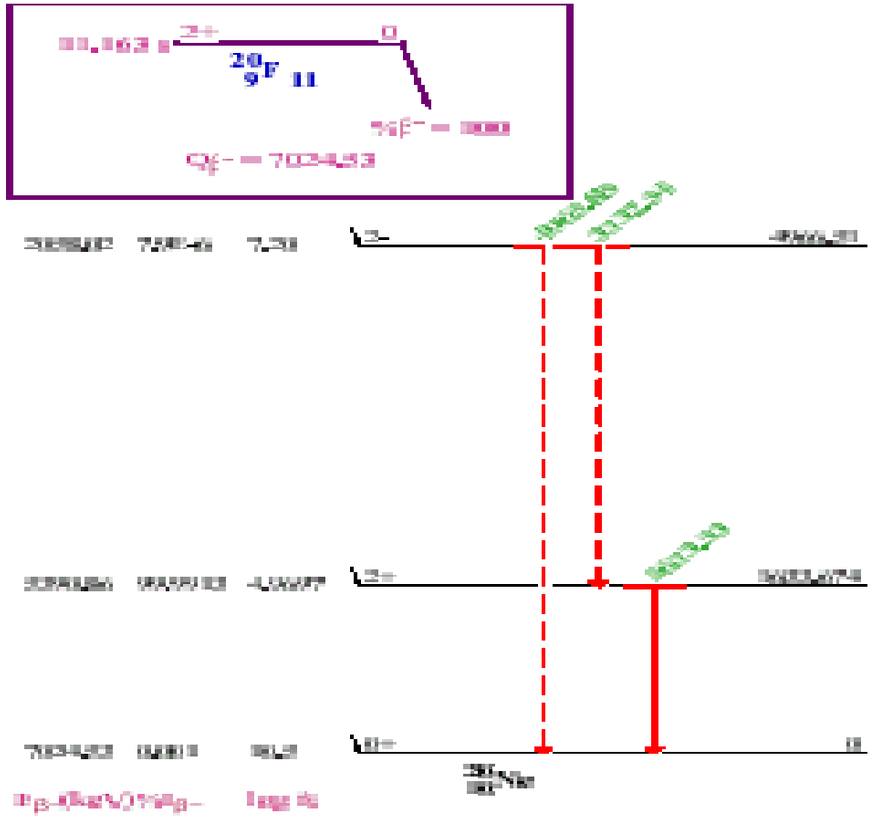

PGAA and NAA spectra

PGAA

- 45 keV to 12 MeV gamma energy range
- Complicated spectrum with hundreds of Gauss-like peaks
- Baseline increasing towards low energies
- Poisson statistics
- Peak positions -> identifying the elements
- Peak areas-> determining quantities

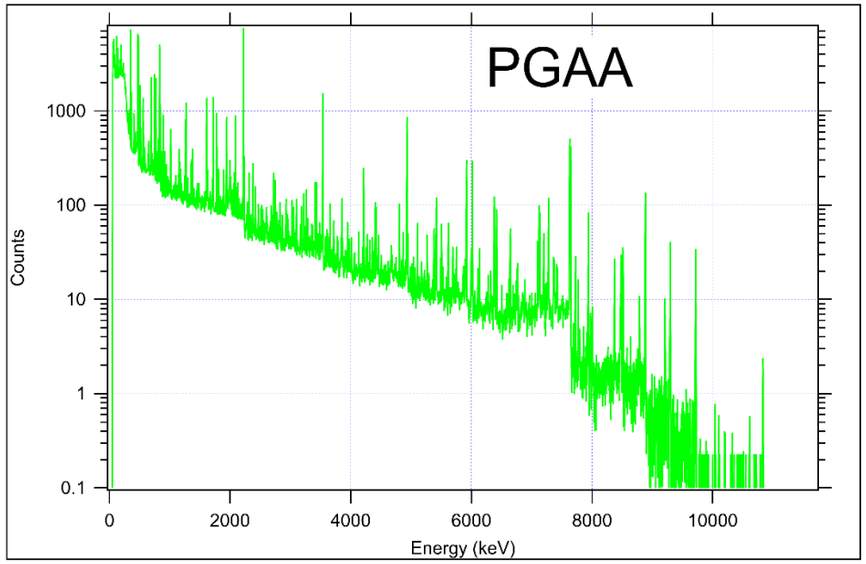

NAA

- 15 keV to 2.8 MeV gamma energy range
- Simpler spectrum with a few (dozen) well separated, Gauss-like peaks
- Baseline increasing towards low energies
- Non-Poisson statistics when measuring at changing count rate
- Peak positions -> identifying the elements
- Peak areas, half lives -> determining quantities

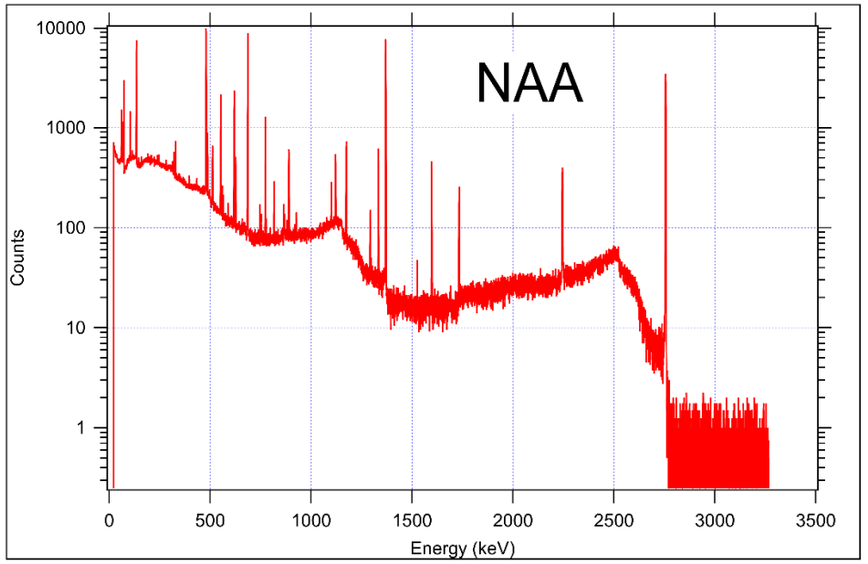

Capture of neutrons – the cross-section

The neutron capture cross section of an isotope of a chemical element is the apparent cross-sectional area that an atom of that isotope presents to absorption and is a measure of the probability of neutron capture.

It is usually measured in barns, i.e. 10^{-24} cm^2 or 10^{-28} m^2

Capture cross section is highly dependent on neutron energy

In general, the likelihood of absorption is proportional to the time the neutron is in the vicinity of the nucleus. The time spent in the vicinity of the nucleus is inversely proportional to the relative velocity between the neutron and nucleus. This is the 1/*v* law.

One expect the highest reaction rate per atom for cold neutrons

Neutrons should be moderated or cooled to maximize the analytical sensitivity of PGAA

1/*v* law

Resonances

$$\sigma = \sigma_0 \frac{v_0}{v}$$

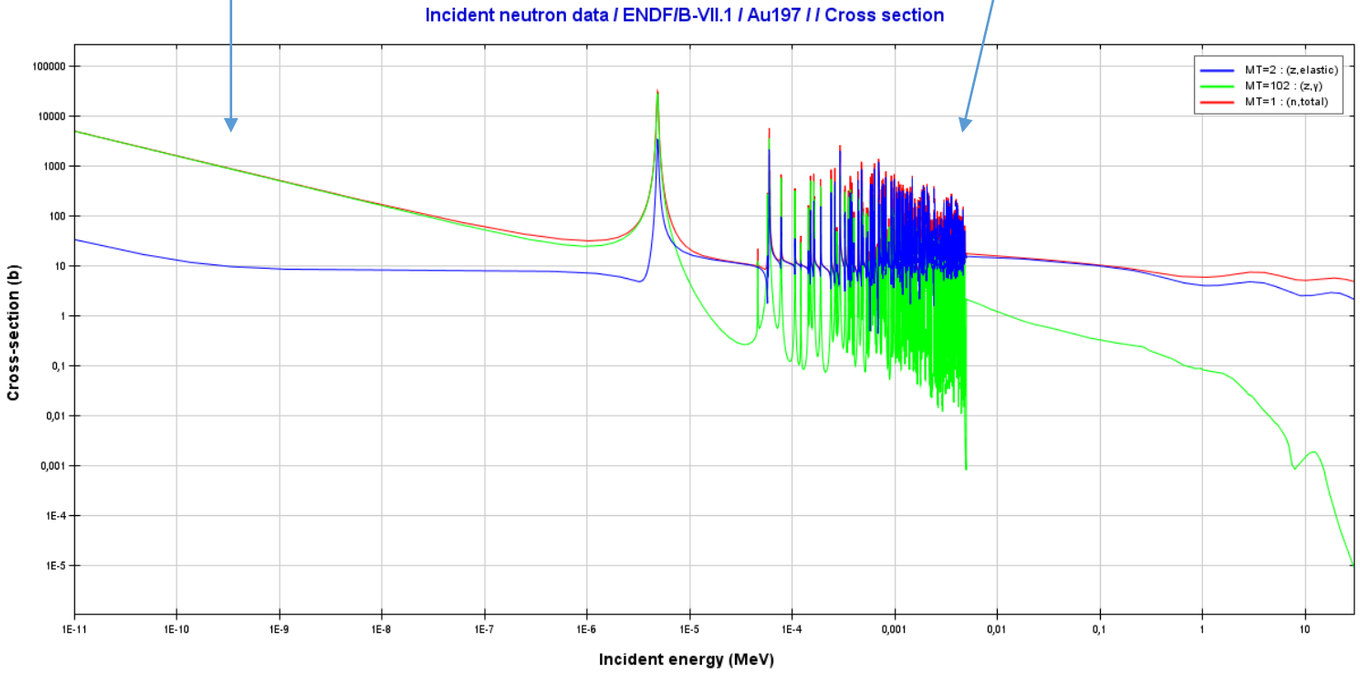

NAA vs. PGAA

Multielement methods
Negligible matrix effect,
Good reproducibility,
Reliable uncertainty budget

NAA

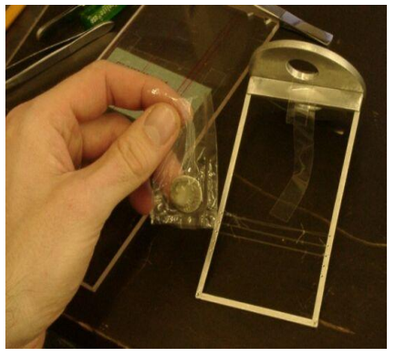

PGAA

•Sample	10 mg	100 mg - 1 g
•Sample preparation	Drying, glass	None/ PTFE bag, vial
•Irradiation	Reactor core	Guided beam of neutrons
•Detection	Separated in time and space	On-line, during the irradiation
•Spectrum	10-100 peaks, 3 MeV	100-5000 peaks, 12 MeV
•Result turnover time	weeks	Few hours
•Detection limits	ppm-ppb	>ppm, %
•Cooling time after irrad.	Several months	1-2 days

Periodic Table for PGAA and NAA

PGAA – major and minor elements

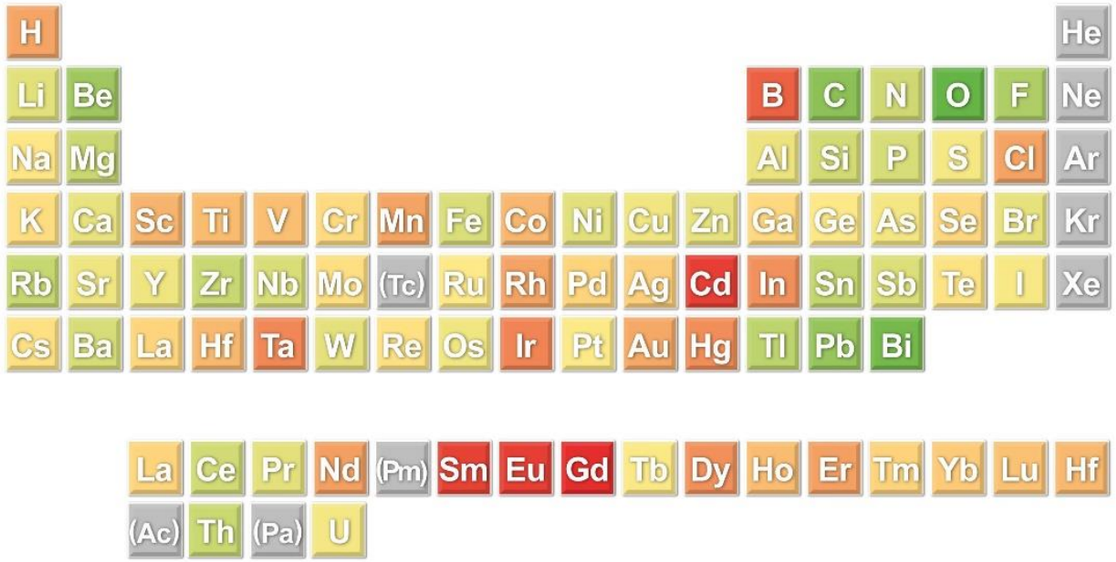

NAA - No light elements!

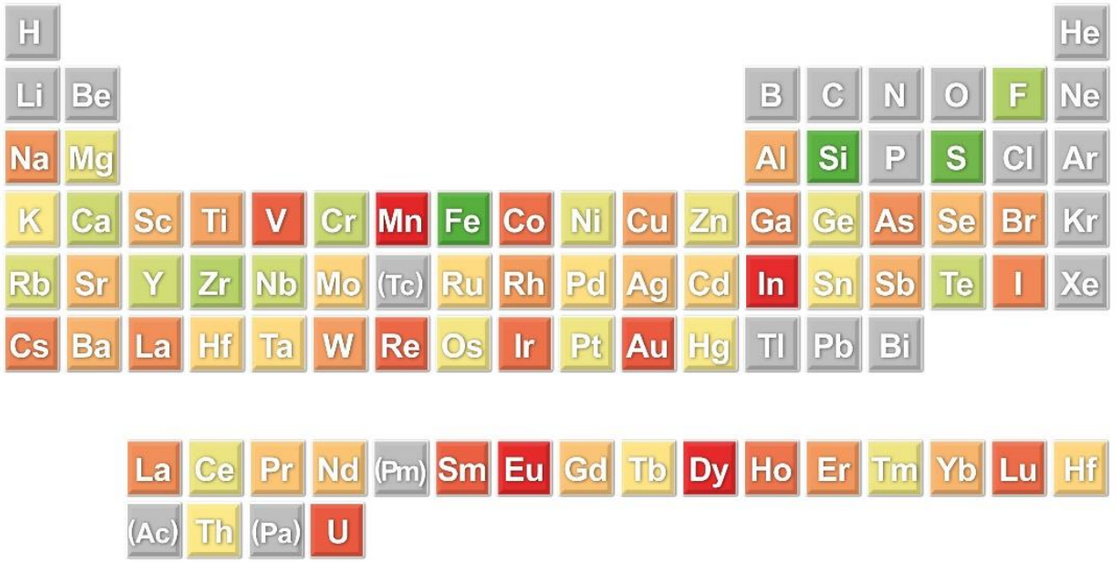

Source: Zs. Révay, C. Stieghorst and R. Müller, TUM

Qualitiative and Quantitative Analysis

Gamma (prompt and decay) radiation is characteristic

- energy → elements (isotopes)
- intensity → quantity

Peak position — Peak area

Energy — Partial gamma-ray production cross section

Nucl.	E (keV)	cross-sec	half-life
^{1}H	2223.249 keV	0.3326 b	-
…			
^{23}Na	1368.6 keV	0.500 b	14.96 h
…			

Decay correction for NAA

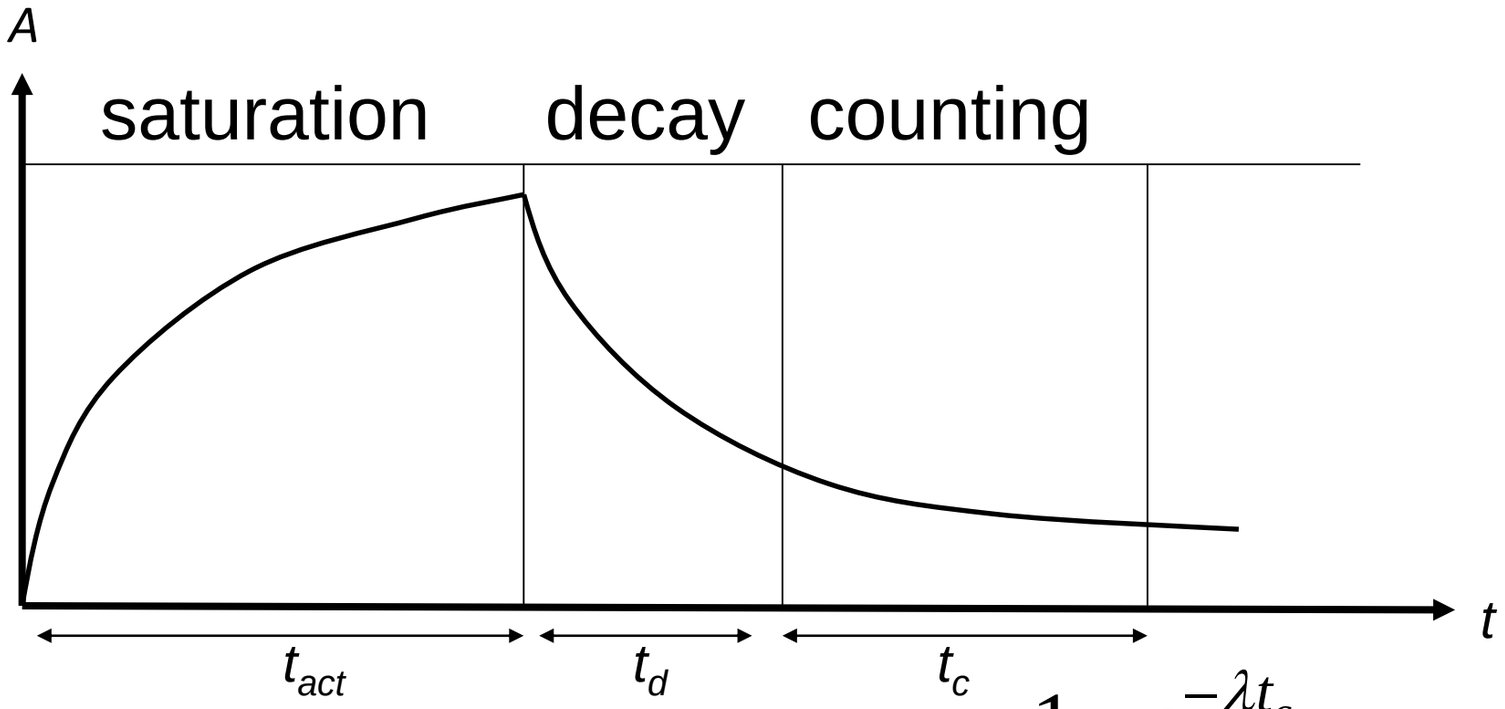

$$S = 1 - e^{-\lambda t_{act}} \qquad D = e^{-\lambda t_d} \qquad C = \frac{1 - e^{-\lambda t_c}}{\lambda t_c}$$

In case of complex activation-decay chain:

$$\frac{dN_1}{dt} = -\Lambda_1 N_1,$$

$$\frac{dN_2}{dt} = -\Lambda_1^* N_1(t) - \Lambda_2 N_2,$$

$$\vdots$$

$$\frac{dN_k}{dt} = -\Lambda_{k-1}^* N_{k-1}(t) - \Lambda_k N_k.$$

$$\Lambda = \lambda + \Phi\sigma$$

$$N_k(t) = \prod_{i=1}^{k-1}(\Lambda_i^*) N_1^0 \sum_{m=1}^{k}\left[\prod_{\substack{n=1 \\ n\neq m}}^{k}\left(\frac{1}{\Lambda_n - \Lambda_m}\right)\exp(-\Lambda_m t)\right],$$

$\lambda = \ln(2)/T_{1/2}$, decay constant

Peak area has to be corrected for saturation: *A'* = *A*/*SDC*

Reaction Rate – general equation

$$R = \int_{E_n=0}^{\infty} \Phi(E_n) \cdot \sigma(E_n)\ dE_n = \int_0^{v_{\mathrm{Cd}}} \sigma(v)\,\varphi'(v)\mathrm{d}v + \int_{E_{\mathrm{Cd}}}^{\infty} \sigma(E)\,\varphi'(E)\mathrm{d}E = G_{\mathrm{th}}\Phi_{\mathrm{th}}\sigma_0 + G_{\mathrm{e}}\Phi_{\mathrm{e}}I_0(\alpha)$$

1/v behavior cancels for slow neutrons:

$$R \equiv \int_{E_{\mathrm{n}}=0}^{\infty} \Phi(E_{\mathrm{n}}) \cdot \sigma(E_{\mathrm{n}})\,\mathrm{d}E_{\mathrm{n}} = \int_{E_{\mathrm{n}}=0}^{\infty} v \cdot n(E_{\mathrm{n}}) \cdot \frac{\sigma_0 v_0}{v}\,\mathrm{d}E_n =$$

$$\sigma_0 \int_{E_n=0}^{\infty} v_0 \cdot n(E_{\mathrm{n}})\,\mathrm{d}E_{\mathrm{n}} = \sigma_0 \cdot \Phi_0$$

R - number of captured neutron per sec

σ - capture cross section (cm^2),

Φ - flux cm^{-2} s^{-1} eV^{-1}

N - number of target nuclides (~ mass)

Determination of chemical composition

$$A_\gamma = m \cdot S \cdot t; \quad S = \frac{N_A}{M} \cdot \underbrace{\theta \cdot \sigma_0 \cdot P_\gamma}_{\sigma_\gamma} \cdot \phi \cdot \varepsilon(E_\gamma) \cdot f(E_\gamma)$$

Fit from the PGAA spectrum

From spectroscopic library

From detector calibration

m : Mass of the element

S : Sensitivity of the analytical peak (cps / mg)

t : measurement time (s)

A_γ : Peak area

N_A : Avogadro-number

M : Molar weight

θ : Isotopic abundance

σ_0 : Neutron capture cross-section

P_γ : Gamma-yield per neutron capture

ϕ : Neutron flux

$\varepsilon(E_\gamma)$: Detector efficiency

$f(E_\gamma)$: Matrix effect correction (neutron self shielding, gamma self absorption)

- We measure concentrations, i.e. ratios of element masses to the cumulative mass of all detected elements.
- No need to know the exact weight of the sample
- No problem if not the entire object is irradiated

Dynamic range of gamma spectra for any nuclide pairs: 10^{6-8}

PGAA

1 mg H together with 1 g Cl

(10 mg water in 1 g CCl_4)

1 mg Cl together with 1 g H

(1 mg Cl in 10 g water)

NAA

it can be increased with repeated counting after cooling, contact counting etc.

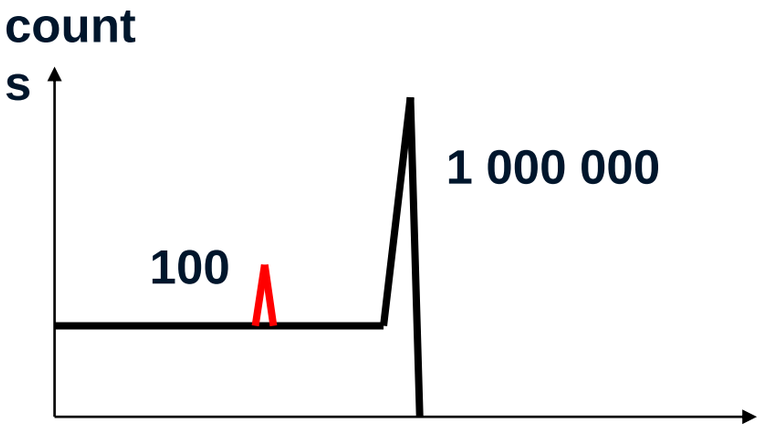

Spatial resolutions vs. detection limits in elemental analysis

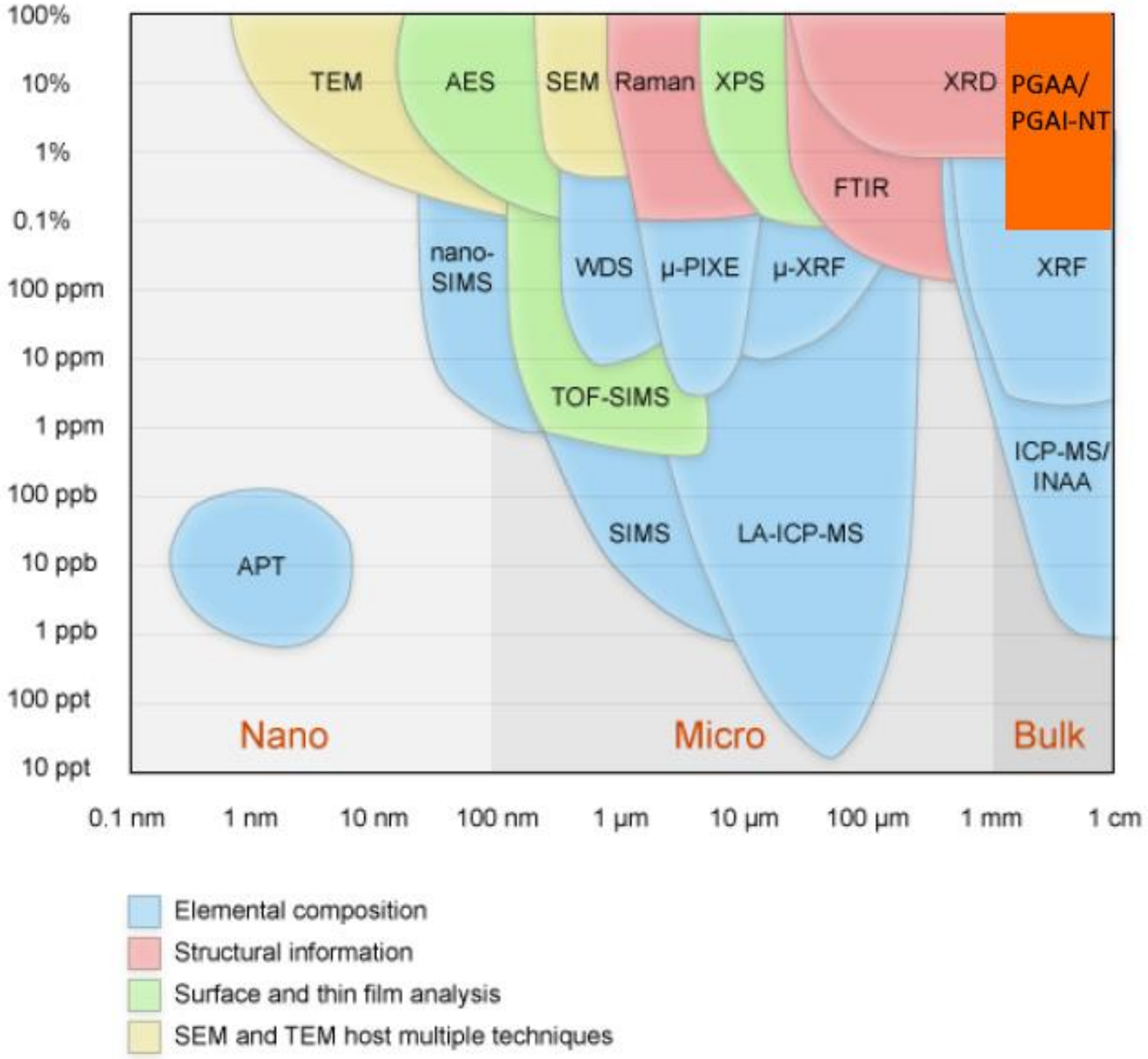

Original figure taken from https://myscope.training/legacy/analysis/introduction/

PGAI-NT:

- Typical spatial resolution for element analysis > 2 mm
- Typical detection limit approx. 0.1%
- Bulk (other methods: near-surface or solution)
- Non-destructive
- Representative
- High metrological quality

Budapest Neutron Centre
Centre for Energy Research

Instrumentation

BNC
Budapest Neutron Centre

BUDAPEST
RESEARCH
REACTOR
1959
2019
60 YEARS
OF RESEARCH
& INNOVATION

Components of the activation analysis

- Neutron source
  - spallation neutron source
  - nuclear reactor
  - neutron generator
  - isotopic neutron source (^{252}Cf, Pu-Be, ...)
  - compact accelerator-driven neutron source
- Moderator (H containing material)
- Shielding against ...
  - Neutrons (PGAA)
  - Gammas
- Pneumatic transfer (a.k.a rabbit) system (only in NAA)
- Automatic sample changer
- Detectors
  - high-purity germanium (HPGe)
  - scintillator (NaI, ...)
  - Low-background counting chamber (NAA)

Budapest Research Reactor

- 10 MW thermal power
- Tank type, Water-cooled, Water-moderated
- 60+ years of operation
- Max. thermal flux in the core: 2×10^{14} cm^{-2} s^{-1}

Reactor type:	Tank-type with beryllium reflector, cooled and moderated with light water
Vessel:	Al-alloy (height: 5685 mm; ∅2300 mm)
Core geometry:	Hexagonal (length: 600 mm; ∅1000 mm)
Fuel:	LEU VVR-M2 (19,75 %)
Equilibrium core	190 fuel elements (5x38 age-group FAs)
Control:	18 control rods = 3 safety rods (B_4C); 14 shim rods (B_4C); 1 automatic control rod (SS - Stainless Steel)
Thermal power:	10 MW
Mean power density:	61.2 kW/litre (in the core)
Neutron flux density in the core:	$2,2*10^{14}$ n/cm^2s (thermal in flux traps) En<0.625 eV $1*10^{14}$ n/cm^2s (in fast channels) En>0.5 MeV
Cooling systems:	Two closed loops (primary and secondary loops)
Pr.cooling water:	$Q_{nominal}$: 1650 m^3/h; T_{inlet}: 45 °C; T_{outlet}: 50 °C

Centre for Energy Research

Cold neutron source at the Budapest

Budapest Neutron Centre

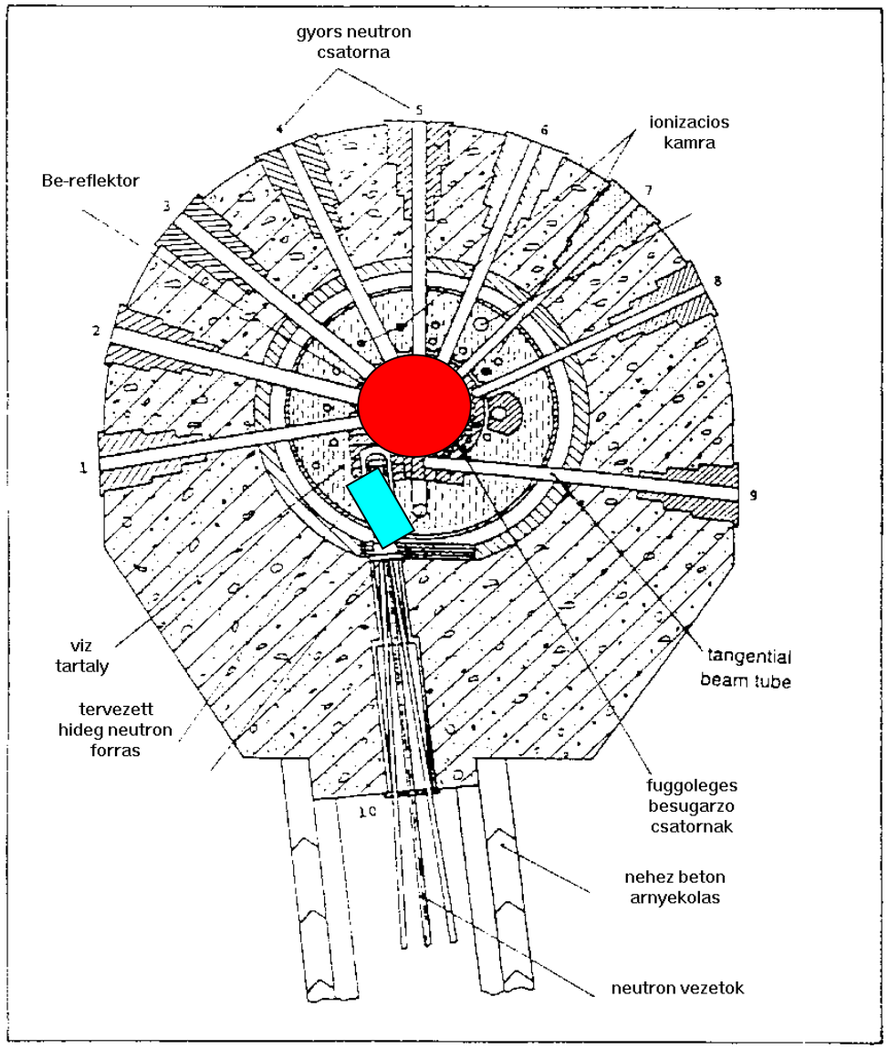

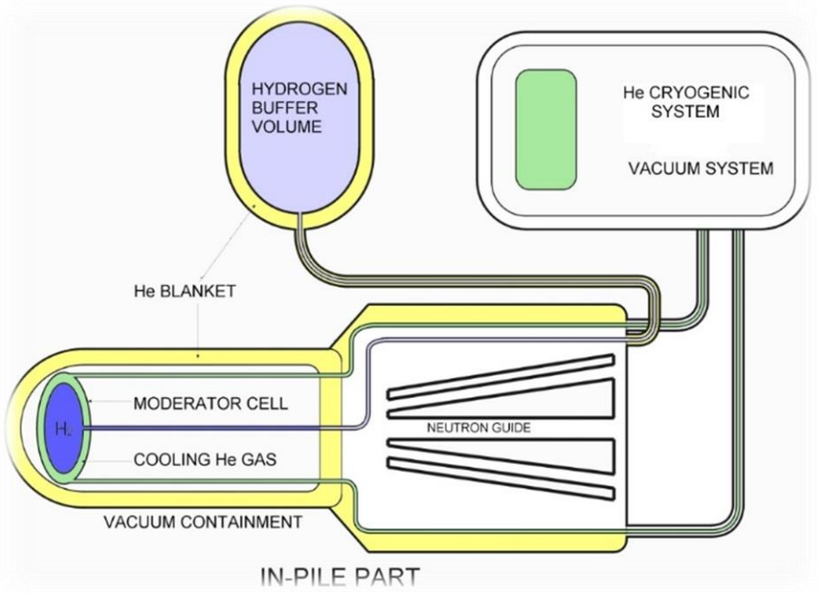

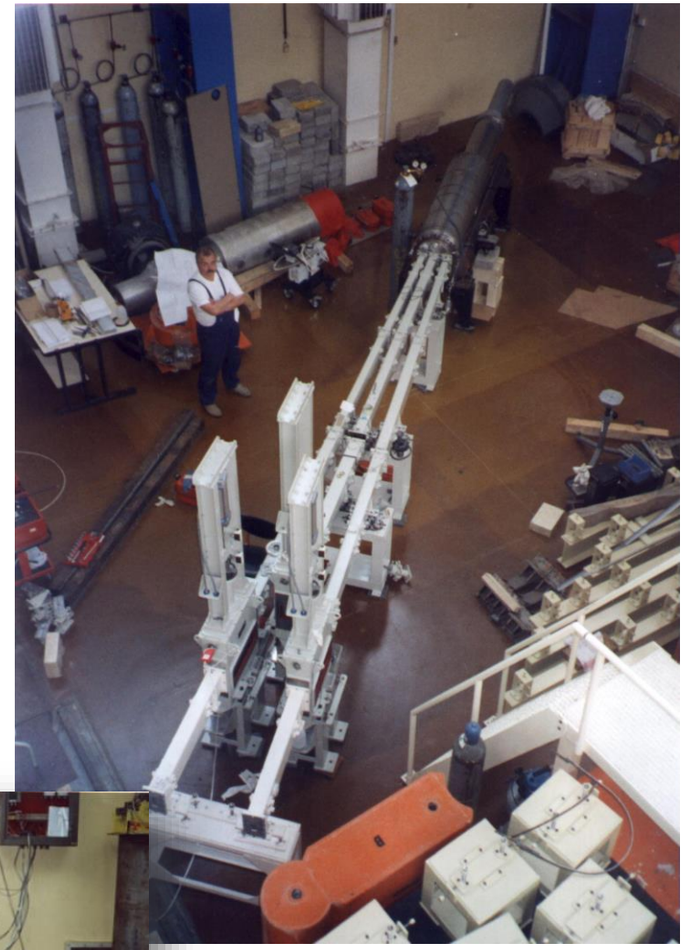

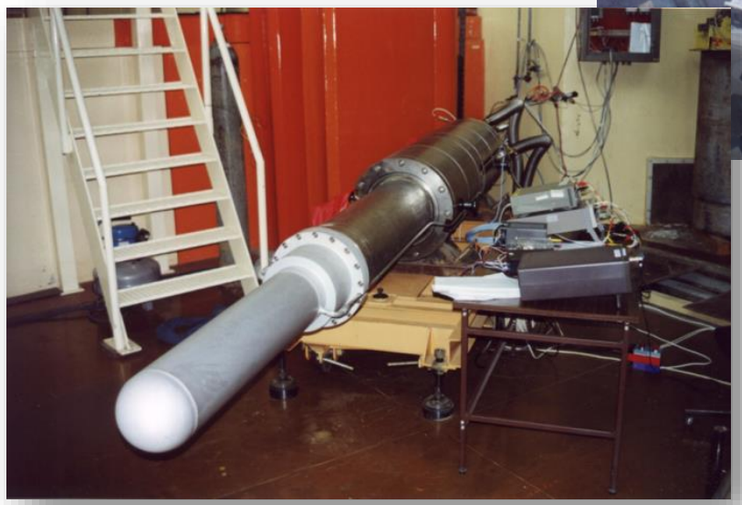

400 cm³, 20 K liquid H_2

Advantages of cold neutron beams

- Higher flux (neutron guides higher throughput)
- every nuclide behaves regularly
  - (follows the 1/*v*-law)
- every nuclide has higher cross section

a higher reaction rate

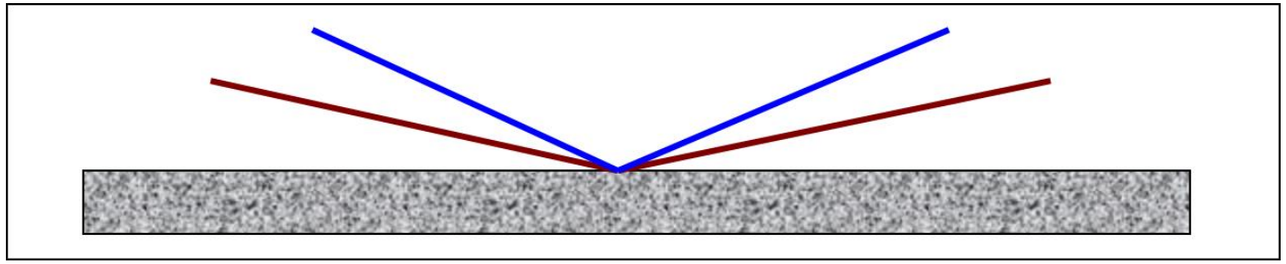

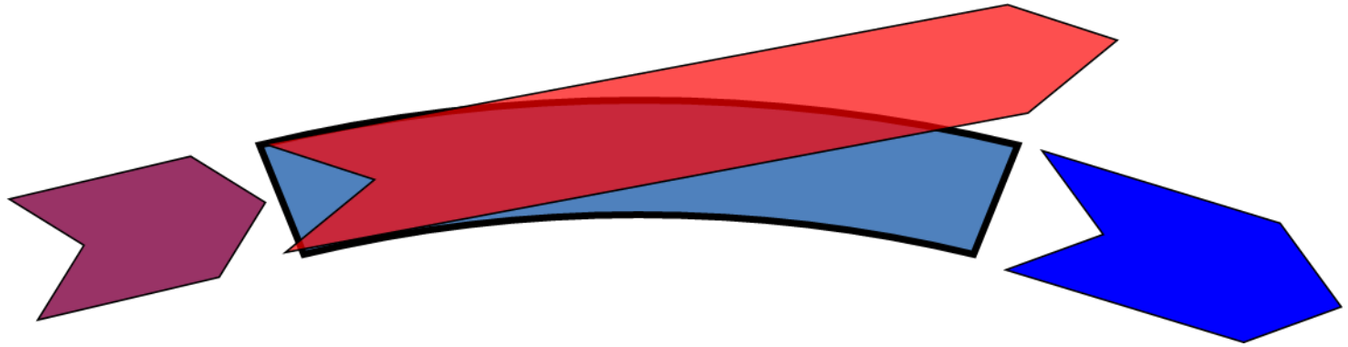

Neutron guides

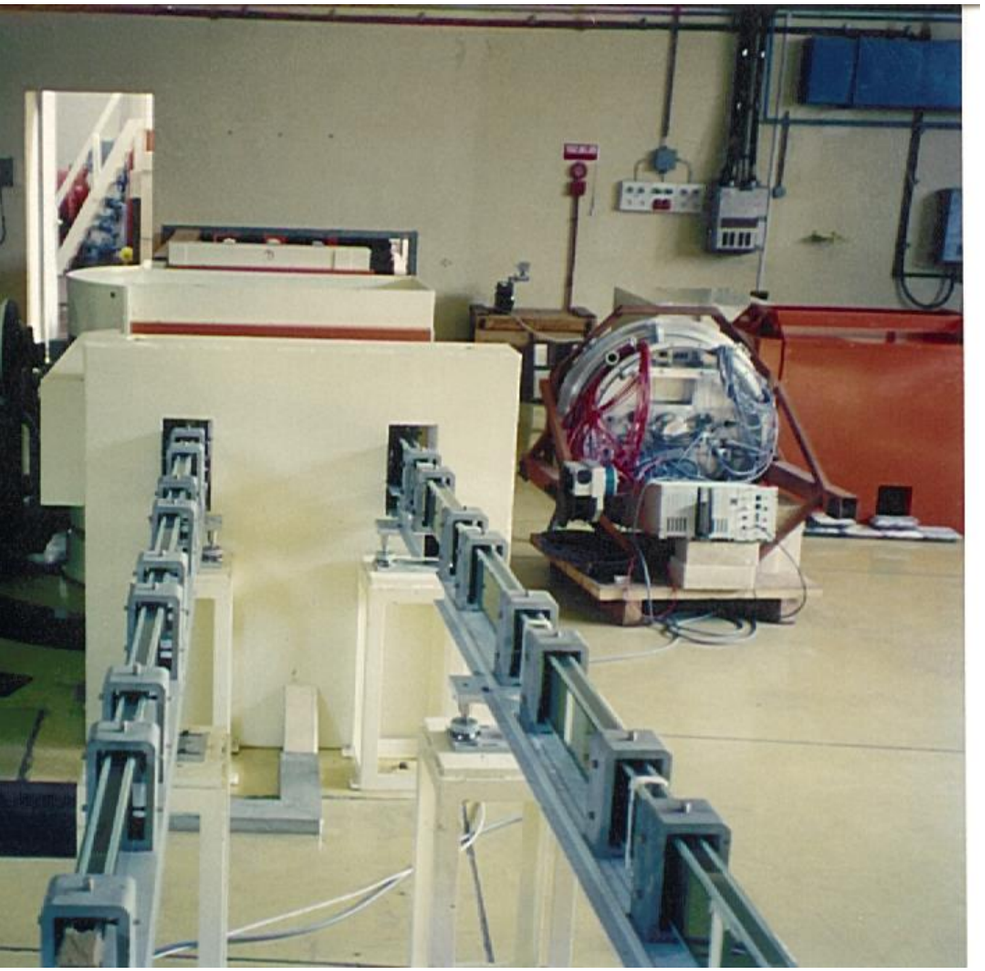

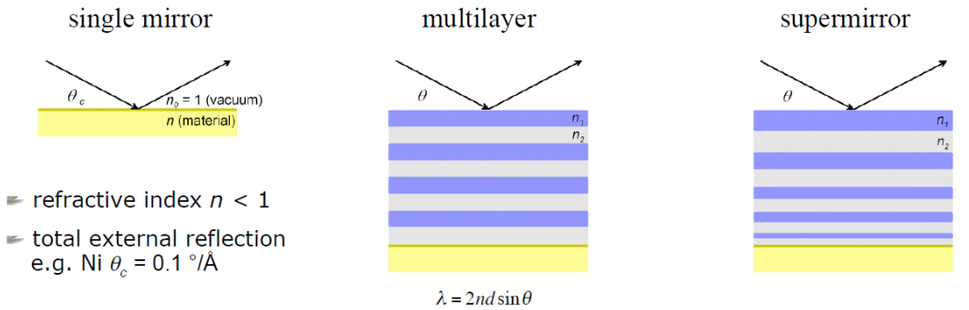

- refractive index $n < 1$
- total external reflection
  e.g. Ni θ_c = 0.1 °/Å

$$\lambda = 2nd\sin\theta$$

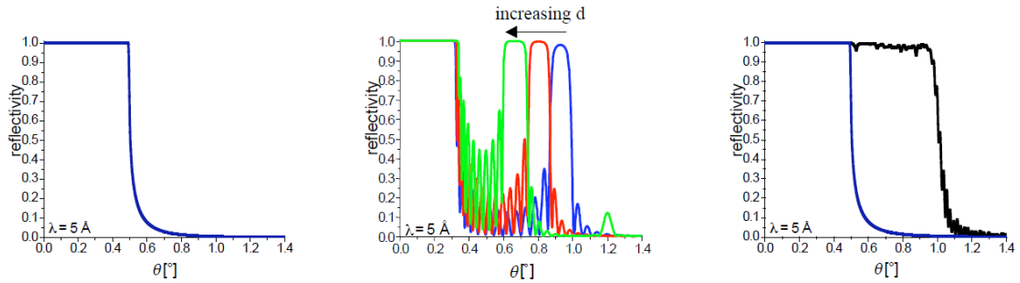

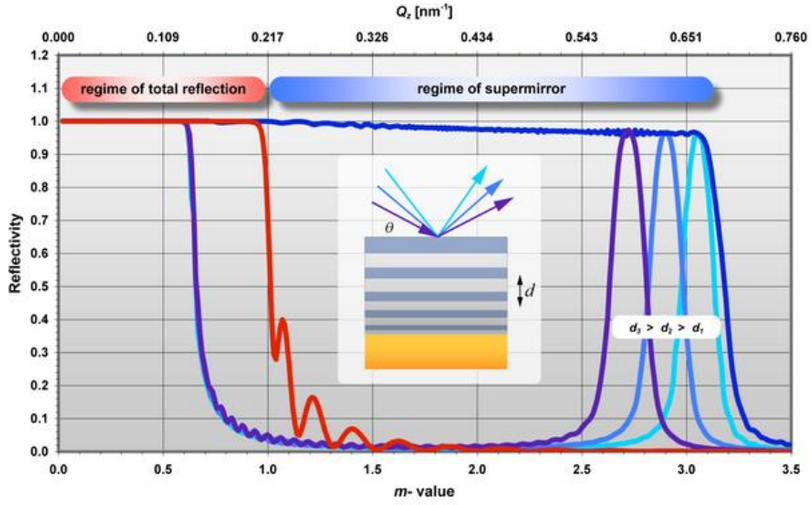

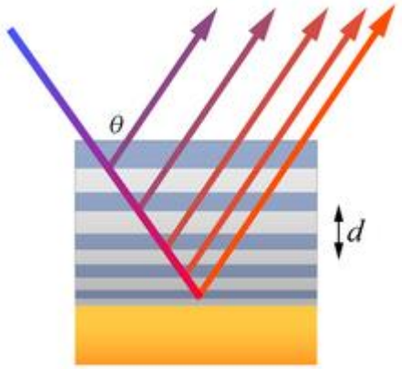

- Ni or supermirror guides
- relatively small losses
- low background

Neutron source -> neutron guide -> PGAA

Neutrons to the sample

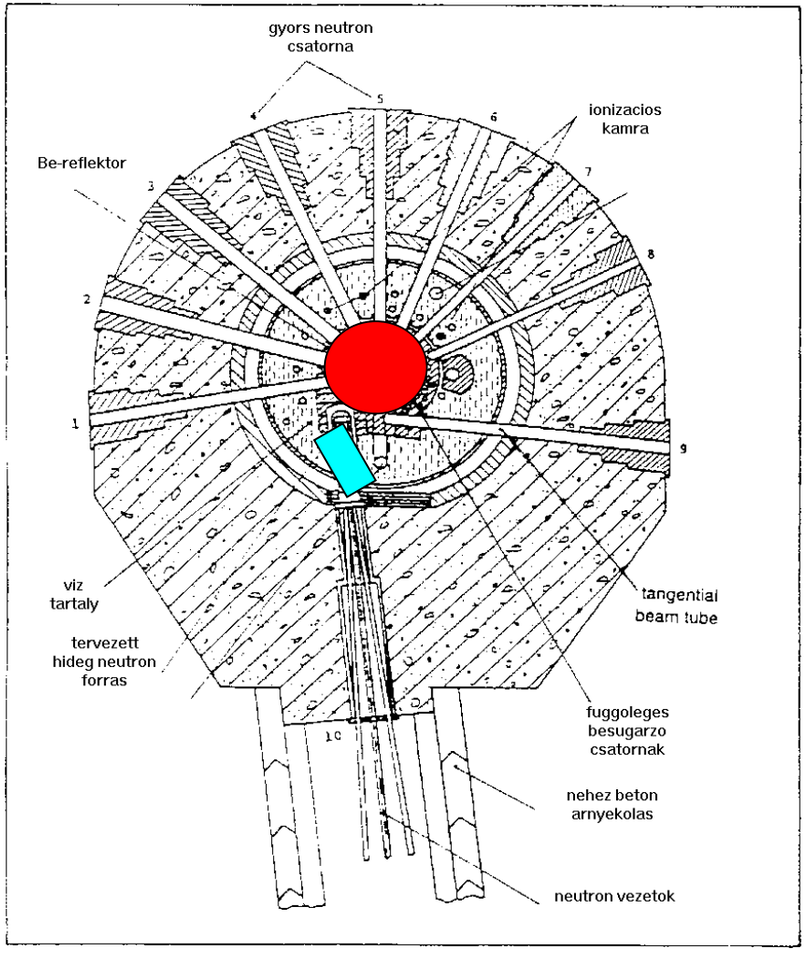

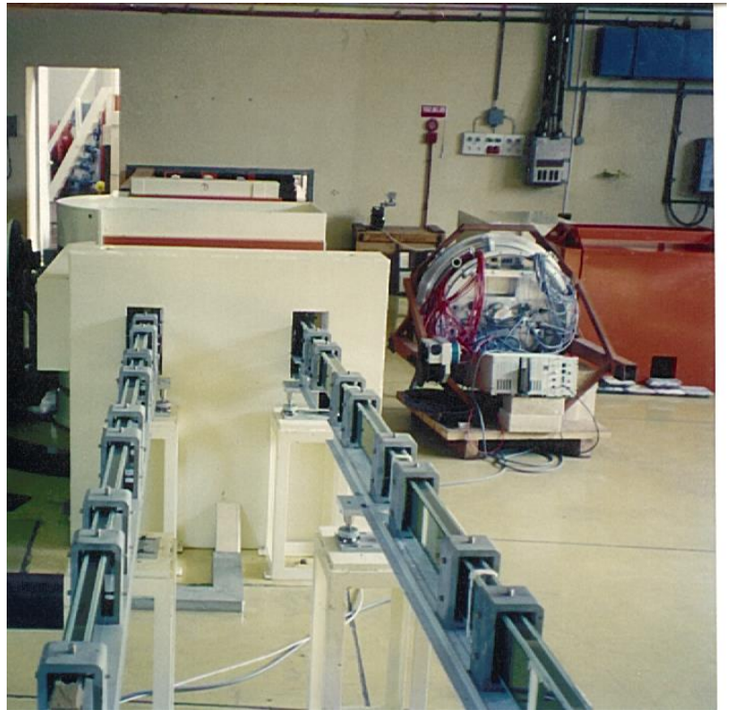

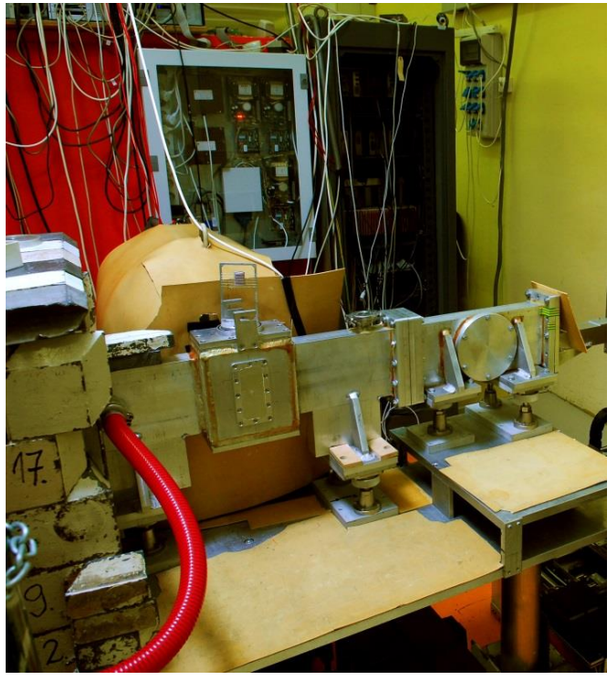

NAA Pneumatic transfer (rabbit) system

Sample to the neutrons

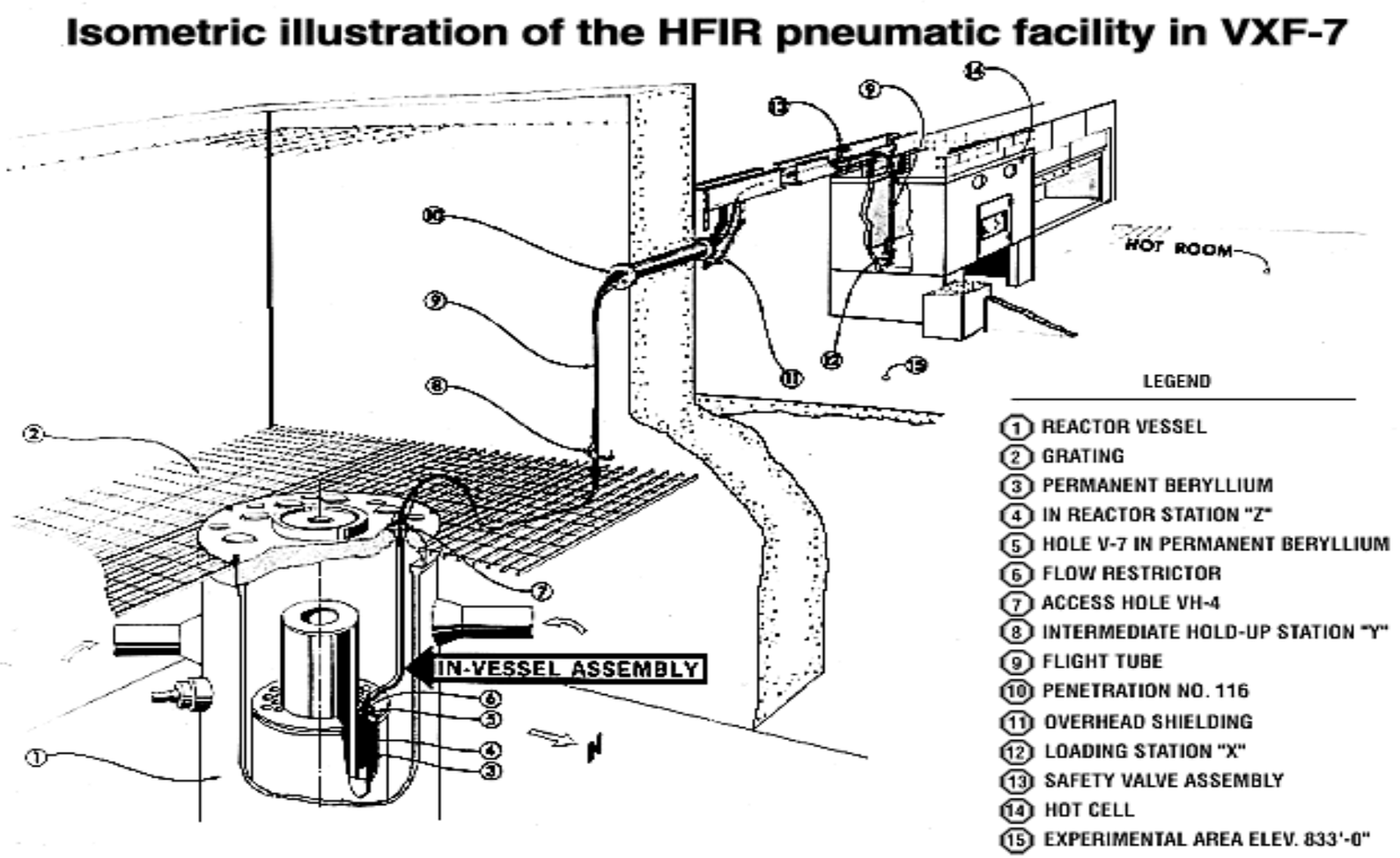

Oak Ridge National Laboratory

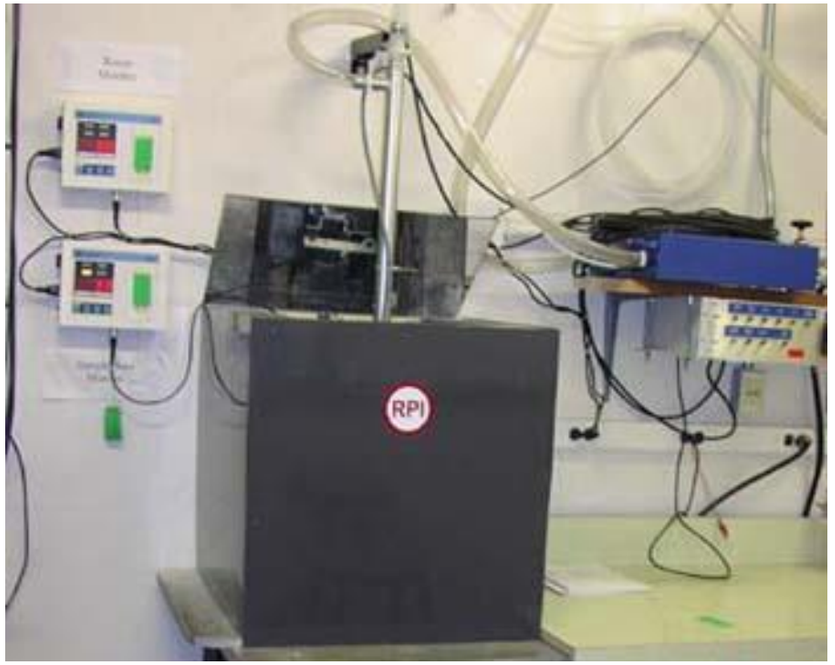

RENSSELAER POLYTECHNIC INSTITUTE ::

Reactor neutron spectrum

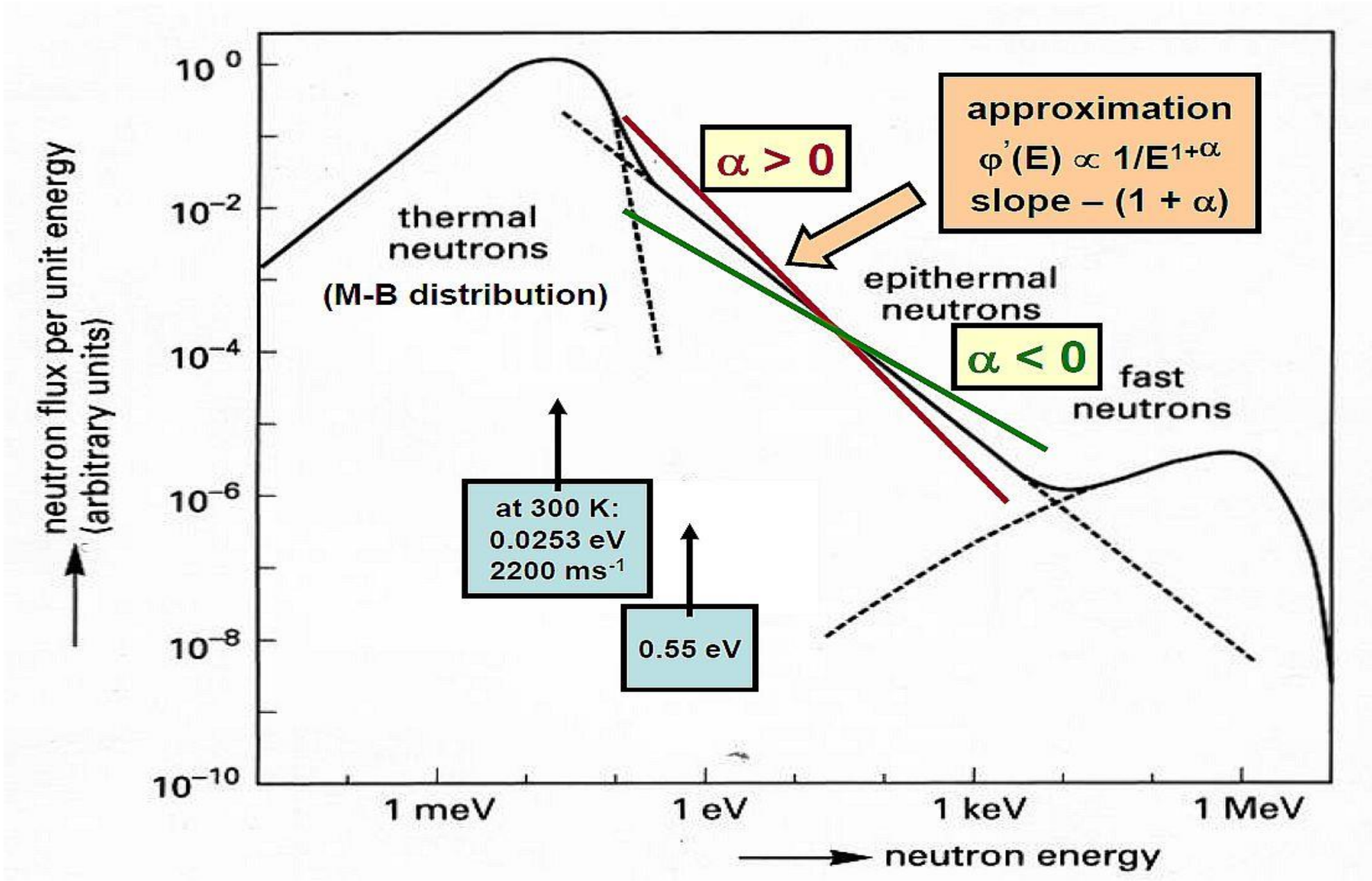

Short irradiations at BNC

Pneumatic rabbit system

$\Phi_{th} = 4.45 \cdot 10^{13}$ n/cm^{2}s

$\Phi_{epi} = 1.28 \cdot 10^{12}$ n/cm^{2}s

$f = \Phi_{th}/\Phi_{epi} = 34.8$, $\alpha = 0.029$

Measured isotopes:

^{24}Na, ^{27}Mg , ^{28}Al,^{38}Cl, ^{49}Ca, ^{51}Ti, ^{52}V, ^{56}Mn, ^{66}Cu, ^{80}Br, ^{87m}Sr, ^{123m}Sn, ^{125m}Sn, ^{128}I, ^{139}Ba

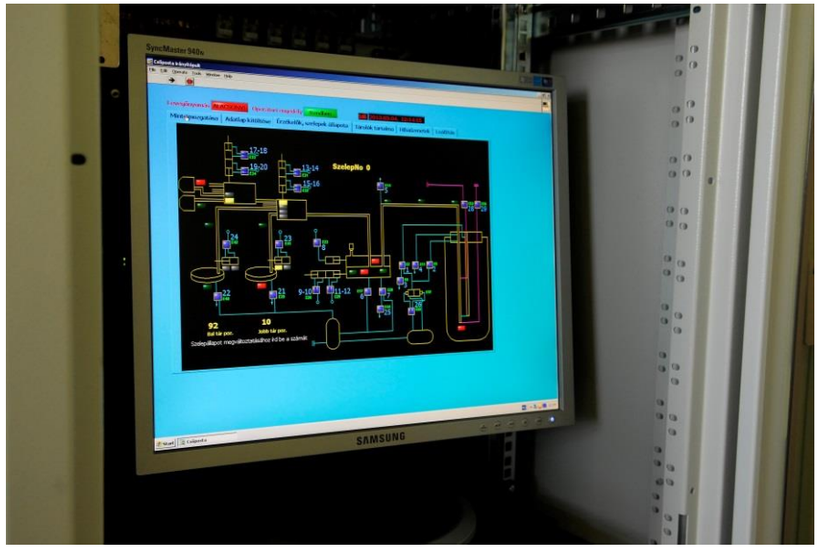

Long irradiations at BNC

BRR No. 17 rotating channel, (∅=54 mm)

$\Phi_{th}=1.76\cdot10^{13}$ n/cm^{2}s

$f = \Phi_{th}/\Phi_{epi}= 47.1$

$\alpha = 0.0249$

20 elements

Measured isotopes:

^{24}Na, ^{42}K, ^{51}Cr, ^{59}Fe, ^{60}Co, ^{58}Co(Ni), ^{65}Zn, ^{69m}Zn, ^{72}Ga, ^{76}As, ^{82}Br, ^{86}Rb, ^{122}Sb, ^{110m}Ag, ^{124}Sb, ^{134}Cs, ^{140}La, ^{153}Sm, ^{182}Ta, ^{187}W

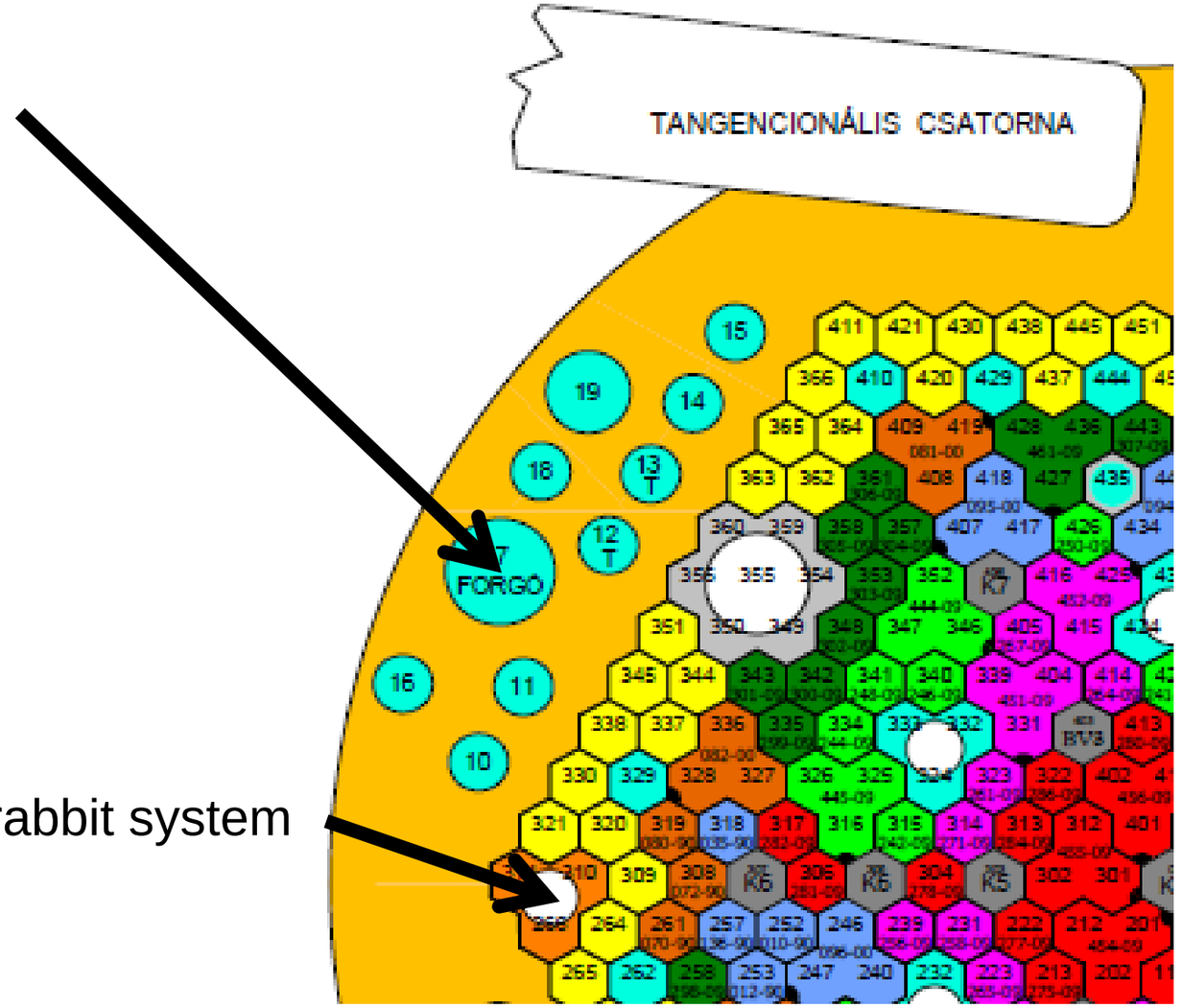

Gamma-ray interactions with the matter

Three major types of interactions between gamma radiation and matter:

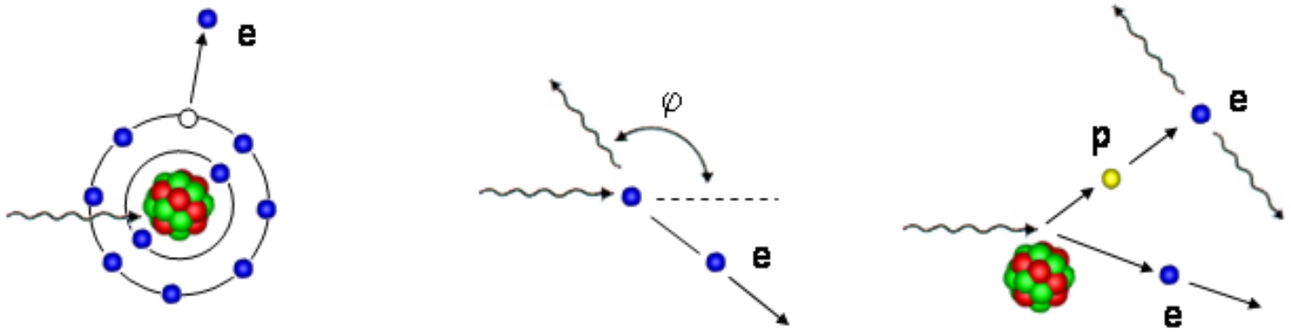

the photoelectric effect (left), the Compton-scattering (middle), and pair production (right).

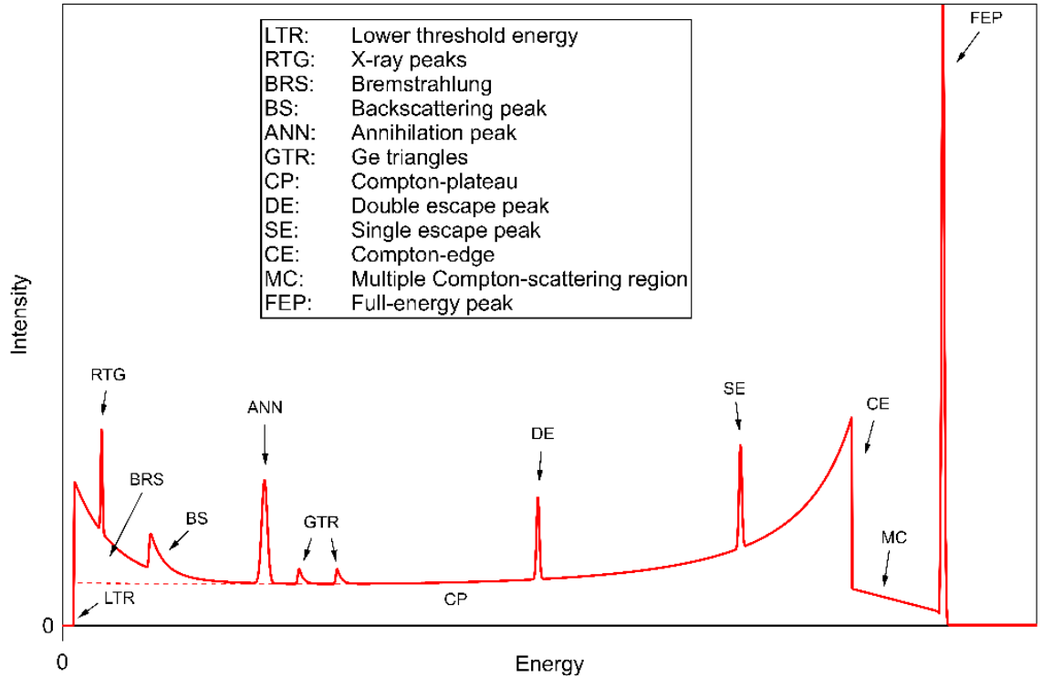

Detectors - Compton suppression

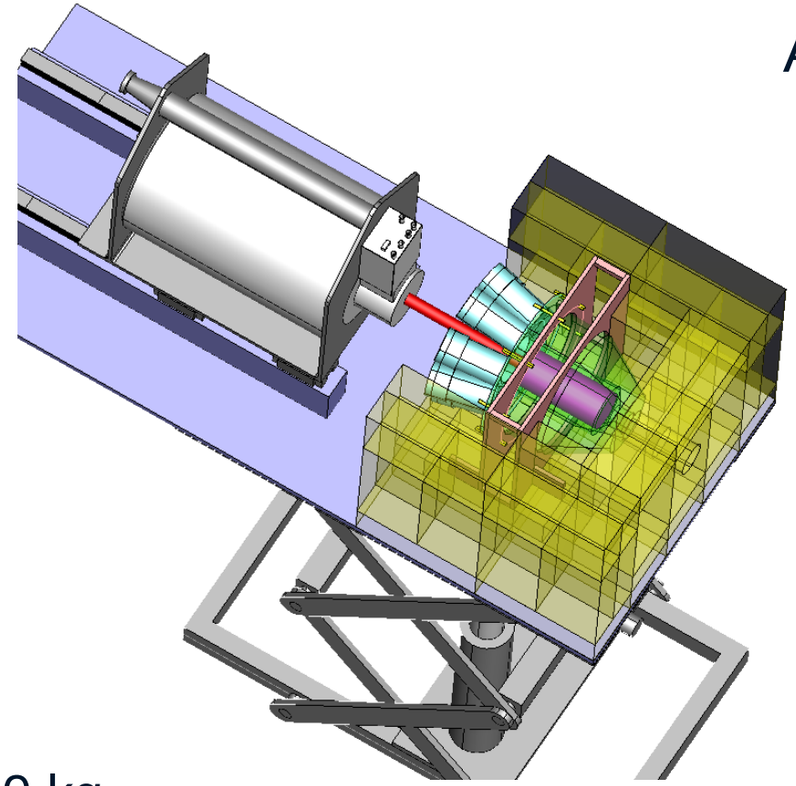

Aim: to reduce the background but not the peak!

i.e. to selectively discard
the events where interaction happened
in both HPGe and suppressor,
and keep all the events interacted
only with HPGe

↓

BETTER
SIGNAL-TO-NOISE
RATIO

20-40 kg
Bi_4GeO_{12} (BGO)

Also reduces room background by more than 2 orders of magnitude

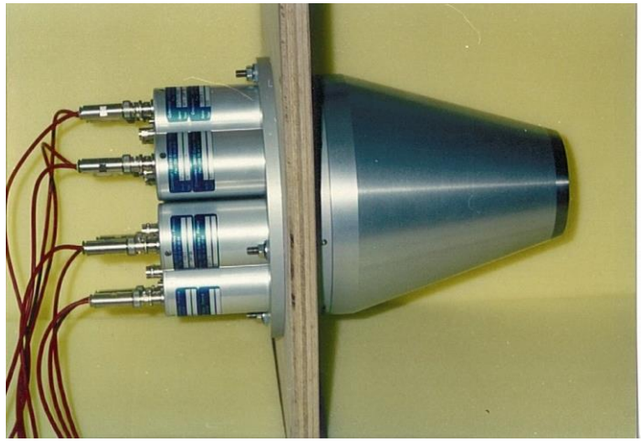

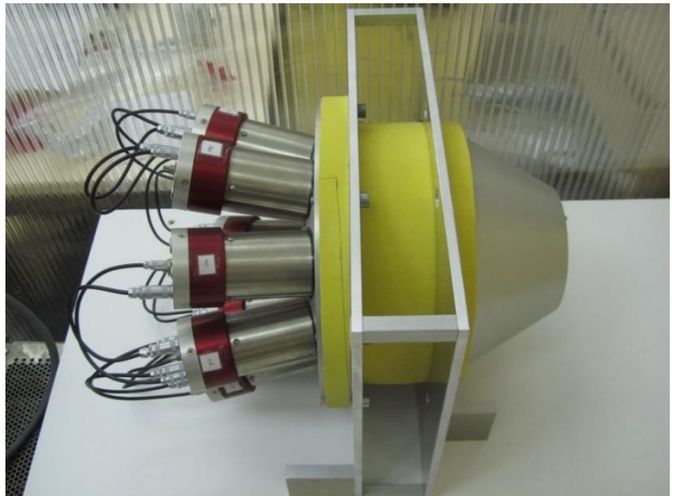

Compton-suppressed gamma detector

Central detector: high-purity Ge, due to best achievable energy resolution

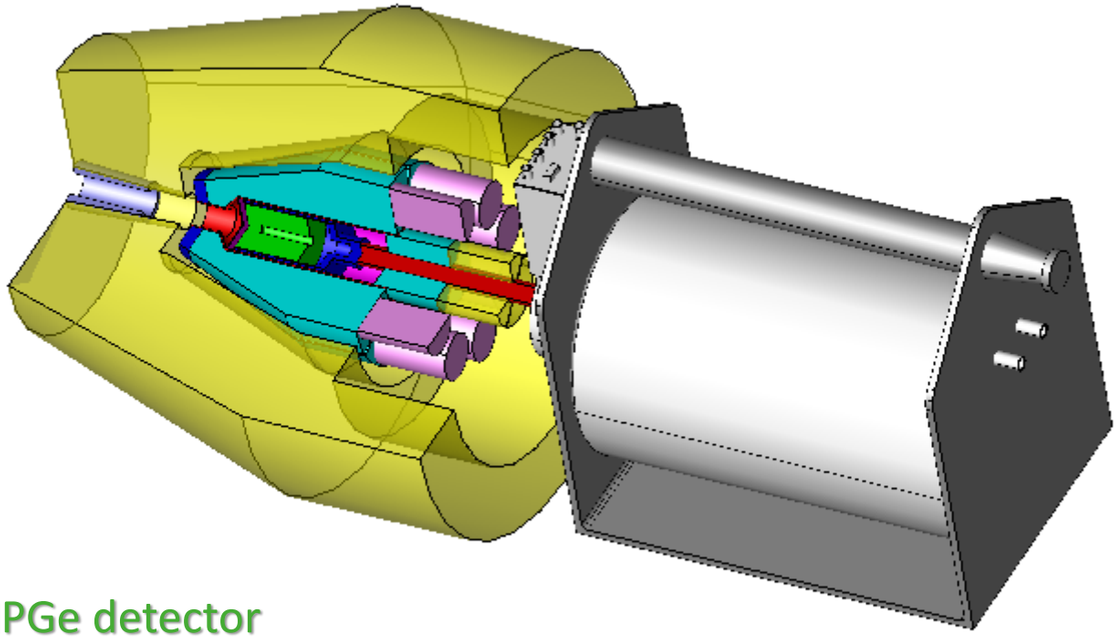

HPGe detector

BGO Compton suppressor detector

Lead shielding

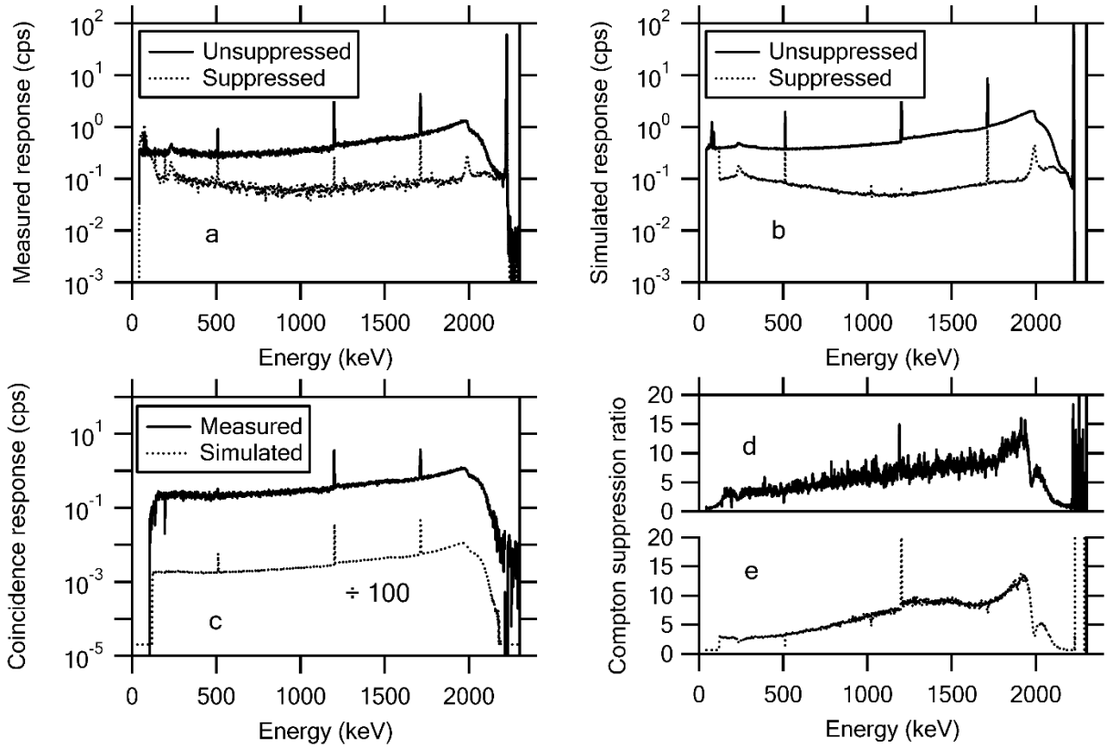

Detector response function for monenergetic gamma radiation (c.f. Compton scattering, pair production)

Two superimposed detector response

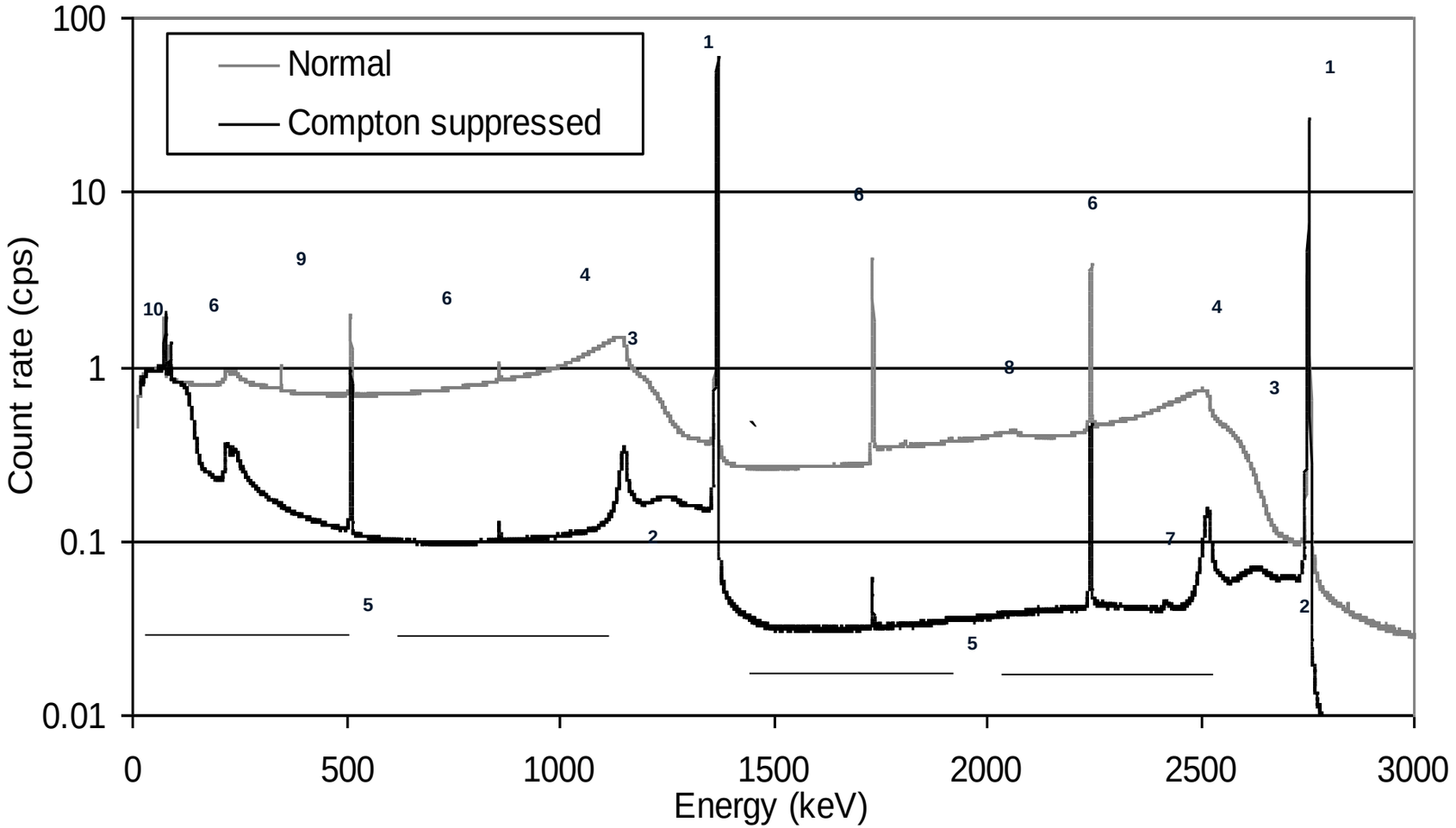

… and in PGAA energy range

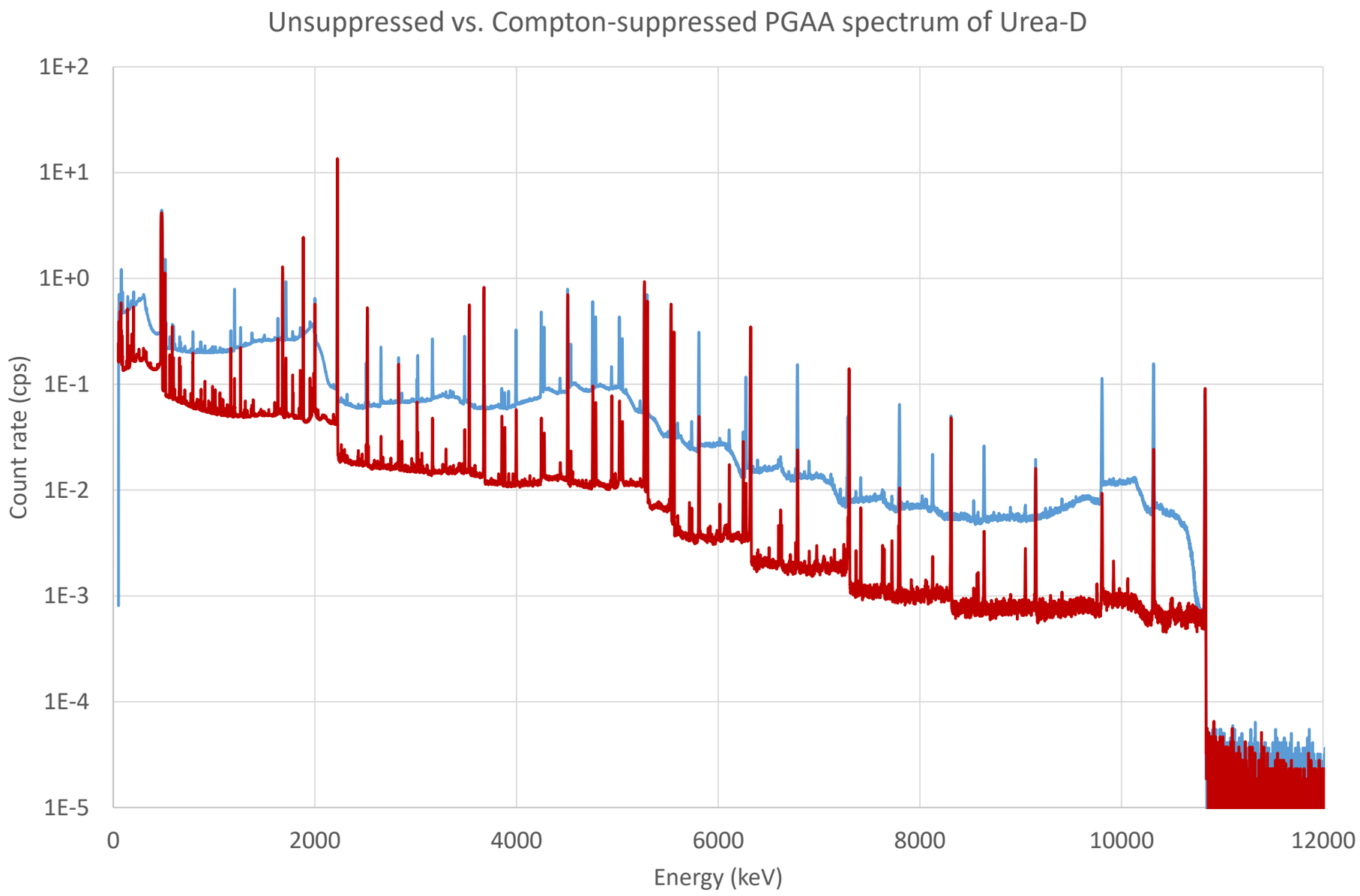

Gamma-spectroscopy for NAA

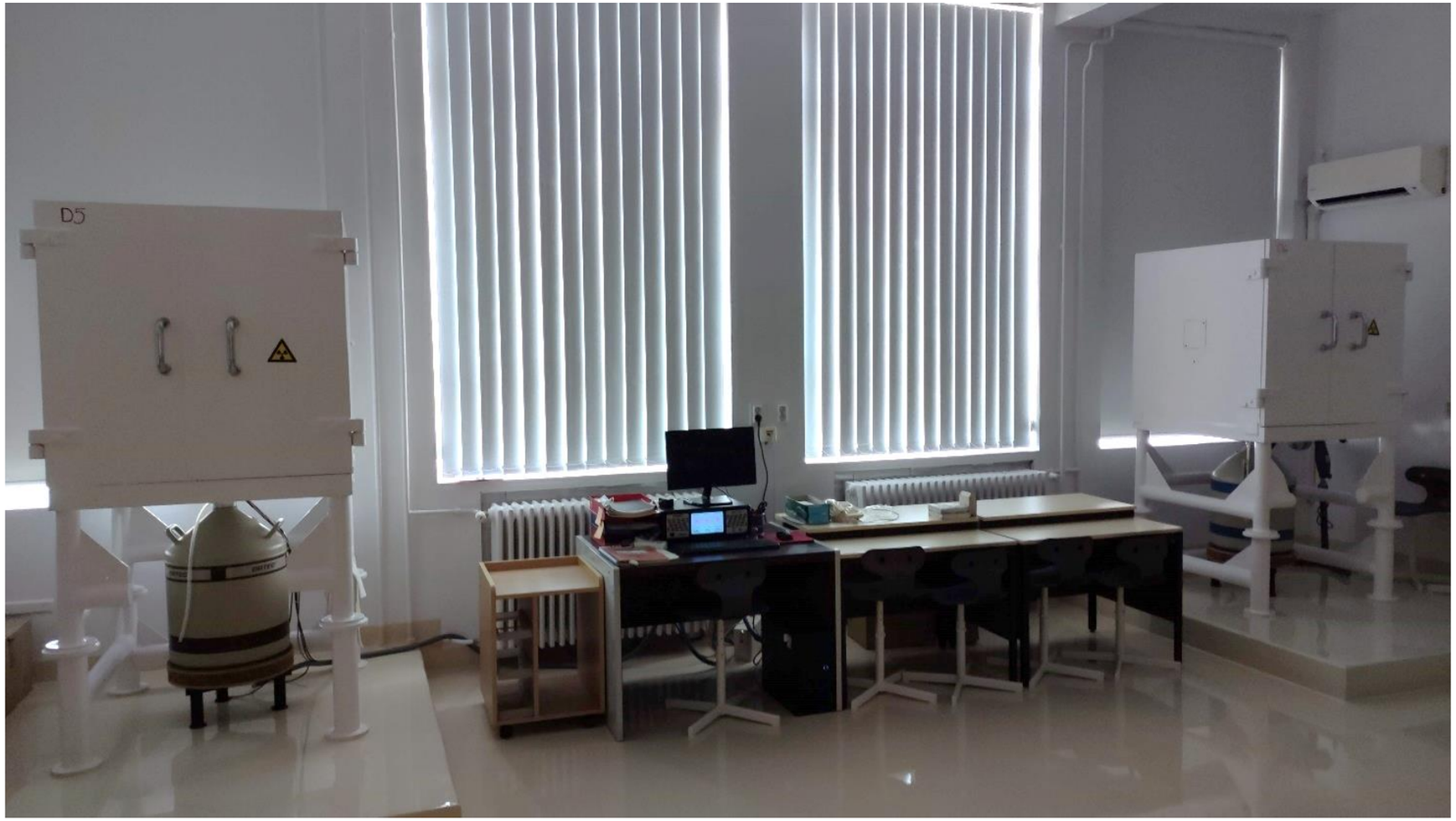

Experimental stations for element analysis at the BNC

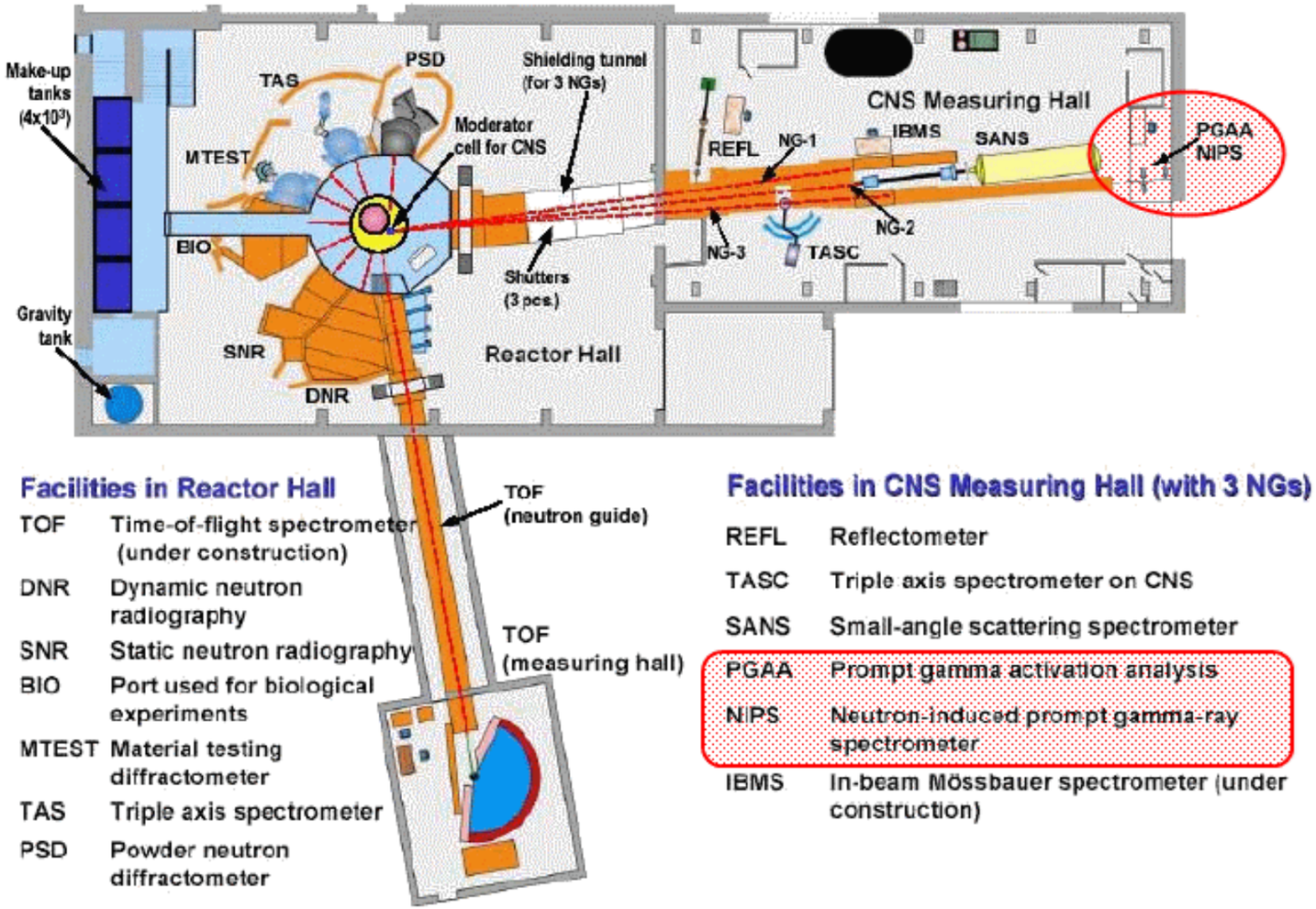

Facilities in Reactor Hall

TOF	Time-of-flight spectrometer (under construction)
DNR	Dynamic neutron radiography
SNR	Static neutron radiography
BIO	Port used for biological experiments
MTEST	Material testing diffractometer
TAS	Triple axis spectrometer
PSD	Powder neutron diffractometer

Facilities in CNS Measuring Hall (with 3 NGs)

REFL	Reflectometer
TASC	Triple axis spectrometer on CNS
SANS	Small-angle scattering spectrometer
PGAA	Prompt gamma activation analysis
NIPS	Neutron-induced prompt gamma-ray spectrometer
IBMS	In-beam Mössbauer spectrometer (under construction)

- PGAA (prompt-gamma activation analysis spectrometer)
  - Increased productivity
  - Automation, reduce manpower
  - Higher throughput for small samples
- NIPS (neutron-induced prompt gamma spectrometer)
  - Specialization for bulky samples, position-sensitive applications
  - Combination with imaging system (NORMA)
- NAA (instrumental neutron activation analysis)
  - High-accuracy trace element analysis of homogeneous samples
  - Often complementary to PGAA in terms of amenable elements and DLs
- DÖME (low-level counting chamber)
  - In-beam activated samples
  - Environmental samples

Present layout of the PGAA-NIPS (NORMA)

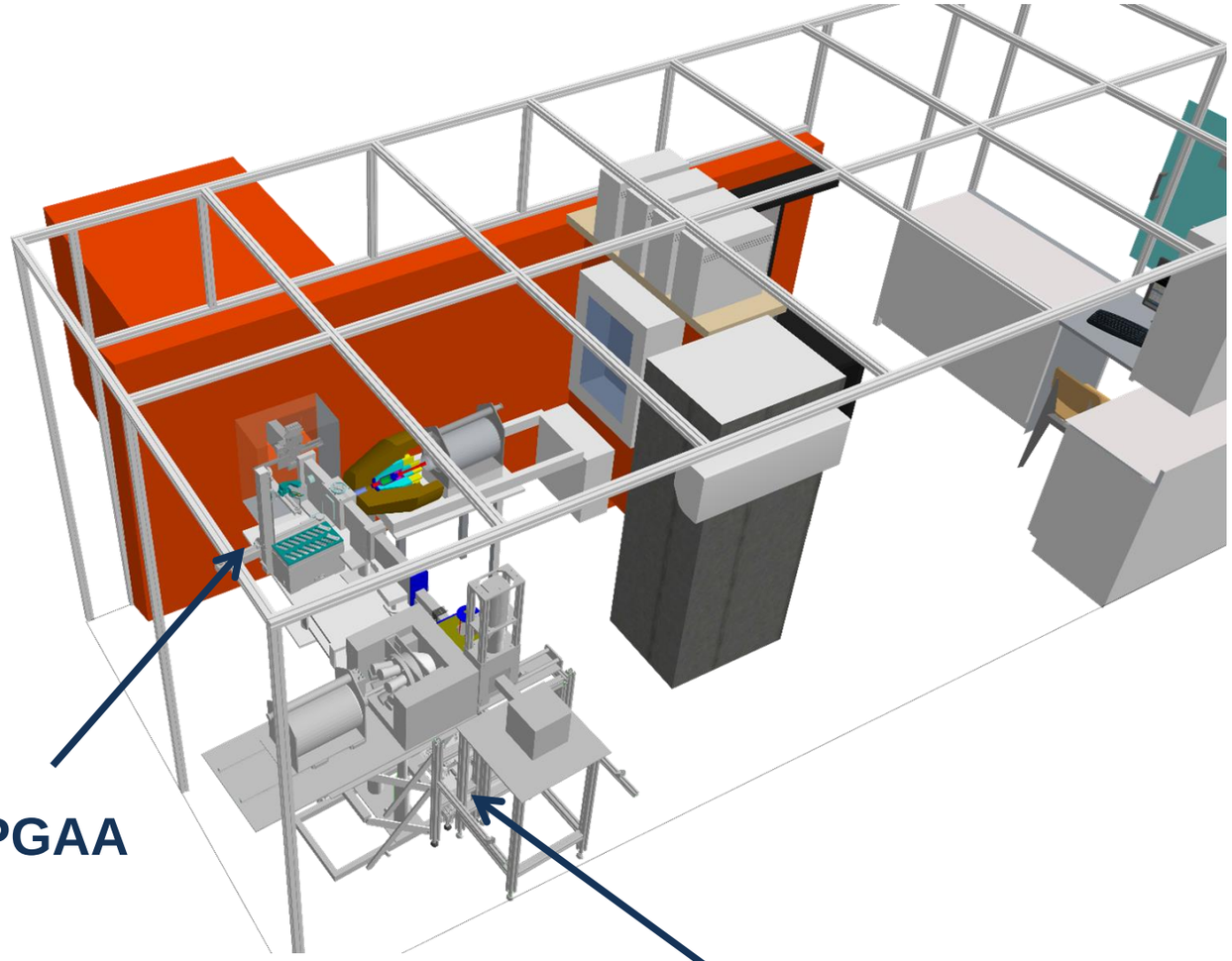

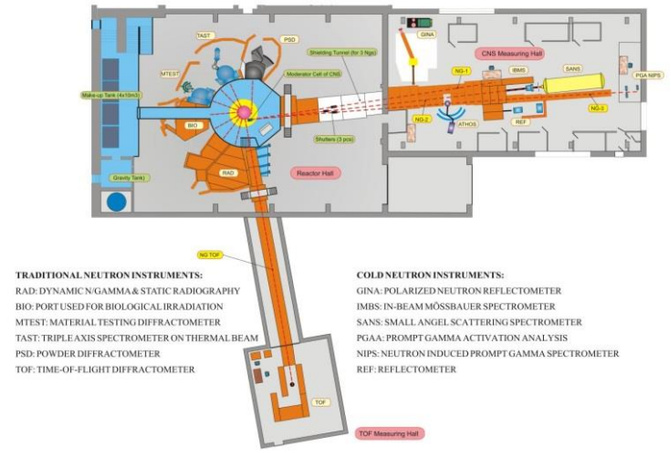

TRADITIONAL NEUTRON INSTRUMENTS:

RAD: DYNAMIC N/GAMMA & STATIC RADIOGRAPHY
BIO: PORT USED FOR BIOLOGICAL IRRADIATION
MTEST: MATERIAL TESTING DIFFRACTOMETER
TAST: TRIPLE AXIS SPECTROMETER ON THERMAL BEAM
PSD: POWDER DIFFRACTOMETER
TOF: TIME-OF-FLIGHT DIFFRACTOMETER

COLD NEUTRON INSTRUMENTS:

GINA: POLARIZED NEUTRON REFLECTOMETER
IMBS: IN-BEAM MÖSSBAUER SPECTROMETER
SANS: SMALL ANGEL SCATTERING SPECTROMETER
PGAA: PROMPT GAMMA ACTIVATION ANALYSIS
NIPS: NEUTRON INDUCED PROMPT GAMMA SPECTROMETER
REF: REFLECTOMETER

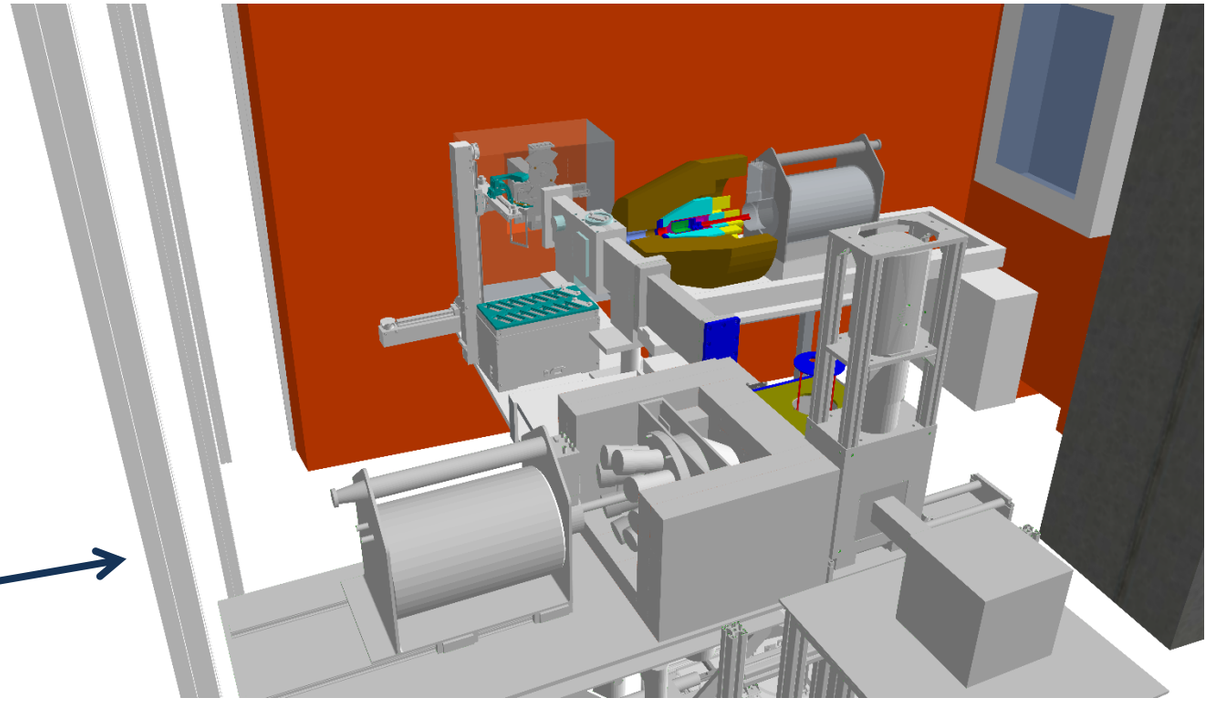

Instrument photos

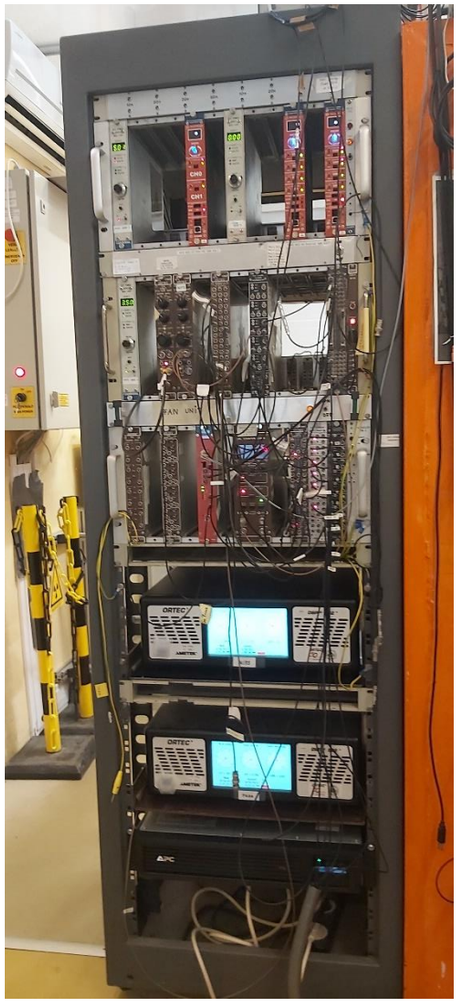

PGAA sample handling

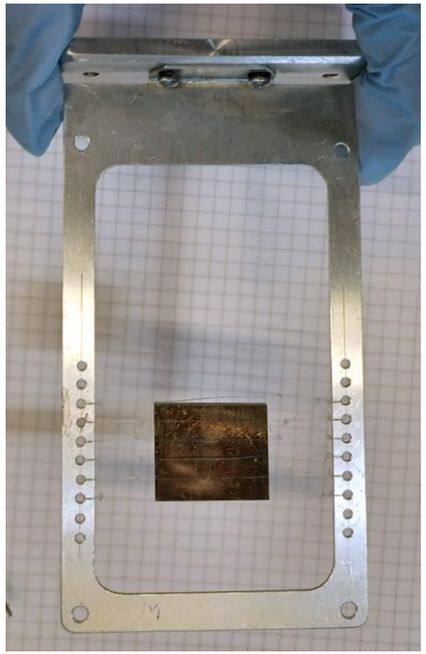

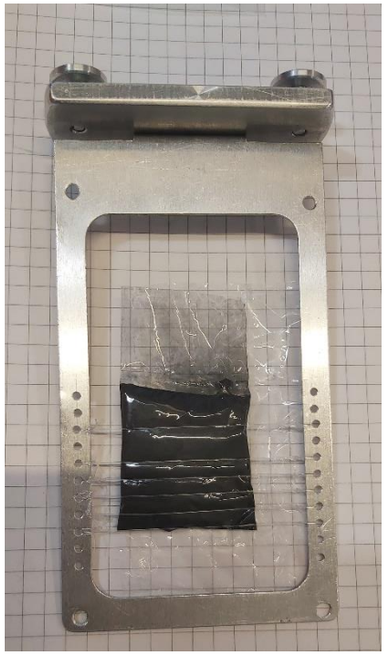

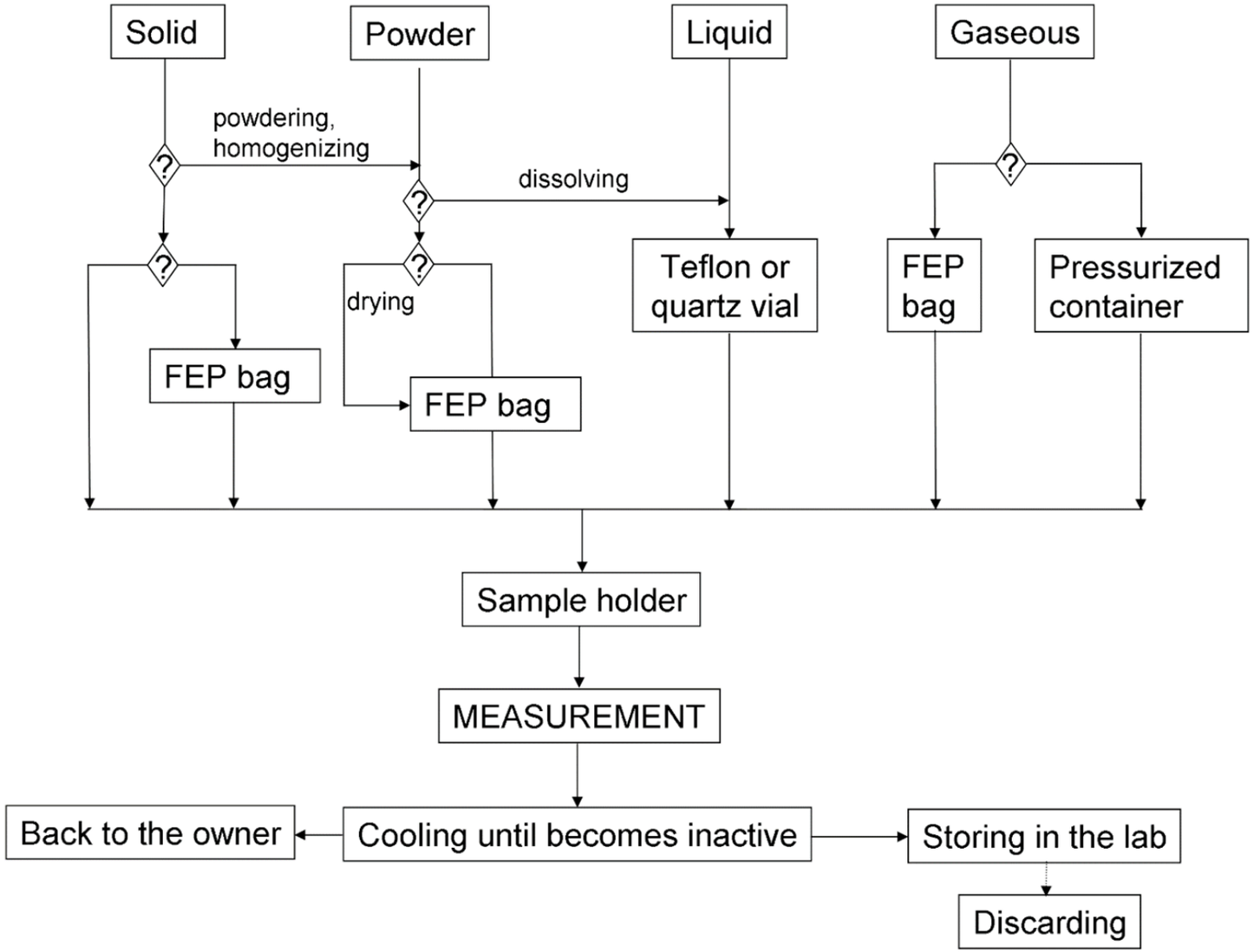

- **10 mg – 1 g sample mass**
- **Powder, solid -> Telfon bag**
- **Liquid -> Teflon vial**
- **Gas -> pressurized container**
- **Remains active only for a few hours (days) after irradiation**

Manual / automatic changer at PGAA

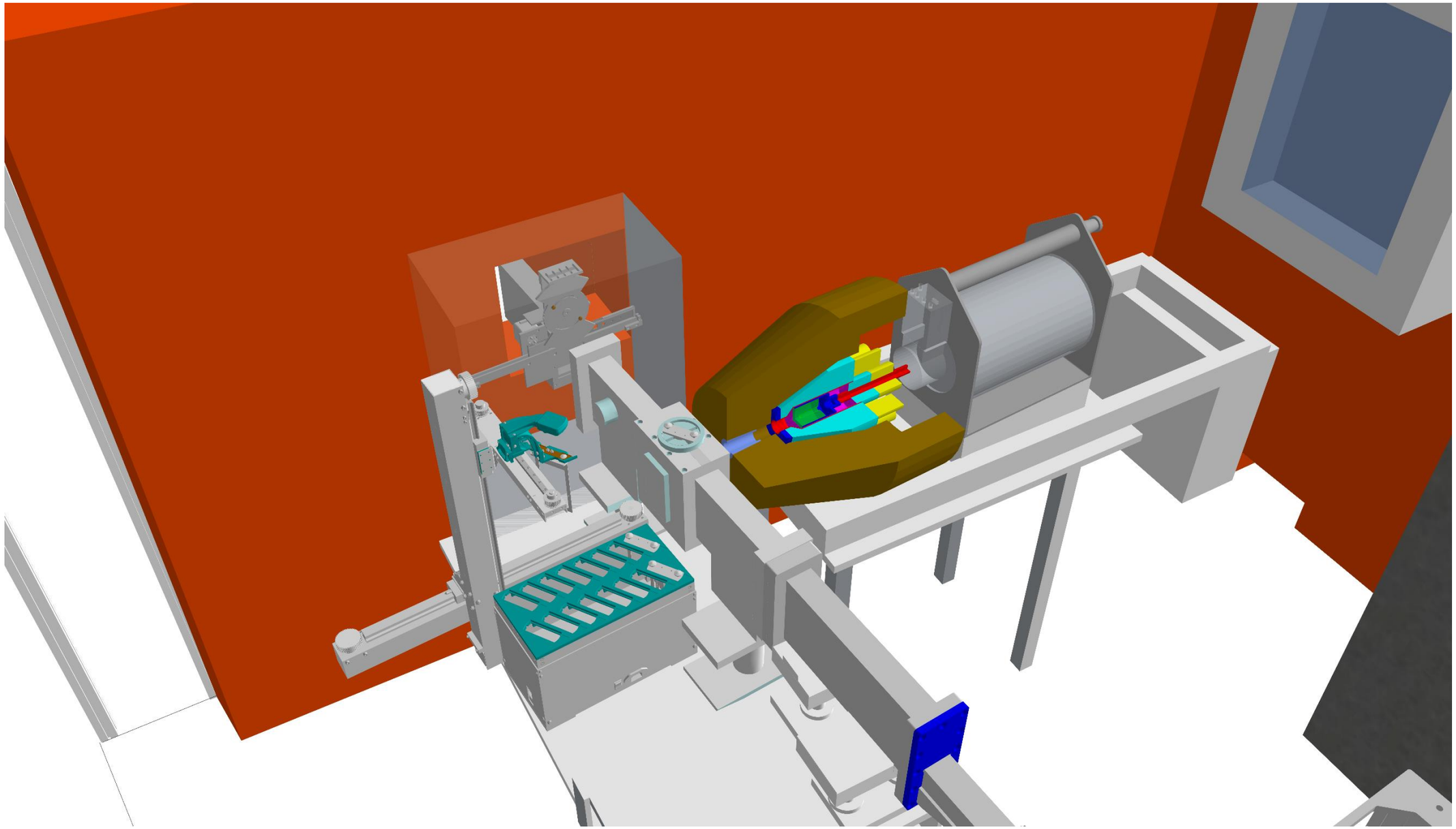

Budapest Neutron Centre
Centre for Energy Research

Methodology

Calibration

Spectroscopy data

Data evaluation

Validation

Spectroscopy

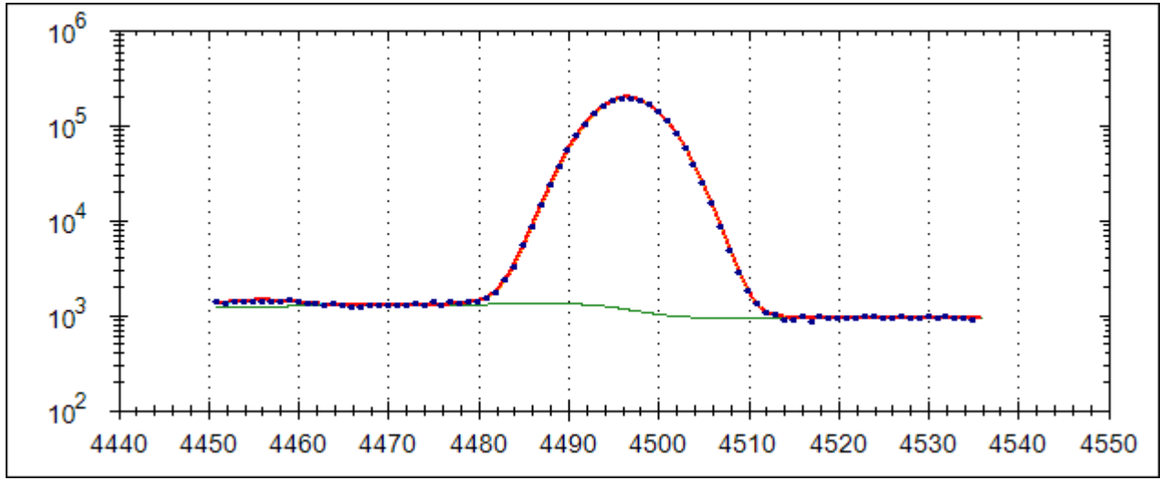

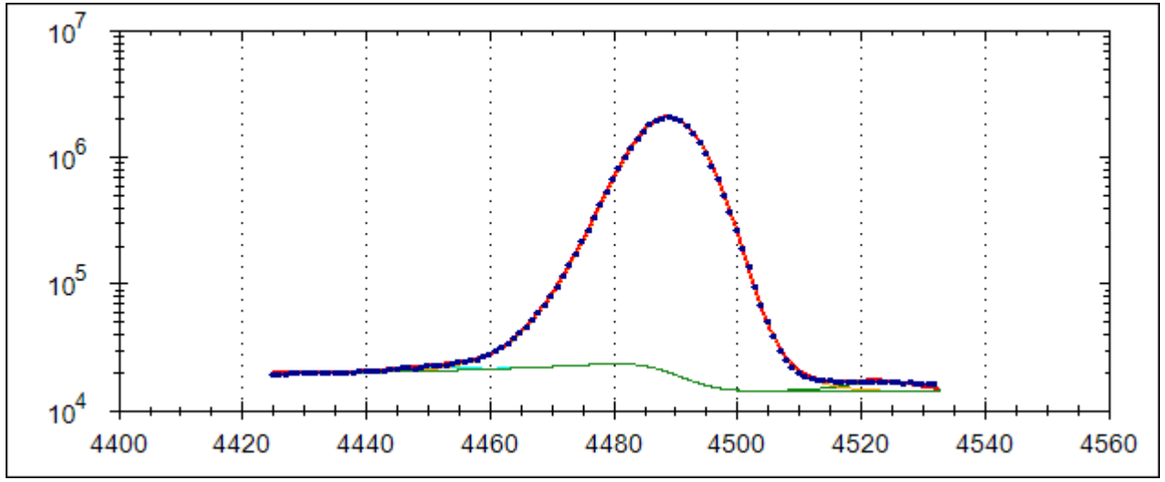

Optimum peak shape

Distorted peak shape

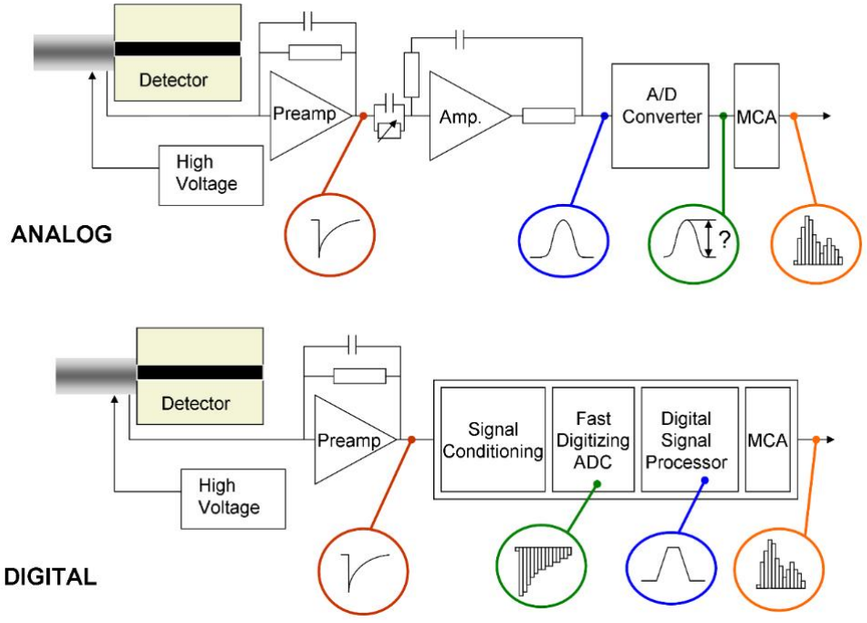

Range of calibration sources

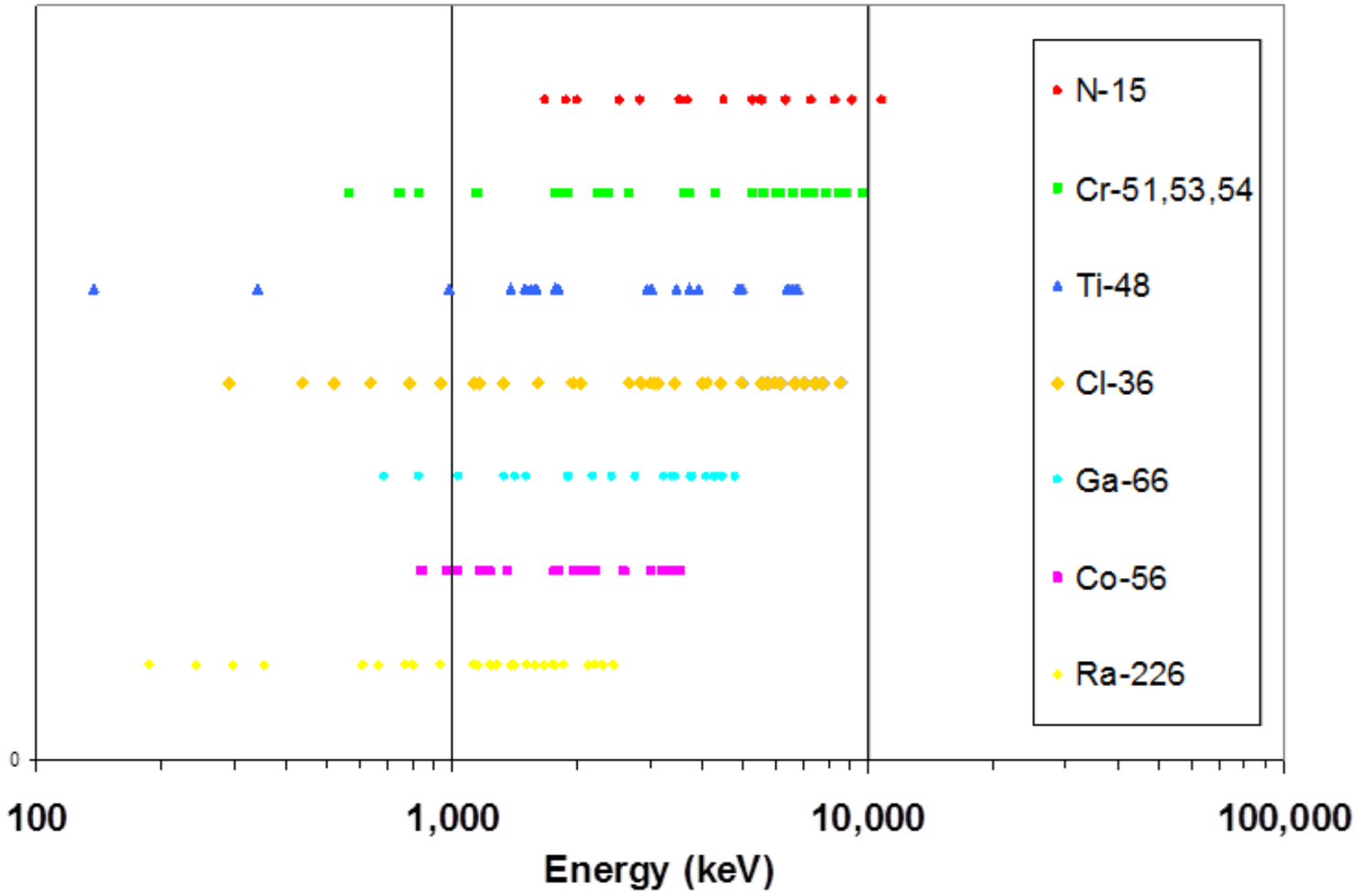

Efficiency and nonlinearity calibration

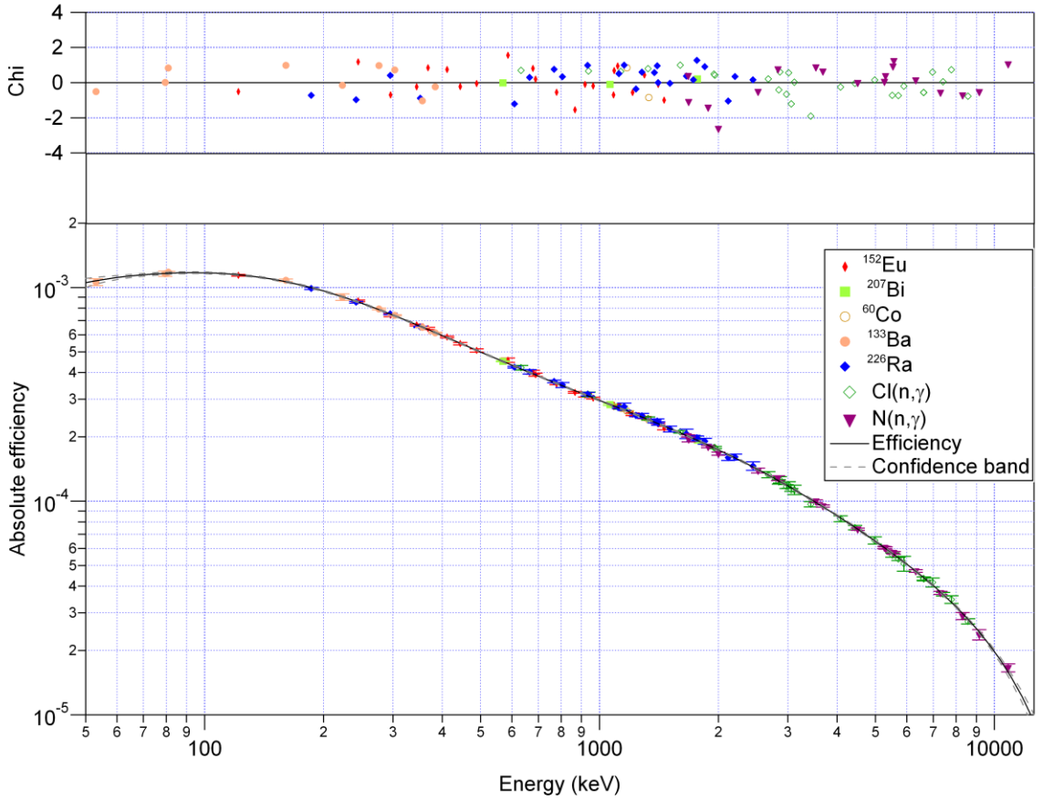

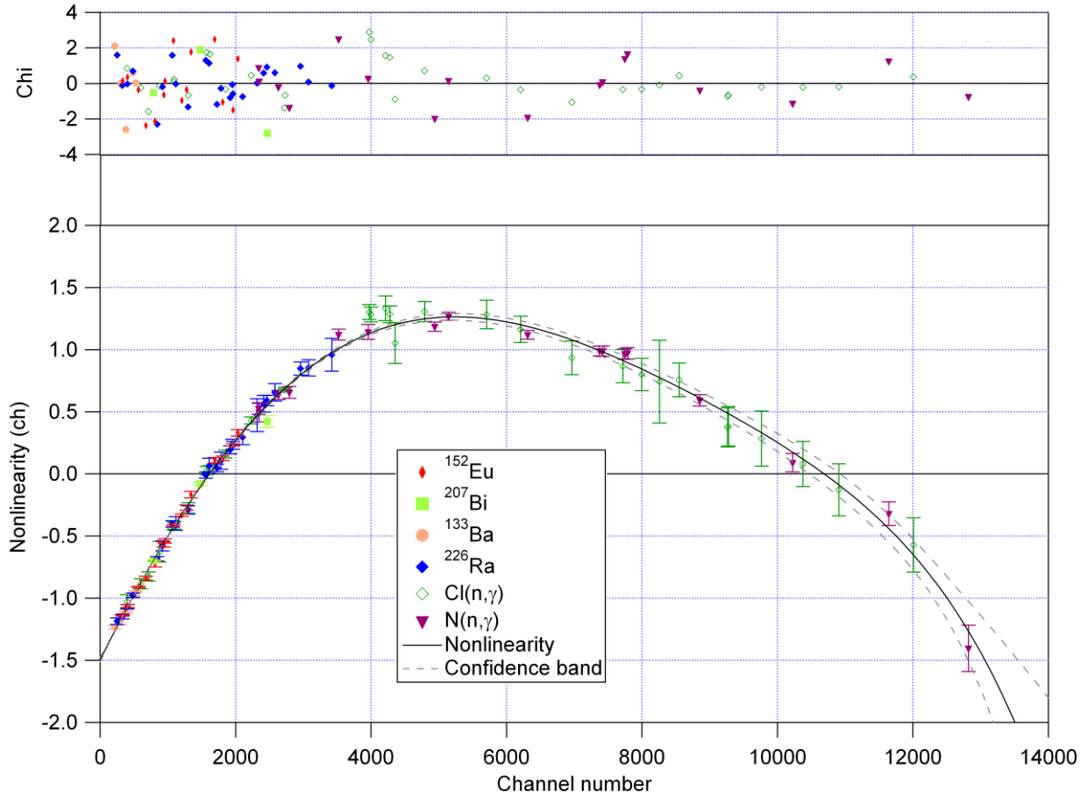

Efficiency = detected events / emitted gamma photons

Nonlinearity is to compensate for a small, but systematic bias in the linear energy-channel correspondence

PGAA spectroscopic library

Z	El	A	MW	#	E	*dE*	σ	dσ%	RI	Area	cps/g
1	H	1	1.01	1	2223.259	*0.019*	0.3326	*0.2*	100.00	100.00	64.183
1	H	2	1.01	2	6250.204	*0.098*	0.000492	*5.0*	0.15	5.00	0.0286
3	Li	6	6.94	5	477.586	*0.050*	0.001399	*5.9*	3.52	10.14	0.1218
3	Li	7	6.94	2	980.559	*0.046*	0.004365	*5.1*	10.97	18.74	0.2251
3	Li	7	6.94	3	1051.817	*0.048*	0.004364	*5.1*	10.97	17.83	0.2141
3	Li	7	6.94	1	2032.310	*0.070*	0.0398	*5.0*	100.00	100.00	1.2007
3	Li	6	6.94	6	6769.633	*0.263*	0.001354	*6.5*	3.40	0.84	0.0101
3	Li	6	6.94	4	7246.800	*0.275*	0.002106	*8.4*	5.29	1.17	0.014
4	Be	9	9.01	4	853.631	*0.011*	0.00165	*8.9*	26.69	100.00	0.0723
4	Be	9	9.01	3	2590.014	*0.025*	0.00188	*8.9*	30.41	49.08	0.0355
4	Be	9	9.01	2	3367.484	*0.035*	0.002924	*8.9*	47.30	58.96	0.0427
4	Be	9	9.01	5	3443.421	*0.036*	0.000993	*8.9*	16.06	19.54	0.0141
4	Be	9	9.01	6	5956.602	*0.092*	0.000146	*9.1*	2.36	1.41	0.001
4	Be	9	9.01	1	6809.579	*0.099*	0.006181	*9.0*	100.00	48.52	0.0351
5	B	10	10.81	1	477.600	*5.000*	712.5	*0.3*	100.00	100.00	39806
6	C	12	12.01	2	1261.708	*0.057*	0.00123	*2.7*	45.58	100.00	0.0306
6	C	12	12.01	3	3684.016	*0.069*	0.001175	*3.5*	43.53	38.02	0.0116
6	C	12	12.01	1	4945.302	*0.066*	0.002699	*2.9*	100.00	60.55	0.0186
7	N	14	14.01	22	583.567	*0.031*	0.000429	*3.3*	1.81	6.93	0.0159
7	N	14	14.01	12	1678.244	*0.029*	0.006254	*1.5*	26.34	47.15	0.1085
7	N	14	14.01	18	1681.174	*0.043*	0.001296	*2.7*	5.46	9.76	0.0225
7	N	14	14.01	21	1853.944	*0.052*	0.000474	*4.5*	2.00	3.31	0.0076
7	N	14	14.01	5	1884.853	*0.031*	0.0145	*1.3*	61.07	100.00	0.2301
7	N	14	14.01	24	1988.532	*0.077*	0.000294	*5.8*	1.24	1.94	0.0045
7	N	14	14.01	15	1999.693	*0.032*	0.003208	*1.7*	13.51	21.12	0.0486
7	N	14	14.01	13	2520.446	*0.039*	0.004246	*1.8*	17.88	22.98	0.0529

Collection of energies, relative emission probabilities and partial gamma-ray production cross-sections for each element

PGAA analysis program ProSpeRo in EXCEL

INPUT MODUL

- **Peak list from Hypermet PC (up to 1200 lines)**
- **PGAA library-25 (~1800 lines)**
- **PGAA library-1% (~6200 lines)**
- **Element data (Molar weights, Oxidation number, γ & n self-absorption)**
- **BKG in equivalent mass**
- **Efficiency**
- **Auxiliary data (Beam temperature, flux, density, thickness)**

DATA EVAULATION MODUL

Iteractive edit of the data by the analyst

OUTPUT MODUL

Zs. Révay, *Determining Elemental Composition Using Prompt-gamma Activation Analysis.*
Analytical Chemistry 81 (2009) 6851-6859

Example of a PGAA analysis report

Spectrum: N22HAM1.MCA Peak list: N22HAM1.pkl Uncertainty calculation: statistical
Live time: 39126.63 s Neutron Flux: 1.50E+8 ±2 %, temp 35 K, BKG: 13 vac08jan Conc. format: ppm / %

Z	El	M	m meas	unc %	m Bkg	unc %	m net	ox. st.	m ox	unc %	c% atom	unc %	c% el/el	unc %	c% el/ox	unc %	c% ox/ox	unc %
1	H	1.008	6.82E-4	0.6	1.15E-5	2.0	6.70E-4	1	5.99E-3	0.6	4.02	1.9	0.187	1.5	0.093	0.9	0.83	1.8
6	C	12.01	0.080	3.8		0.0	0.08	4	0.29	3.8	40	2.5	22	3.2	11.1	3.4	41	2.4
9	F	19	4.89E-2	5.	2.06E-4	20.	4.87E-2	-1	4.87E-2	5.	16	4.	14	4.	6.8	5.	6.8	5.
12	Mg	24.31	1.08E-2	5.		0.0	1.08E-2	2	1.79E-2	5.	2.7	5.	3.0	5.	1.5	5.	2.5	5.
13	Al	26.98	1.06E-2	1.6	1.73E-3	3.0	8.84E-3	3	1.67E-2	2.0	1.98	2.7	2.47	2.4	1.23	2.1	2.32	2.6
14	Si	28.09	0.064	2.1		0.0	0.06	4	0.14	2.1	13.7	2.5	17.8	2.2	8.8	2.1	18.9	2.4
15	p	30.97	7.23E-3	5.		0.0	7.23E-3	5	1.66E-2	5.	1.4	6.	2.0	6.	1.0	5.	2.3	6.
17	Cl	35.45	7.99E-4	39.		0.0	7.99E-4	-1	7.99E-4	39.	0.1	39.	0.2	39.	0.11	39.	0.11	39.
19	K	39.1	3.78E-2	2.4		0.0	3.78E-2	1	4.56E-2	2.4	5.9	2.9	10.6	2.5	5.3	2.4	6.3	2.8
20	Ca	40.08	0.092	2.4		0.0	0.09	2	0.13	2.4	13.9	2.7	26	2.1	12.8	2.2	18.0	2.6
22	Ti	47.87	8.30E-4	2.4		0.0	8.30E-4	4	1.39E-3	2.4	0.105	3.0	0.23	2.7	0.115	2.5	0.193	2.9
24	Cr	52	1.21E-5	49.		0.0	1.21E-5	3	1.77E-5	49.	10 ppm	49.	30 ppm	49.	20 ppm	49.	20 ppm	49.
25	Mn	54.94	2.35E-3	3.8	3.18E-6	10.	2.35E-3	3	3.37E-3	3.8	0.26	4.	0.65	4.0	0.33	3.8	0.47	4.
27	Co	58.93	1.08E-5	15.		0.0	1.08E-5	2	1.38E-5	15.	11 ppm	15.	30 ppm	15.	15 ppm	15.	19 ppm	15.
28	Ni	58.69	3.35E-5	11.		0.0	3.35E-5	2	4.27E-5	11.	35 ppm	11.	90 ppm	11.	50 ppm	11.	60 ppm	11.
34	Se	78.96	2.59E-4	8.		0.0	2.59E-4	4	3.64E-4	8.	200 ppm	9.	0.07	8.	360 ppm	8.	0.051	8.
38	Sr	87.62	9.19E-4	5.		0.0	9.19E-4	2	1.09E-3	5.	0.063	5.	0.26	5.	0.13	5.	0.15	5.
48	Cd	112.4	1.07E-6	1.9		0.0	1.07E-6	2	1.22E-6	1.9	0.58 ppm	2.6	3.0 ppm	2.3	1.49 ppm	2.0	1.70 ppm	2.6
49	In	114.8	3.63E-6	8.		0.0	3.63E-6	3	4.39E-6	8.	1.9 ppm	8.	10 ppm	8.	5.0 ppm	8.	6.1 ppm	8.
50	Sn	118.7	3.13E-3	6.		0.0	3.13E-3	2	3.55E-3	6.	0.16	6.	0.87	6.	0.43	6.	0.49	6.
60	Nd	144.2	1.13E-5	8.		0.0	1.13E-5	3	1.32E-5	8.	4.7 ppm	9.	31 ppm	8.	16 ppm	8.	18 ppm	9.
62	Sm	150.4	6.74E-7	1.6		0.0	6.74E-7	3	7.82E-7	1.6	0.271ppm	2.4	1.88 ppm	2.1	0.94 ppm	1.8	1.09 ppm	2.4
64	Gd	157.3	9.60E-7	19.		0.0	9.60E-7	3	1.11E-6	19.	0.4 ppm	19.	3 ppm	19.	1.3 ppm	19.	1.5 ppm	19.
		0																
		0																
		0																
							0.35818	2.6	0.71964	1.3	100.31		100.36		49.78		100.43	

Quantification limit for 50 % - O calculated 0.36146 50 % O/ total
mass without O 0.35818

self-abs.: no (recalc.: Ctrl+Shift+S) thickness (mm) : 1 density: 2.7 oxide: yes

version: 3.2.2 (2008.04.21)

Centre for Energy Research

Hyperlab for peak fitting

Budapest Neutron Centre

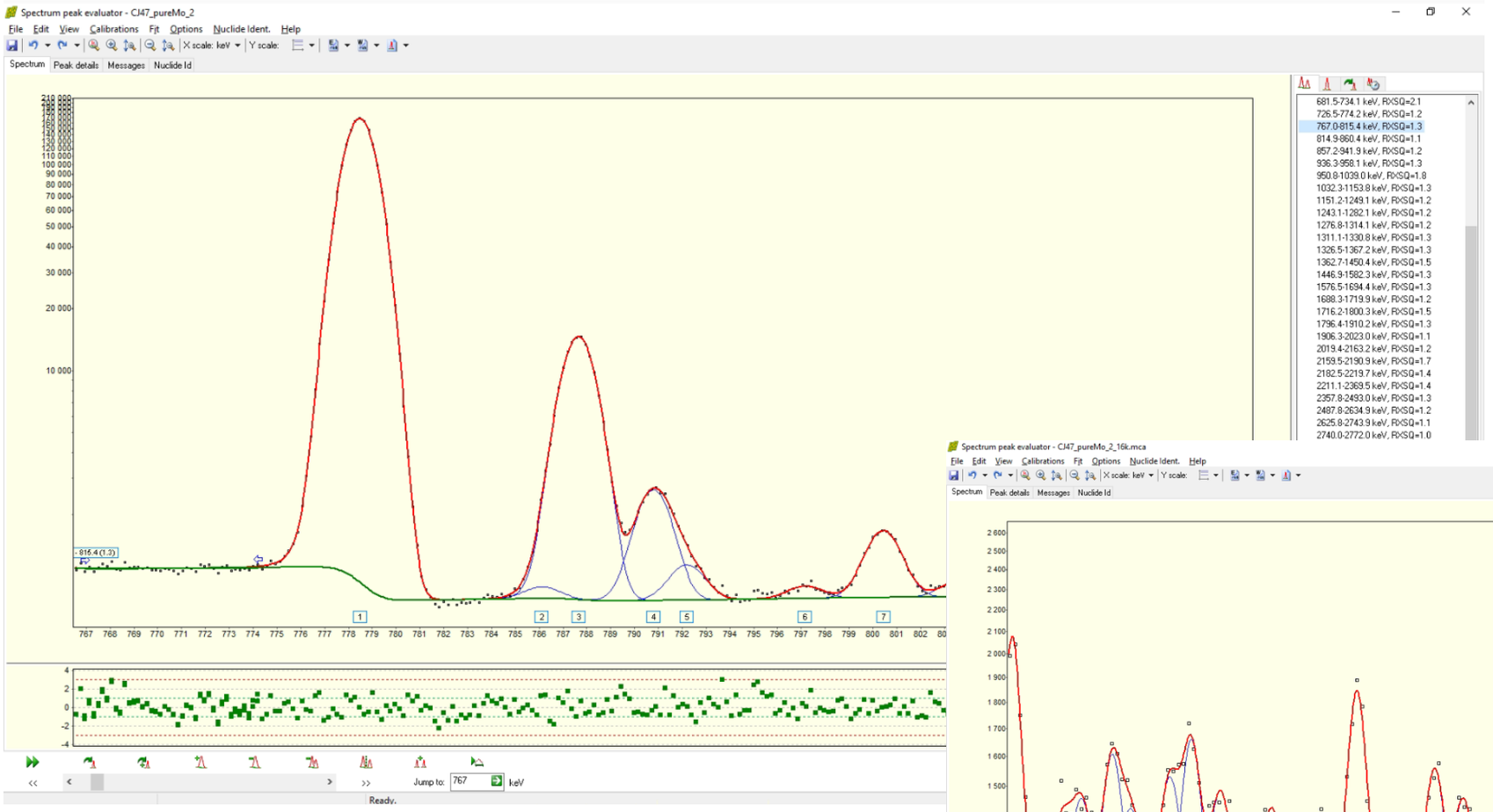

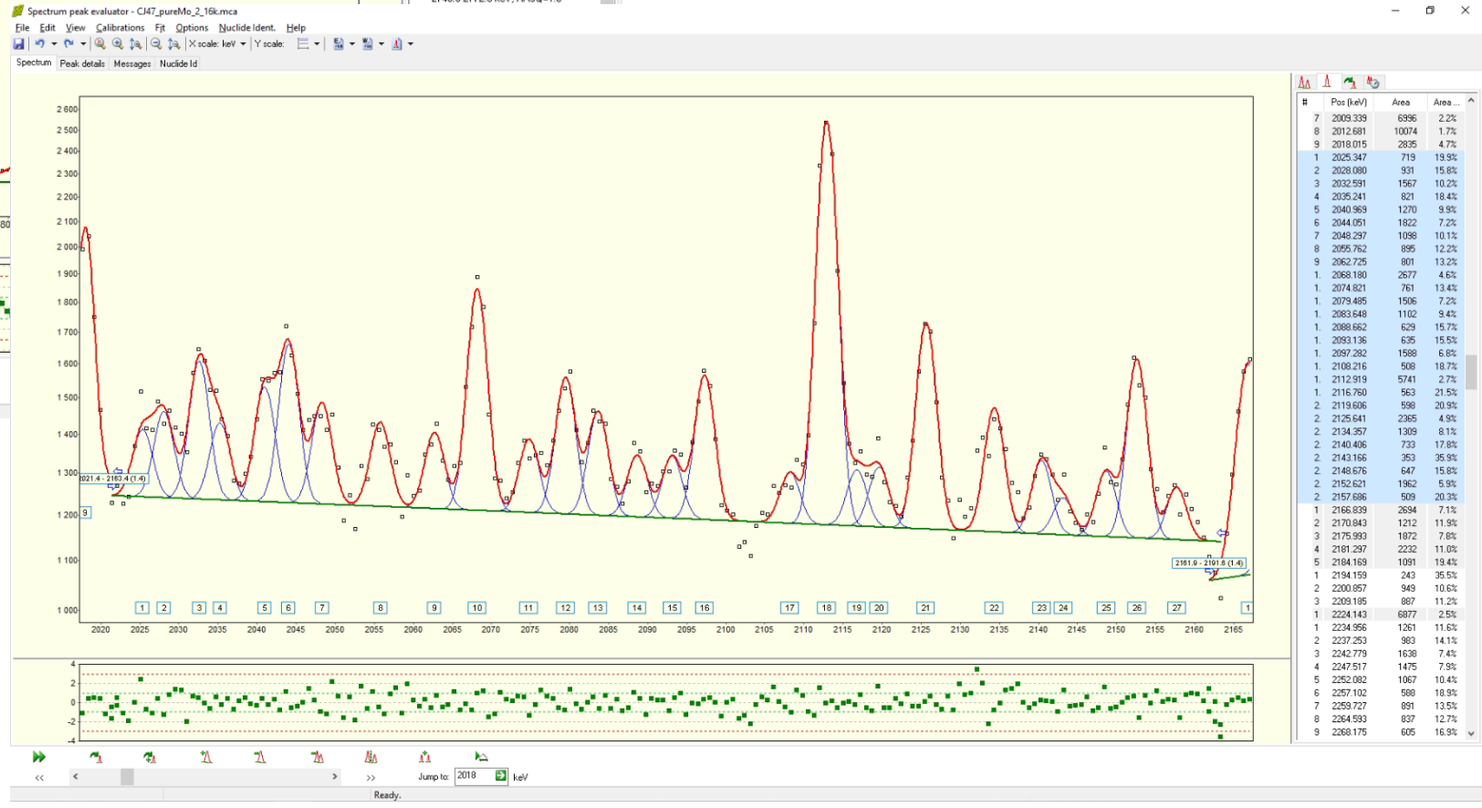

k_0 approach of NAA

$$\frac{N_p/t_m}{(N_p/t_m)_*} = \frac{w}{w^*} \cdot \frac{S \cdot D \cdot C}{S^* \cdot D^* \cdot C^*} \cdot \frac{M^*}{M} \cdot \frac{\theta}{\theta^*} \cdot \frac{\gamma}{\gamma^*} \cdot \frac{\sigma_0}{\sigma_0^*} \cdot \frac{f+Q_0}{f+Q_0^*} \cdot \frac{\varepsilon_p}{\varepsilon_p^*}$$

k_0: compound nuclear constant

$$c_x(ppm) = \frac{\left[\frac{N_{p,x}}{t_m \cdot S \cdot D \cdot C \cdot W}\right]}{A_{sp,Au}} \cdot \frac{1}{k_{0,Au}(x)} \cdot \frac{f+Q_{0,Au}(\alpha)}{f+Q_{0,x}(\alpha)} \cdot \frac{\varepsilon_{p,Au}}{\varepsilon_{p,x}} \cdot 10^6$$

$$f = \frac{\Phi_{th}}{\Phi_e}, Q_0 = \frac{I_0}{\sigma_{th}}, \quad A_{sp,x} = N_{p,x}/t_m \cdot S \cdot D \cdot C \cdot W$$

α : epitermal shape factor

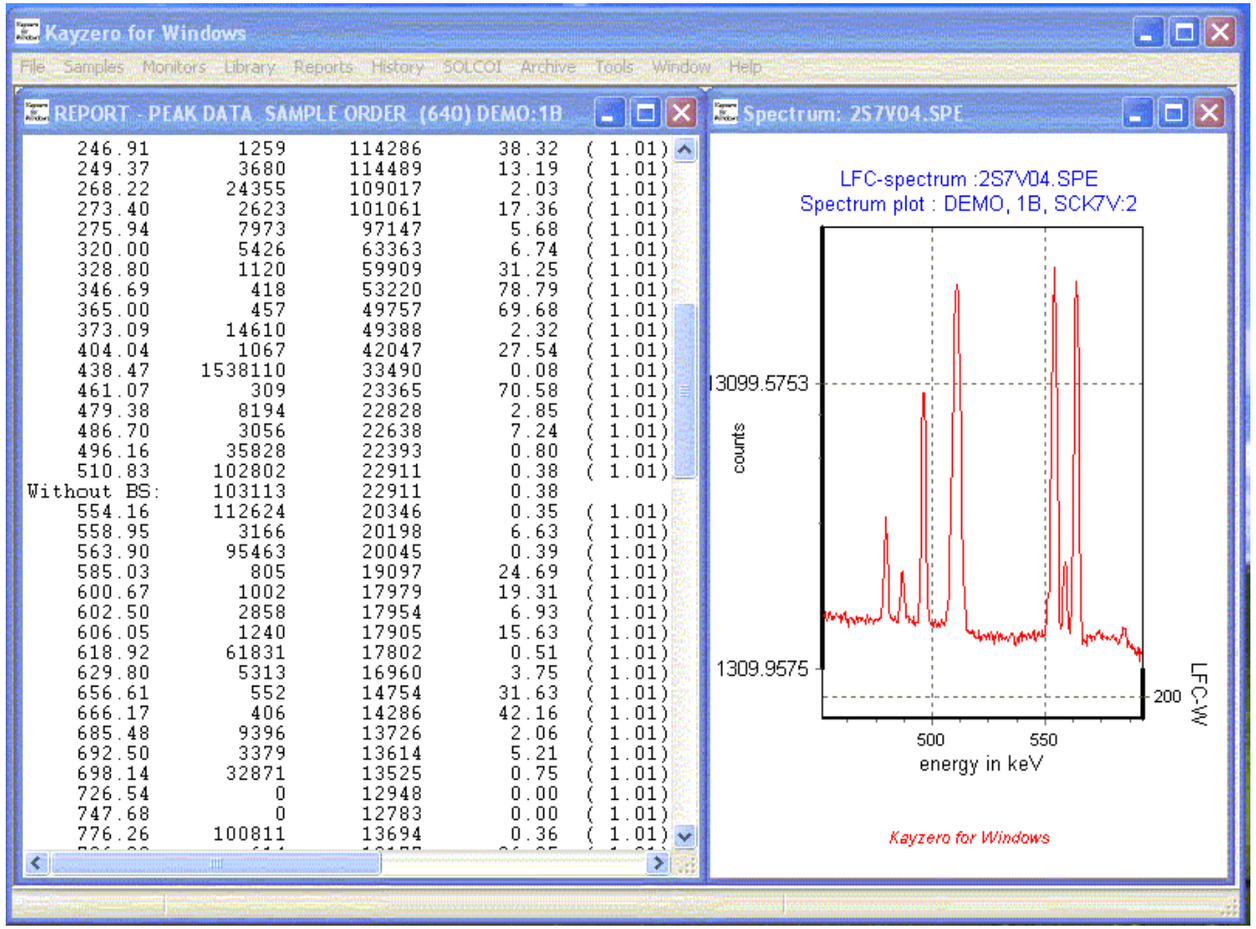

PGAA vs. NAA

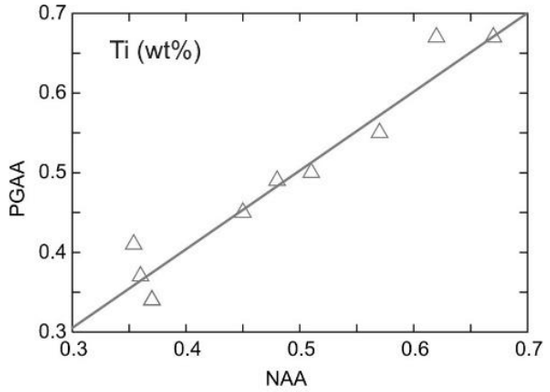
Ti (wt%)
PGAA
NAA

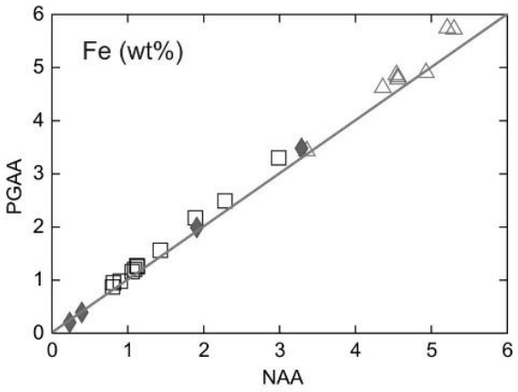
Fe (wt%)
PGAA
NAA

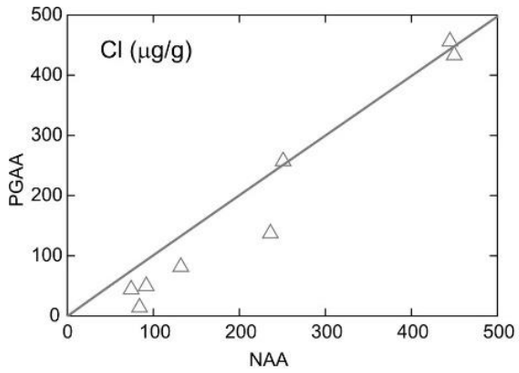
Cl (μg/g)
PGAA
NAA

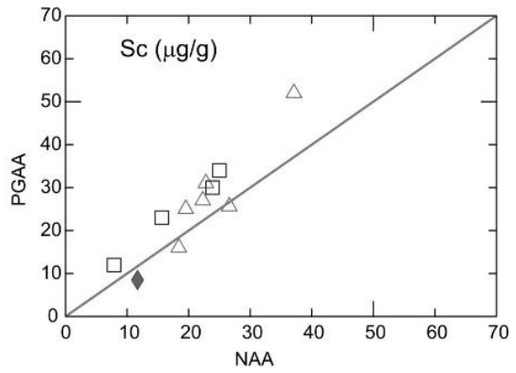
Sc (μg/g)
PGAA
NAA

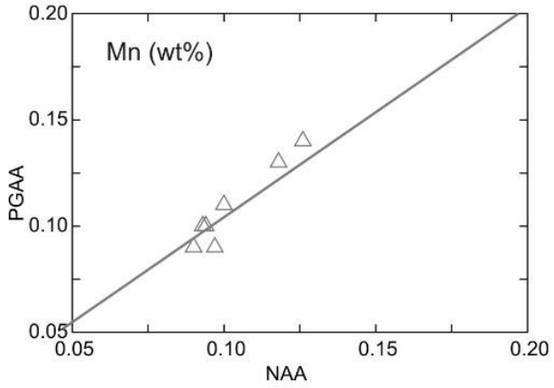
Mn (wt%)
PGAA
NAA

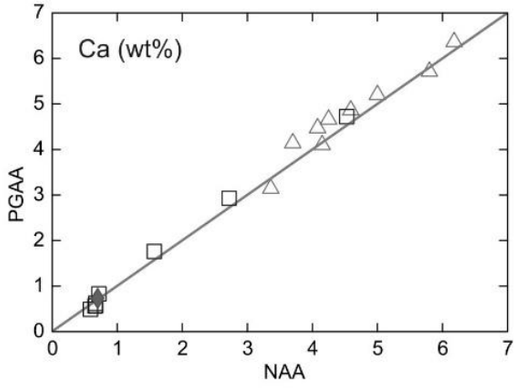
Ca (wt%)
PGAA
NAA

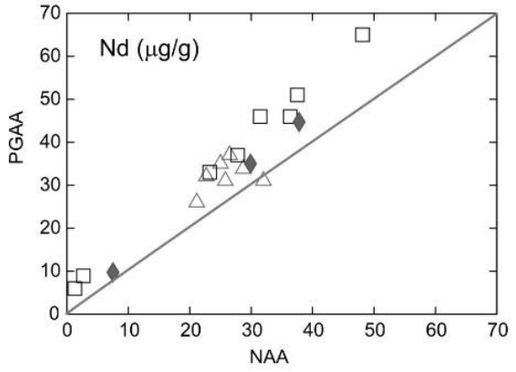
Nd (μg/g)
PGAA
NAA

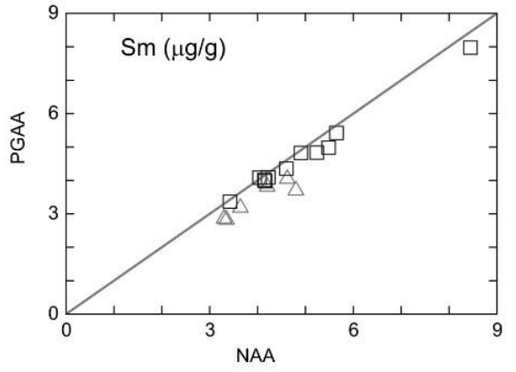
Sm (μg/g)
PGAA
NAA

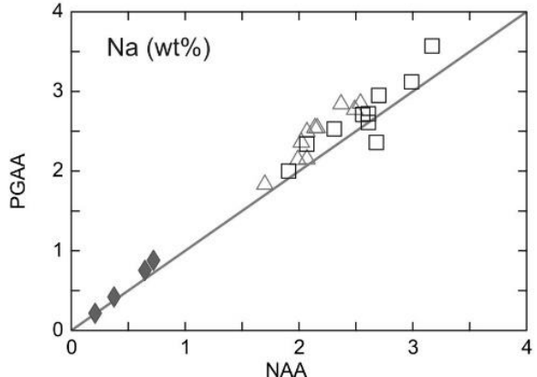
Na (wt%)
PGAA
NAA

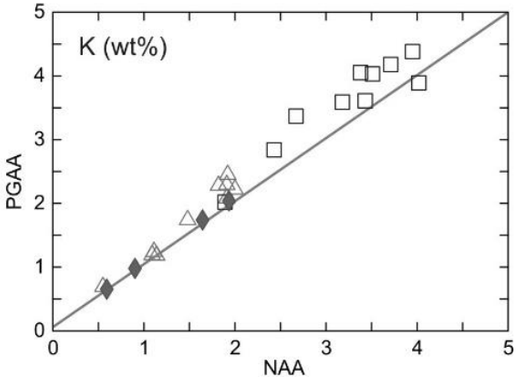
K (wt%)
PGAA
NAA

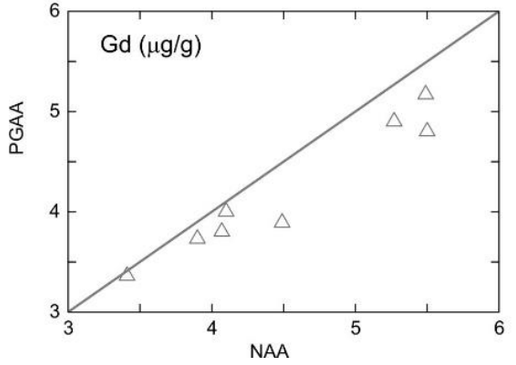
Gd (μg/g)
PGAA
NAA

Validation – geological standards

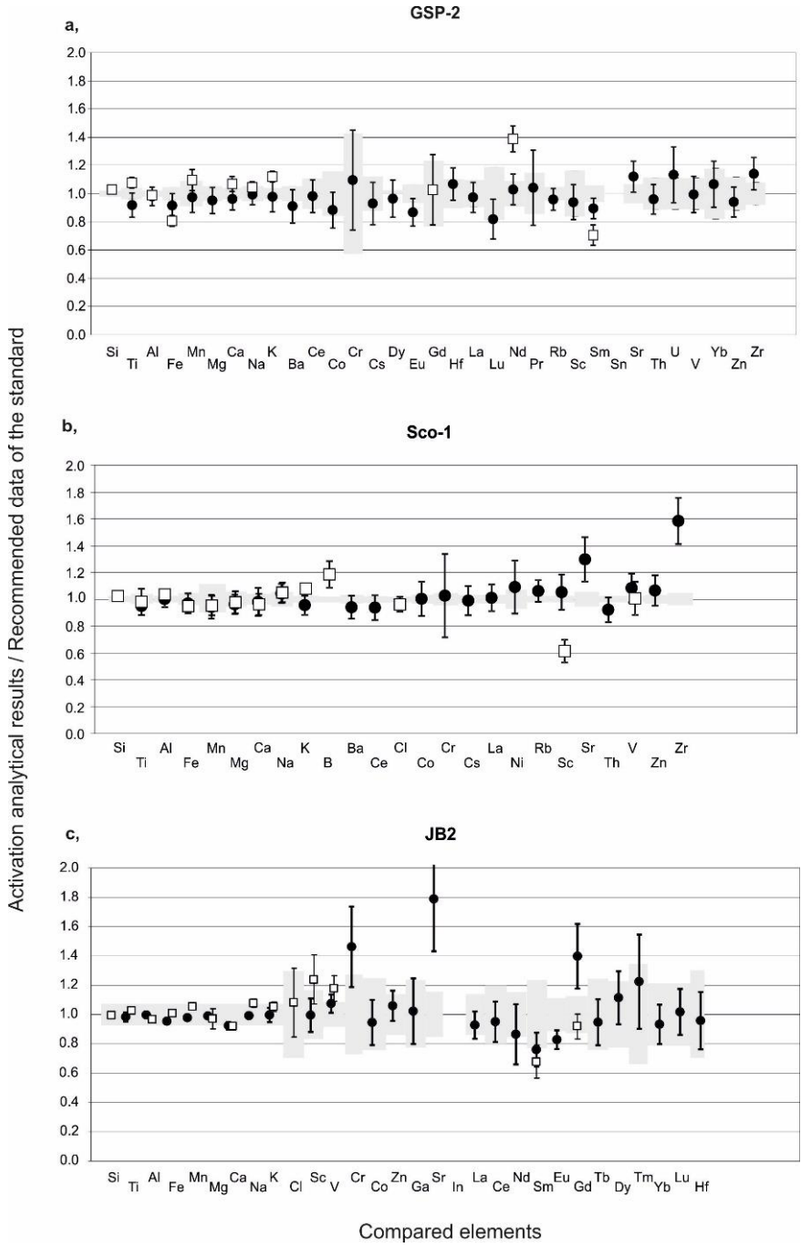

PGAA (empty squares)

NAA (black dots)

Budapest Neutron Centre
Centre for Energy Research

Special or combined techniques

Position-sensitive measurements by scanning

Radiography-driven PGAA

In-situ PGAA

BNC
Budapest Neutron Centre

BUDAPEST
RESEARCH
REACTOR
1959 2019
60 YEARS
OF RESEARCH
& INNOVATION

Position-sensitive PGAA:

- Tomographic principle (PGI, PGA-CT, NT)
  - Detecting integrated information along the path of the neutrons, repeating this at several points and angles
  - Mathematical reconstruction is needed
  - The whole sample has to be measured

- Isovolume approach (PGAI)
  - Collimation: the source of analytical information is the so-called isovolume
  - Scanning the sample, recording localized data
  - Signal vs. position instantly gives the raw result
  - Pointwise correction for neutron self shielding and gamma self attenuation is required (Monte Carlo)
  - Measurement of the whole sample is not a must

The isovolume concept

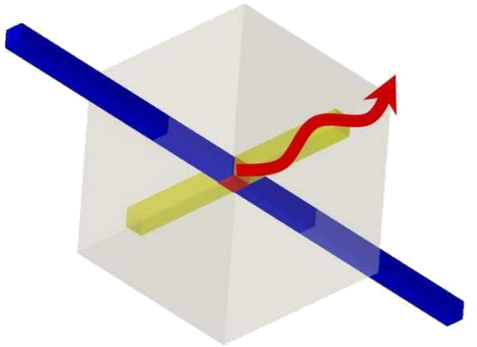

a) Isovolume geometry:
Gamma collimator size < Sample thickness

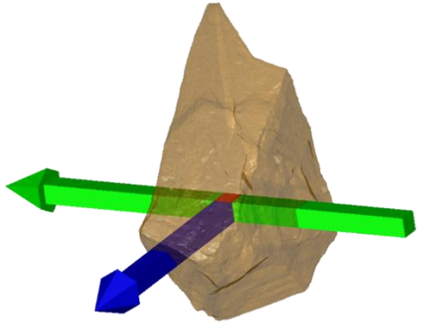

b) Chord geometry:
Gamma collimator size > Sample thickness

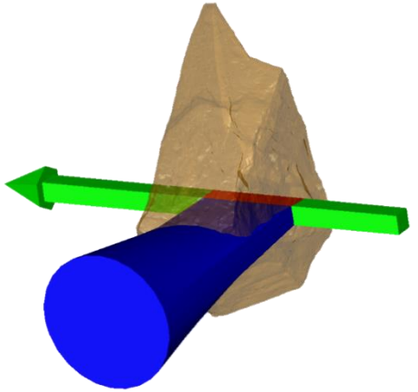

Direct elemental imaging with PGAI

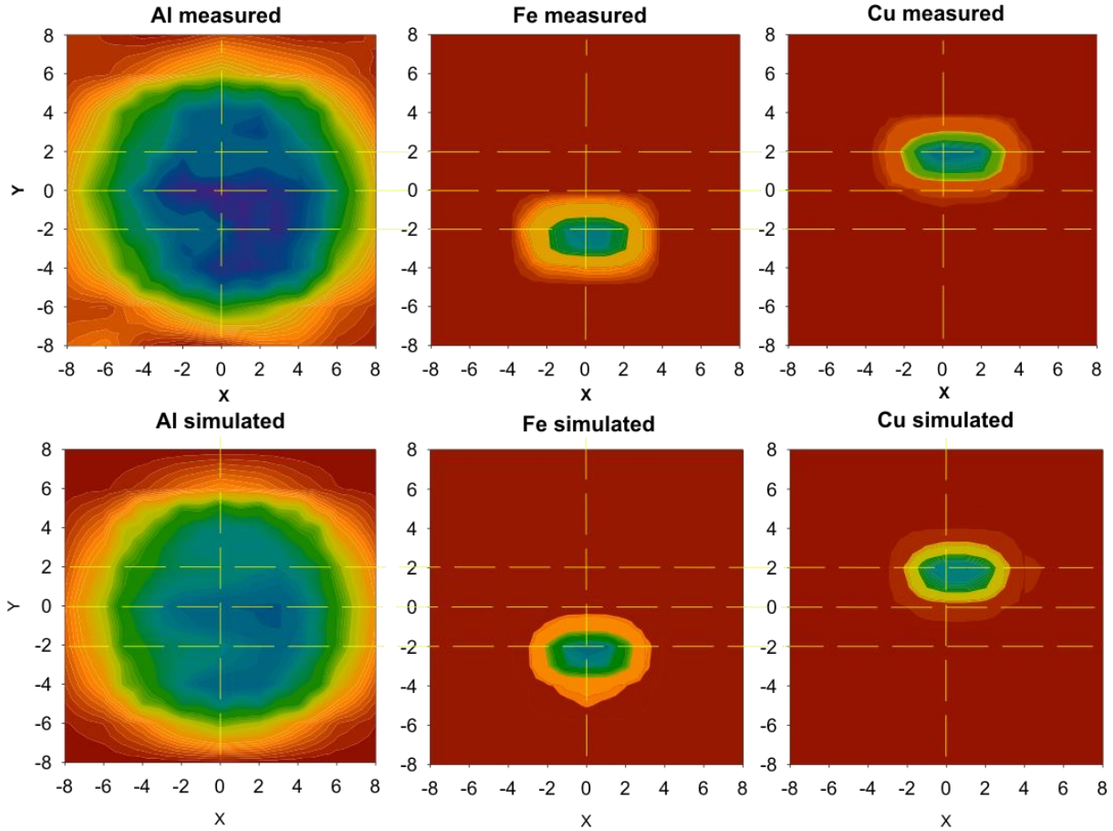

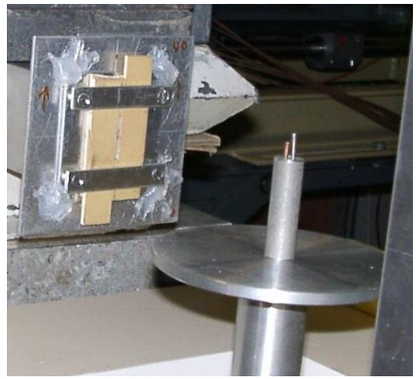

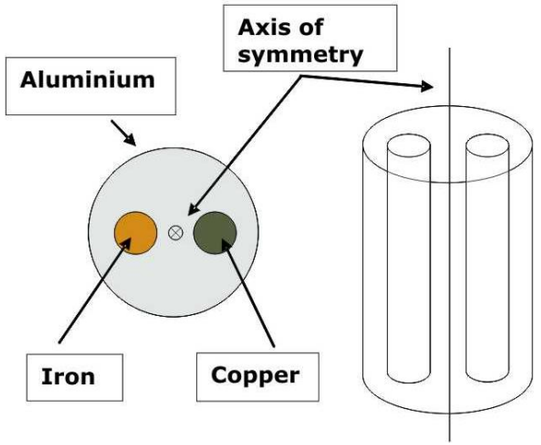

- Systematic scanning of the sample
- 2500 s acq. time per point (altogether 5 days!)

Z. Kis, T. Belgya and L. Szentmiklósi, Monte Carlo simulations towards semi-quantitative prompt gamma activation imaging, *Nucl. Instruments Methods A.*, 2011, **638**, 143–146.

Applied Radiation and Isotopes 67 (2009) 2070–2074

Contents lists available at ScienceDirect

Applied Radiation and Isotopes

journal homepage: www.elsevier.com/locate/apradiso

PGAA, PGAI and NT with cold neutrons: Test measurement on a meteorite sample

Lea Canella [a,*], Petra Kudějová [a,b], Ralf Schulze [b], Andreas Türler [a], Jan Jolie [b]

[a] Technische Universität München, Institut für Radiochemie, Lichtenbergstr. 1, 85748 Garching, Germany
[b] Universität zu Köln, Institut für Kernphysik, 50937 Köln, Germany

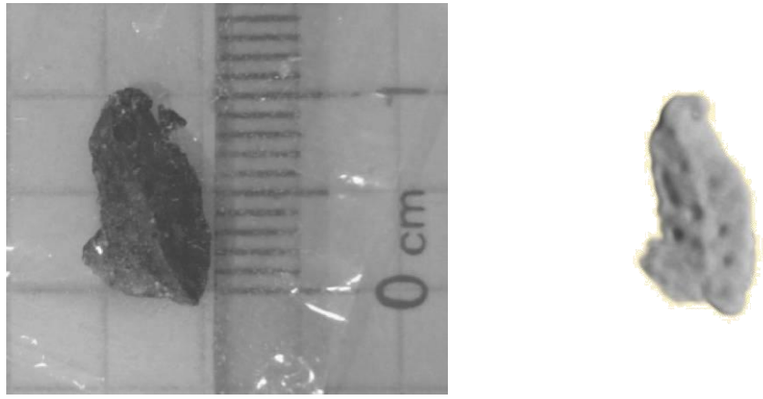

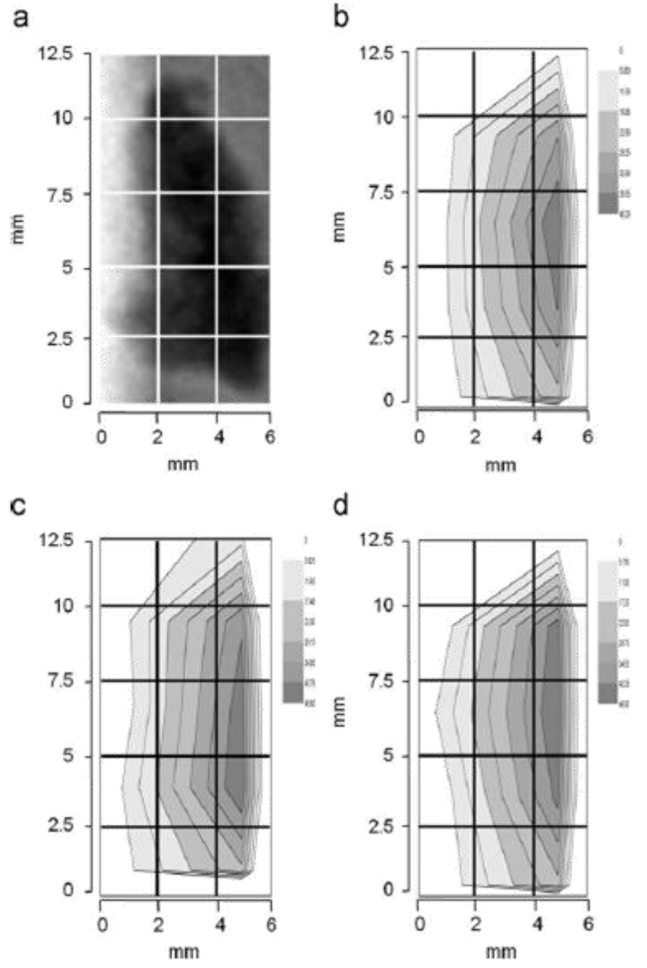

Fig. 4. 2D distribution of the main elements Fe, Si and Mg obtained with PGAI. (a) Radiography of Allende meteorite. (b) Si 2D distribution. (c) Fe 2D distribution. (d) Mg 2D distribution.

3D Elemental maps of a fibula

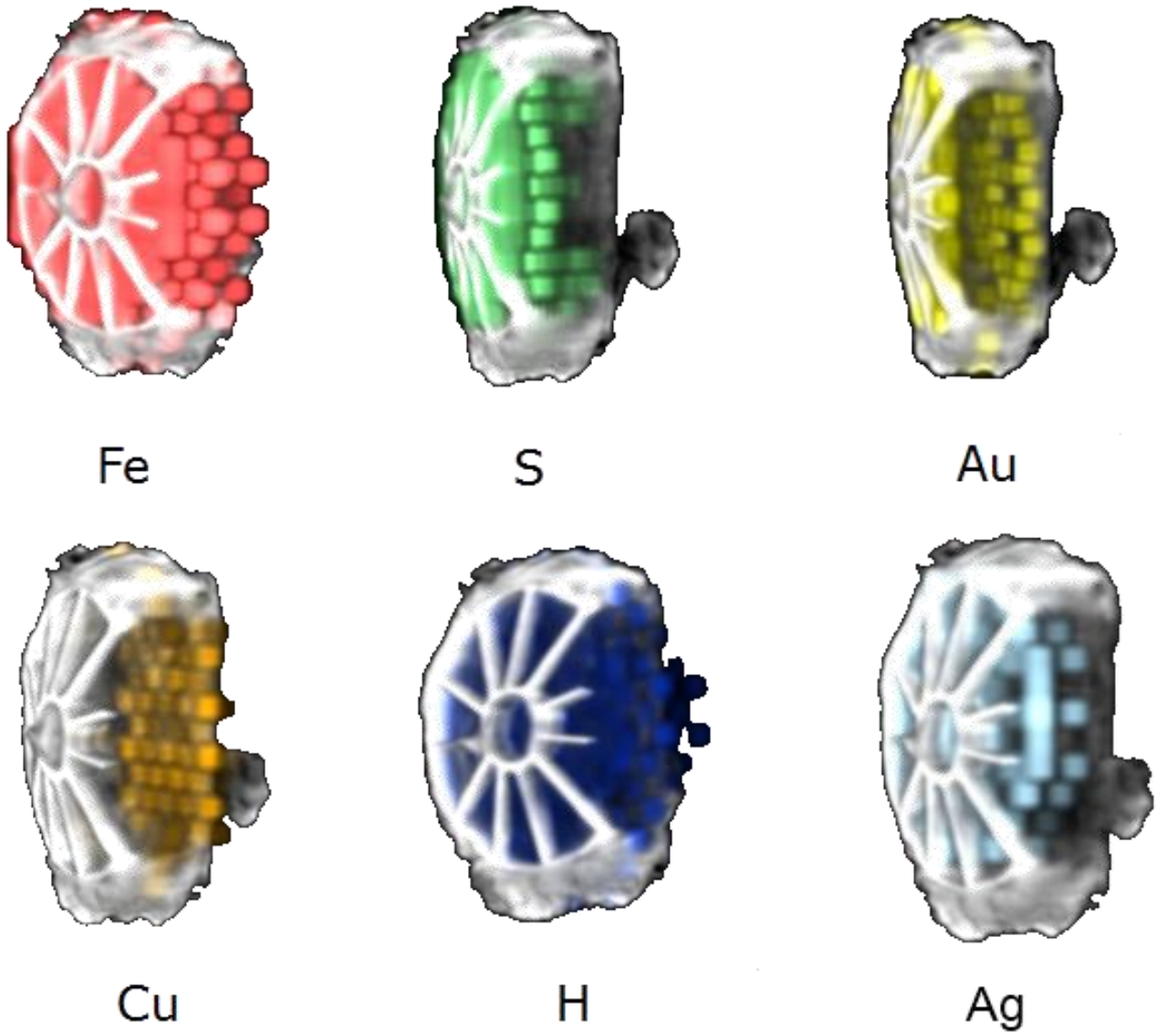

R. Schulze, L. Szentmiklósi, P. Kudejova, L. Canella, Z. Kis, T. Belgya, J. Jolie, M. Ebert, T. Materna, K. T. Biró and Z. Hajnal, The ANCIENT CHARM project at FRM II: Three-dimensional elemental mapping by prompt gamma activation imaging and neutron tomography, *J. Anal. At. Spectrom.*, 2013, **28**, 1508–1512.

Radiography/Tomography-driven PGAI (PGAI-NR, PGAI-NT)

- PGAI (prompt-gamma activation imaging)
  - 3D PGAA, pointwise scanning, 2-3 mm resolution at best
  - Collimate the neutron beam and the gamma detection,
  - Requires high flux, very time consuming

- Neutron Radiography/Tomography
  - Good spatial resolution
  - Fast
  - Needs a beam with low divergence

- Radiography/Tomography-driven PGAI
  - Most real objects are made of some distinct, by themself homogeneous parts
  - Visualize and locate the interesting regions first, prompt-γ measurement only where it is needed for the conclusive result
  - Often no need for mm-resolution
  - Can save substantial beam time
  - Requires 3D coordinate transfer and good repositioning of the object

The operation of a PGAI-NR(NT) setup

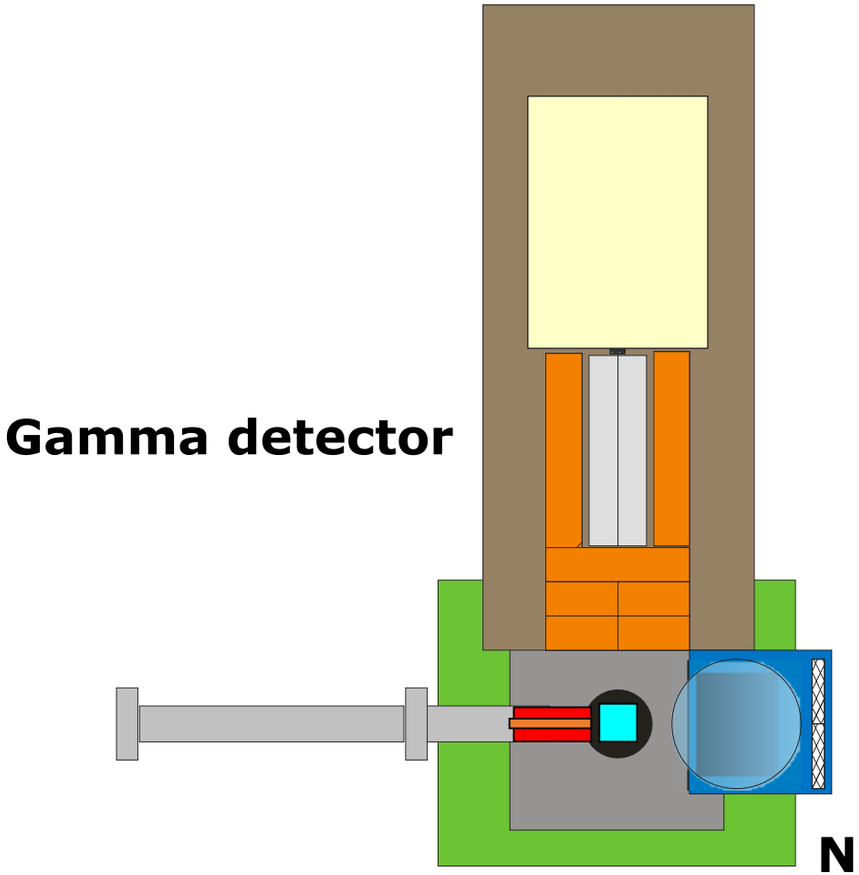

NORMA –a configuration of NIPS for imaging

NORMA: neutron optics and radiography for material analysis

- *Sample chamber (A)—Al house lined with ^{6}Li-polymer sheets :*
- AlMgSi0.5 alloy →less neutron activation
- inner volume: 20×20×20 cm^{3} →larger objects
- removable side panels →easy handling

- *Sample stage (B)—xyzω movements :*
- maximum load: 5 kg
- travel distance: 200 mm

- *Imaging system (C)—CCD-based neutron imaging :*
- 100 µm thick ^{6}Li/ZnS scintillator (green light)
- silver-free quartz mirror
- ANDOR iKon-M CCD camera (cooled, 16bit, 1024×1024 px)

- *Gamma detection (D)—Compton-suppressed HPGe detector :*
- Canberra GR2318/S HPGe detector + Bismuth Germanate (BGO) scintillator
- Canberra DSP–2060 digital signal processor
- 10-cm lead shielding with exchangeable collimators

- *Data acquisition—Integrated control software :*
- sample stage, gamma spectrometer and camera

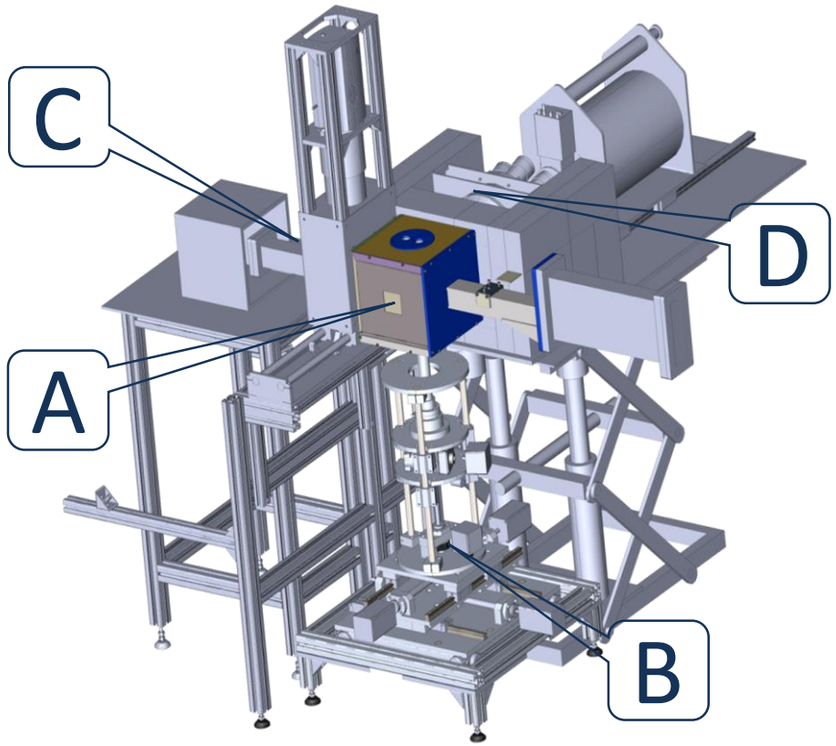

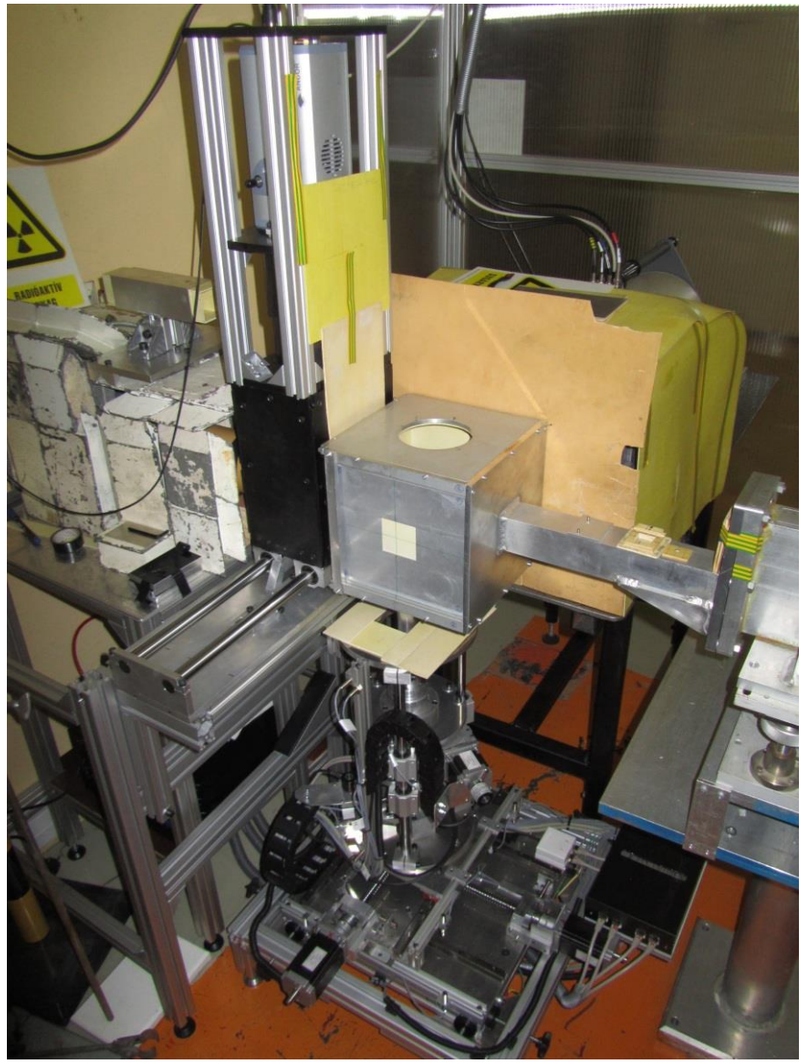

First permanent PGAI-NT facility in the world !
Startup in 2012

Centre for Energy Research

Custom-made sample holders

Gentle sample holders (a combination of Al motorized sample stage with ABS polymer for contact areas off neutron beam) for precious artifacts by additive manufacturing (a.k.a. 3D printing).

a) Photograph of a bronze casted spearhead.

b) photorealistic STL digital model.

c) 3D AM copy of the object.

d) CAD concept and the

(e-f) realization of a custom sample interlock coupling the sample and the standard sample stage of the NIPS-NORMA station at BNC

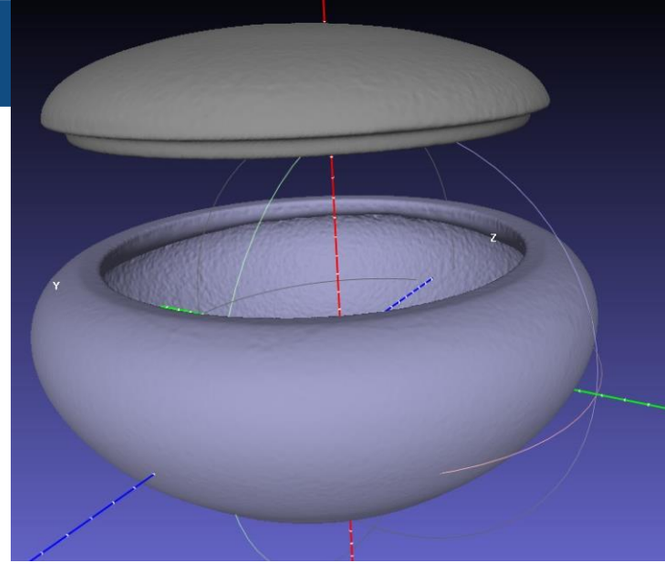

L. Szentmiklósi et al., Use of 3D mesh geometries and additive manufacturing in neutron beam experiments, J. Radioanal. Nucl. Chem. (2019) 320:451–457

Visualization of the results

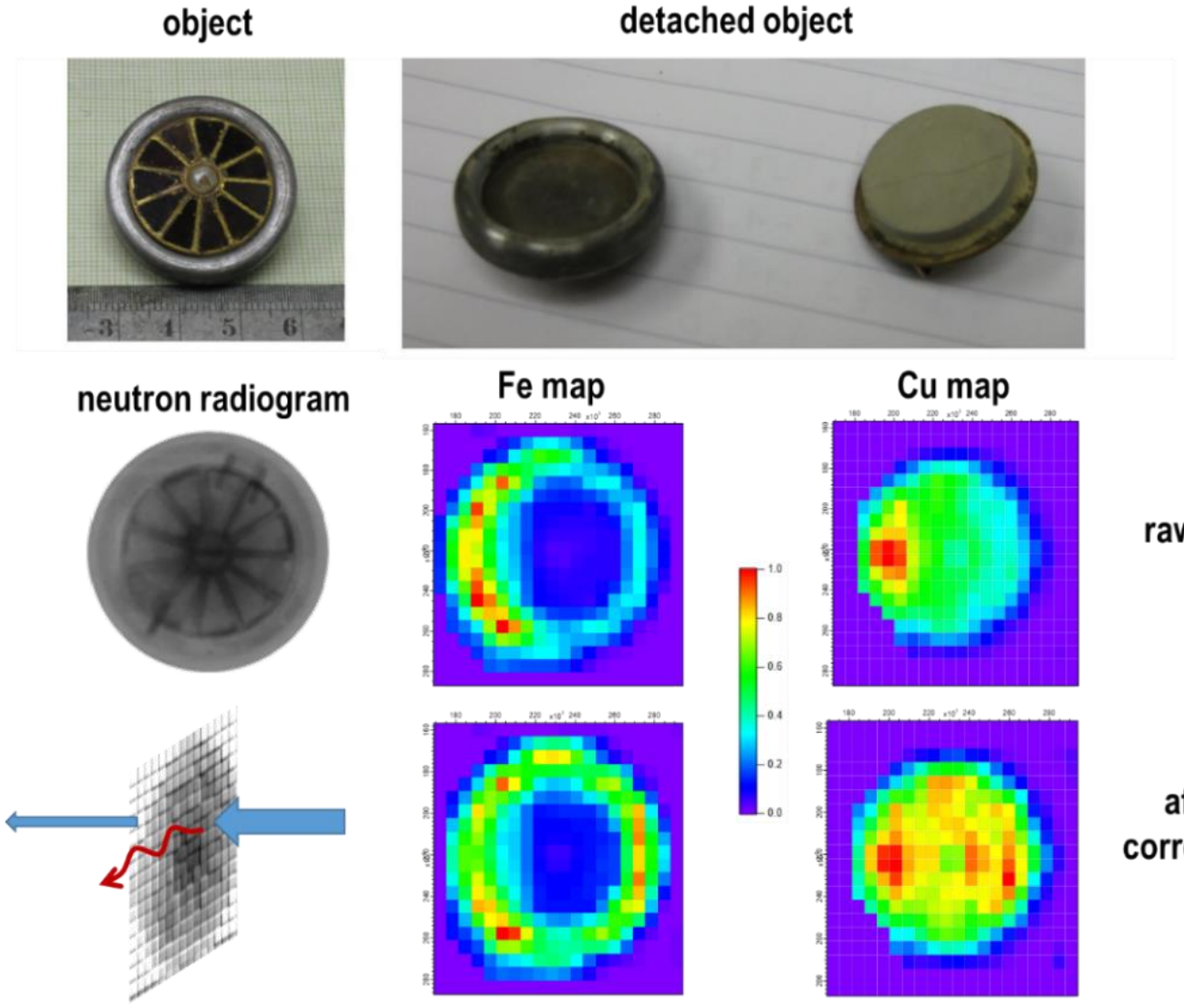

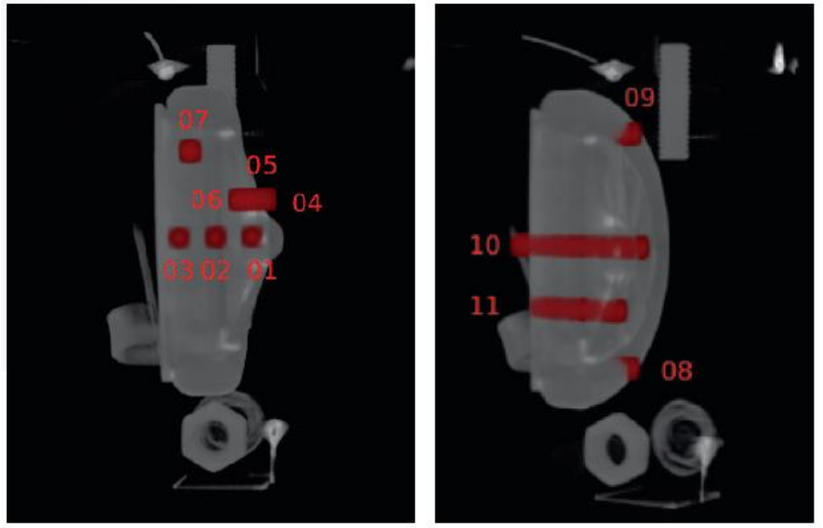

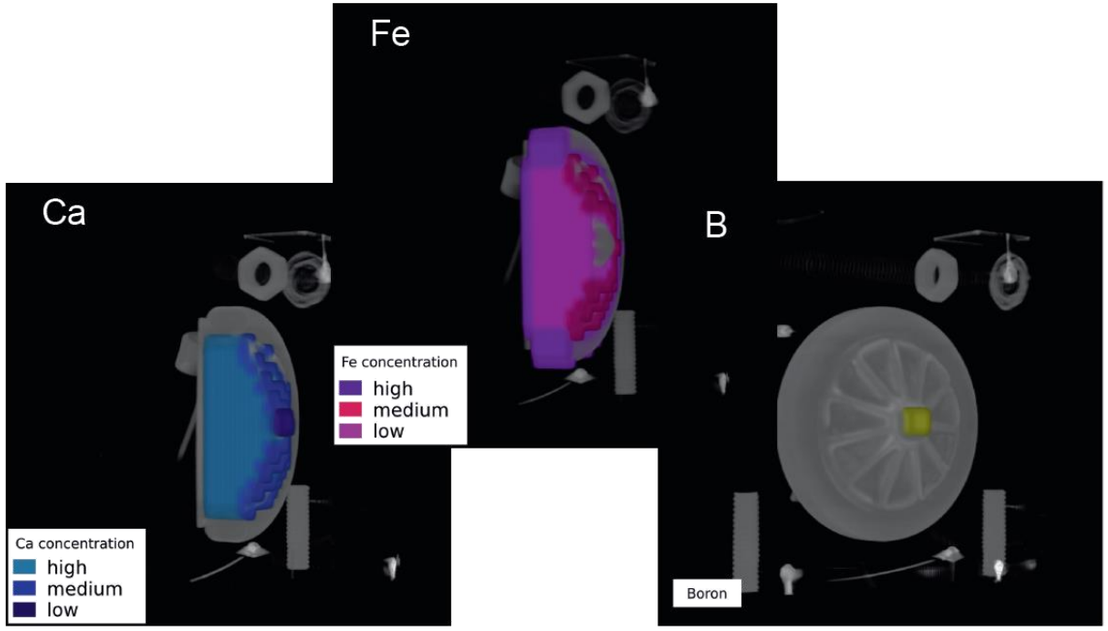

Note the difference in spatial resolution

3D element maps and NT data are visualized together

Scanning the ^{10}B surface-density profile for

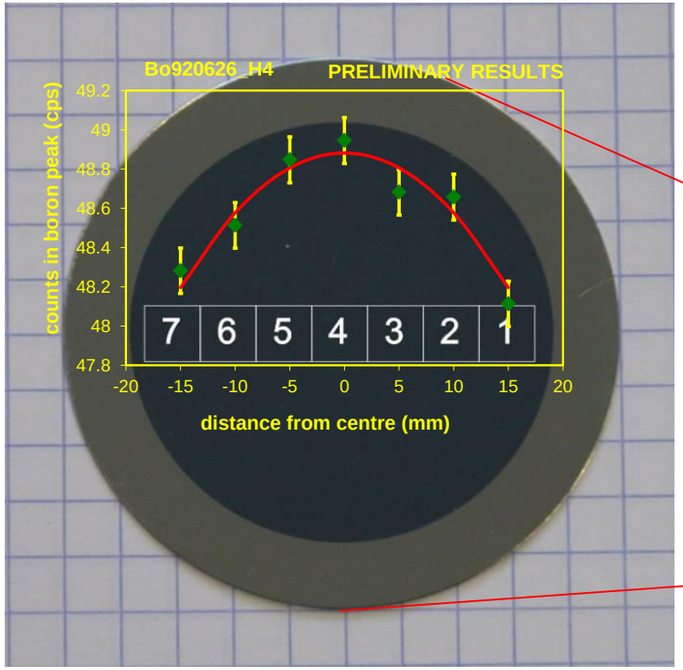

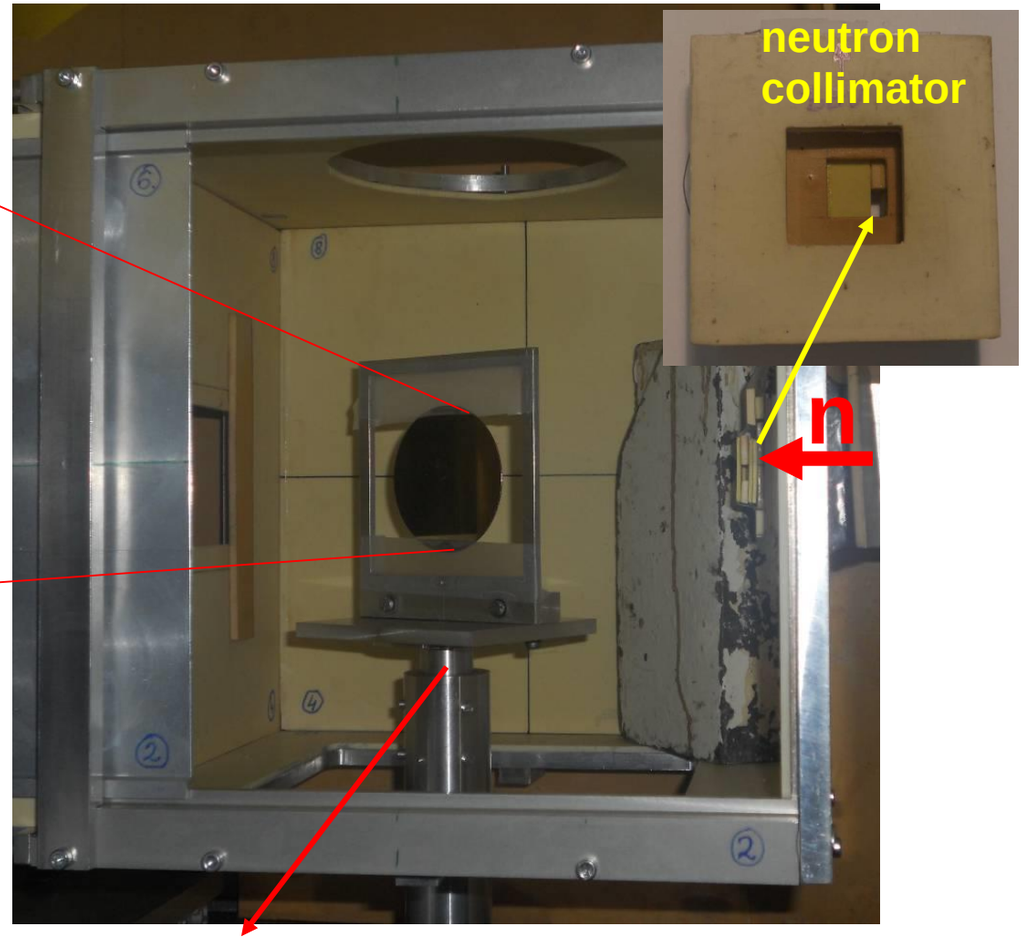

- ^{10}B IRMM sample, 30 µg/cm^2
- ϕ 38mm spot
- ϕ 50mm SS backing
- sample at 30° to beam axis
- 2.5 × 5 mm^2 collimation
  (5 × 5 mm^2 projection on sample)

Sample support + motorized stage

Direct element profiling by PGAI

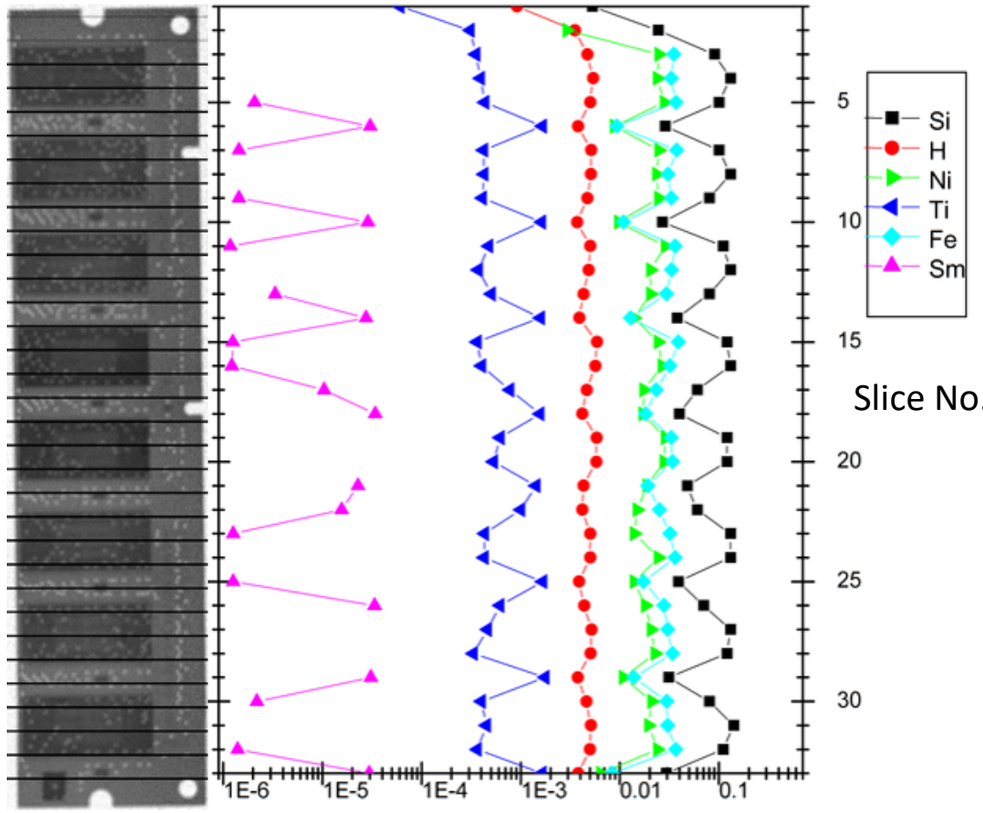

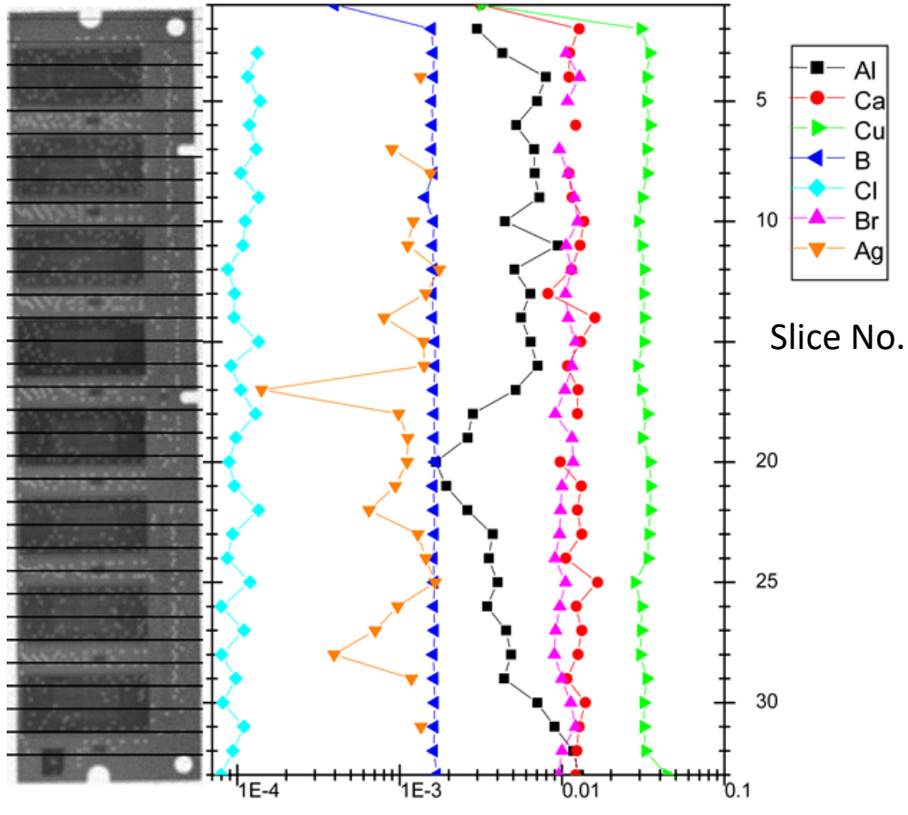

Linear scan of a stepper motor

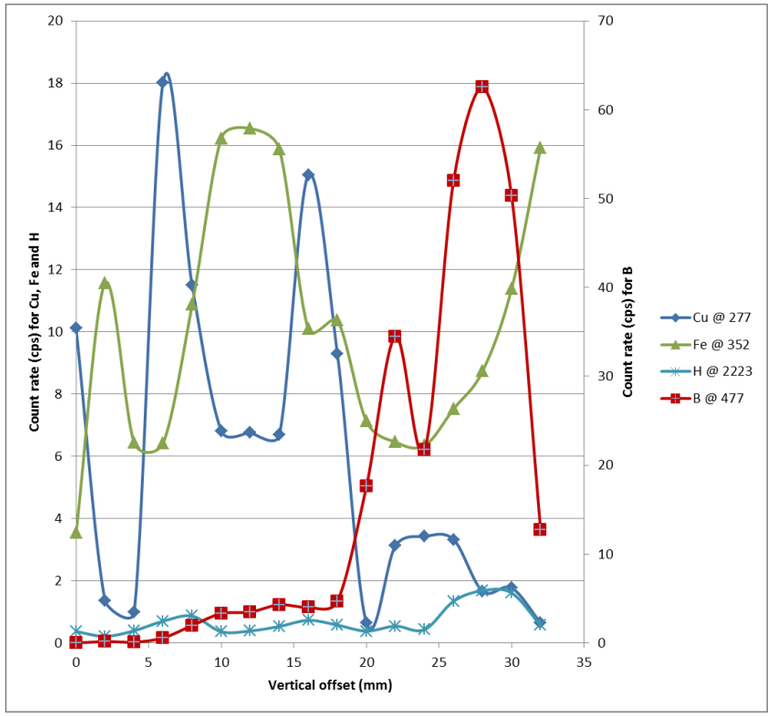

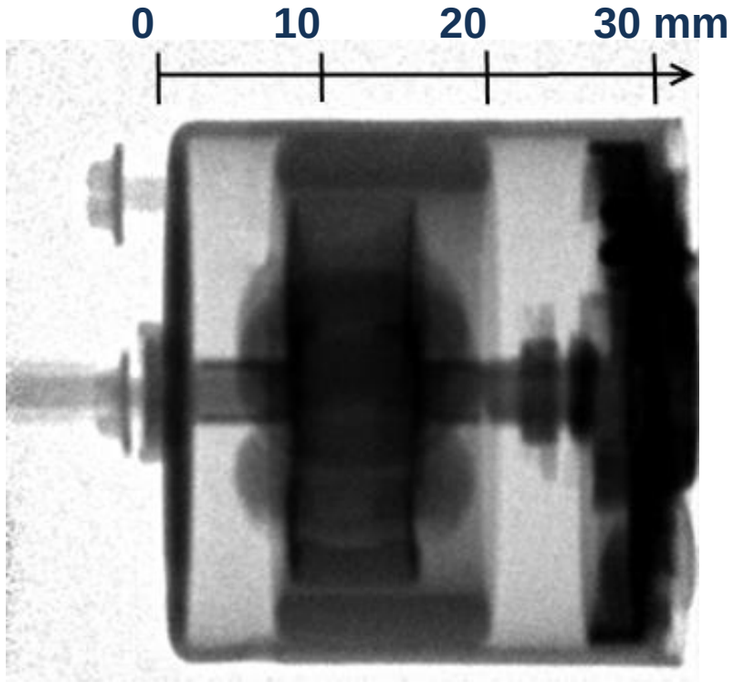

Quantitative Analysis and Distribution of

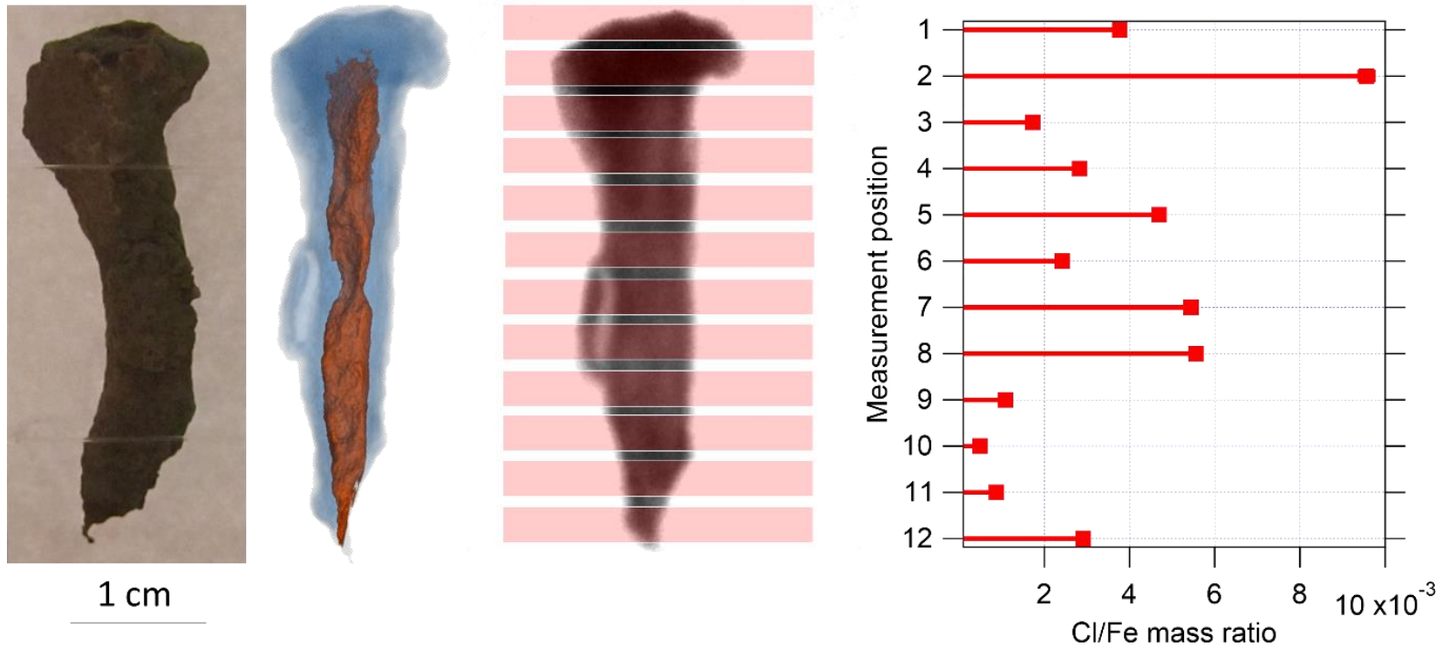

The photo (taken from a different viewpoint), the segmented 3D neutron tomogram (orange: metallic iron, blue: corroded regions), and the pointwise Cl/Fe mass fractions of a corroded iron nail from PGAI

Watkinson et al, Archaeometry (56) 2014 841–859

Scanning of Damaged reactor fuel element

- Hydrogen content profiling in E110G Zr fuel cladding of VVR-440 nuclear power reactors, following a simulated LOCA event
- PGAA is a direct way to quantify H, unlike the neutron imaging used so far: 100-1800 ppm

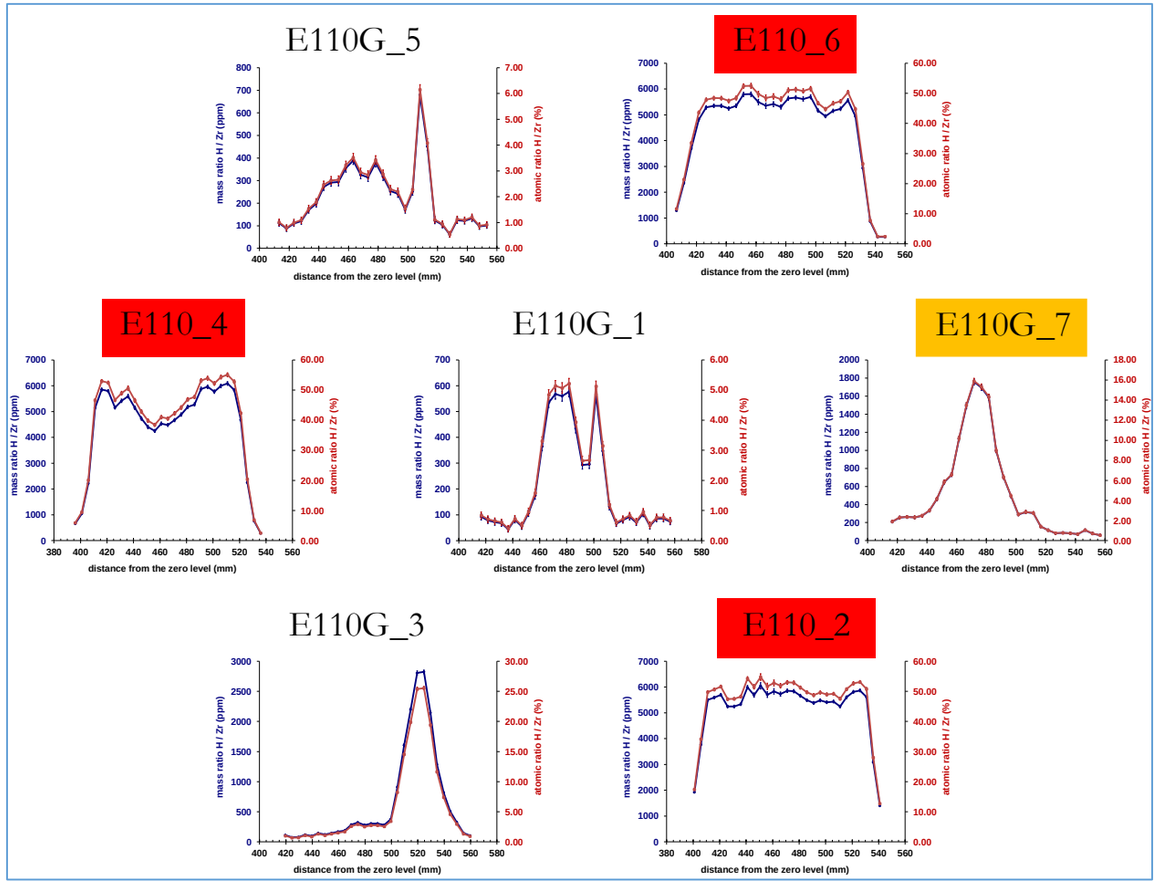

Zoltán Kis et al: Lokális hidrogéntartalom mérése roncsolásmentes neutronos módszerekkel cirkónium fűtőelemburkolatok hossztengelye mentén, Nukleon 2019. december XII. (2019) 223 (in Hungarian)

Non-destructive analysis of sea urchin (*Parascutella*

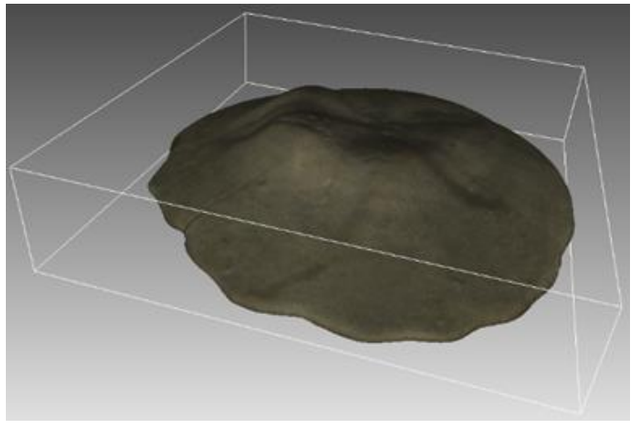

3D rendered textured mesh model with the aligned bounding box for characteristic linear dimension analysis

Boglárka Maróti, Bálint Polonkai, Veronika Szilágyi, Zoltán Kis, Zsolt Kasztovszky, László Szentmiklósi, Balázs Székely:

Joint application of structured-light optical scanning, neutron tomography and position-sensitive prompt gamma activation analysis for the non-destructive structural and compositional characterization of fossil echinoids,

NDT&E International 115 (2020) 102295 DOI: 10.1016/j.ndteint.2020.102295

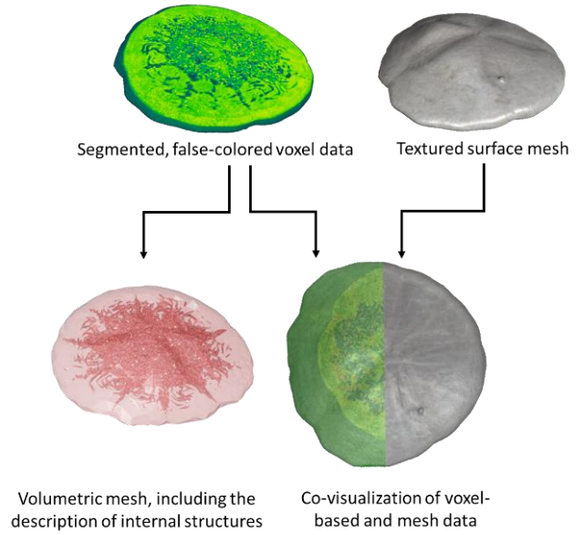

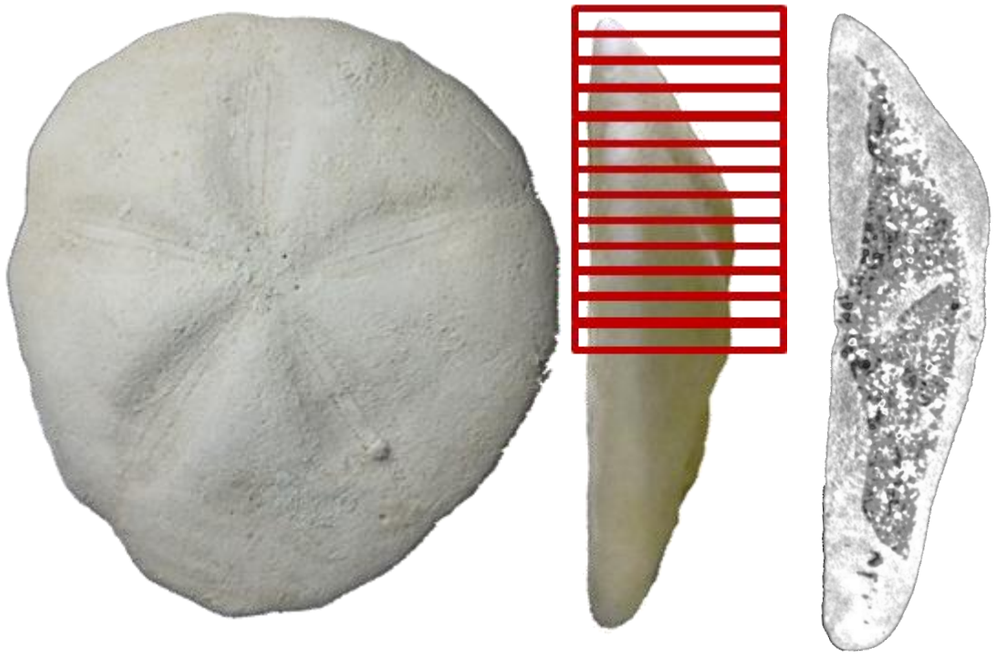

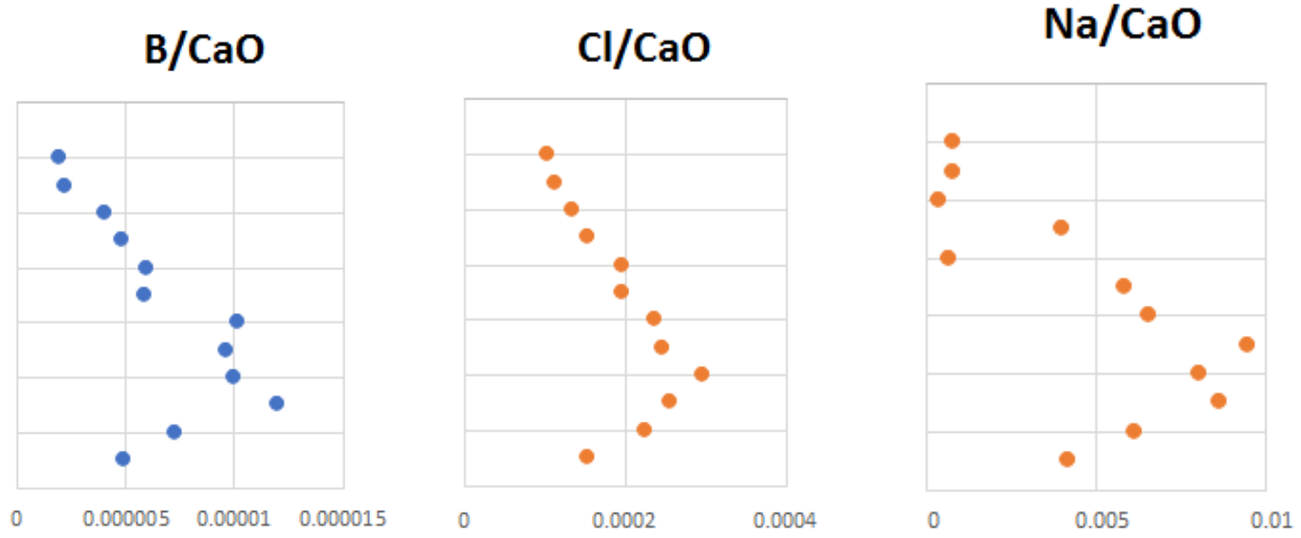

Element profiling along a radius of the sea urchins

PGAI-NR of items in a sealed Pb container

Components of the benchmark sample:

Cu balls

Aluminum cylinder

Uranium oxide (U_3O_8)

Iron skrew

…in a Lead container

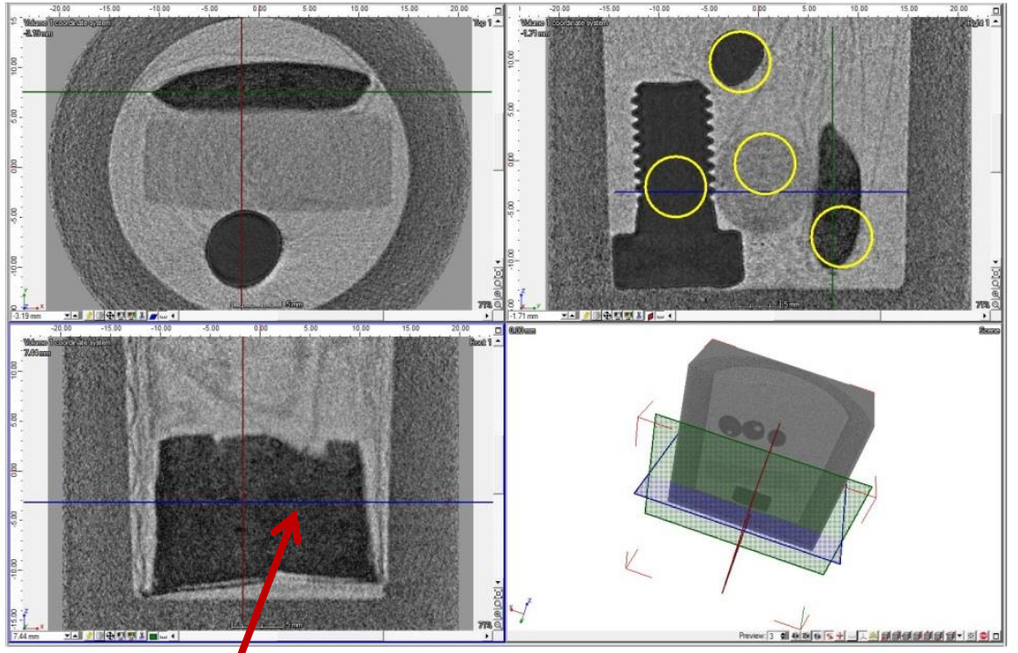

Uranium-containing material in a FEP bag

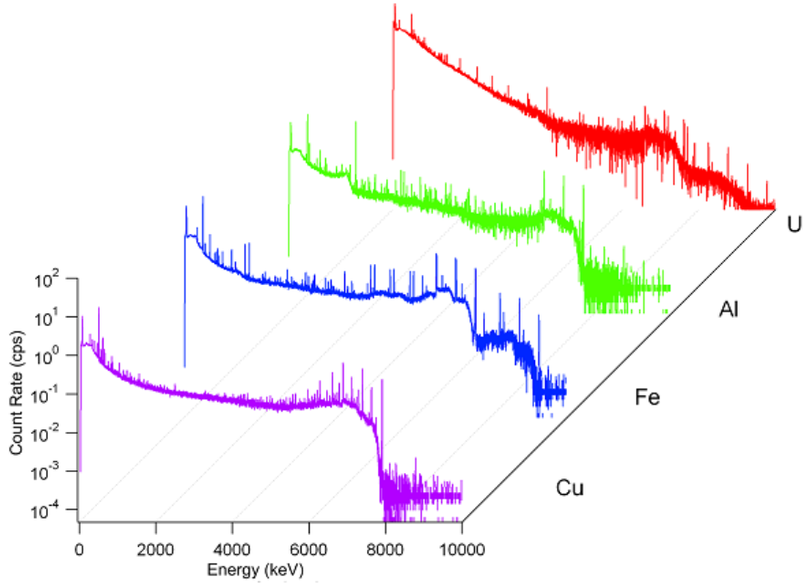

L. Szentmiklósi et al, Anal. Methods 2015 (7) 3157

Centre for Energy Research

What is in the pottery? Herbs for the afterlife

Budapest Neutron Centre

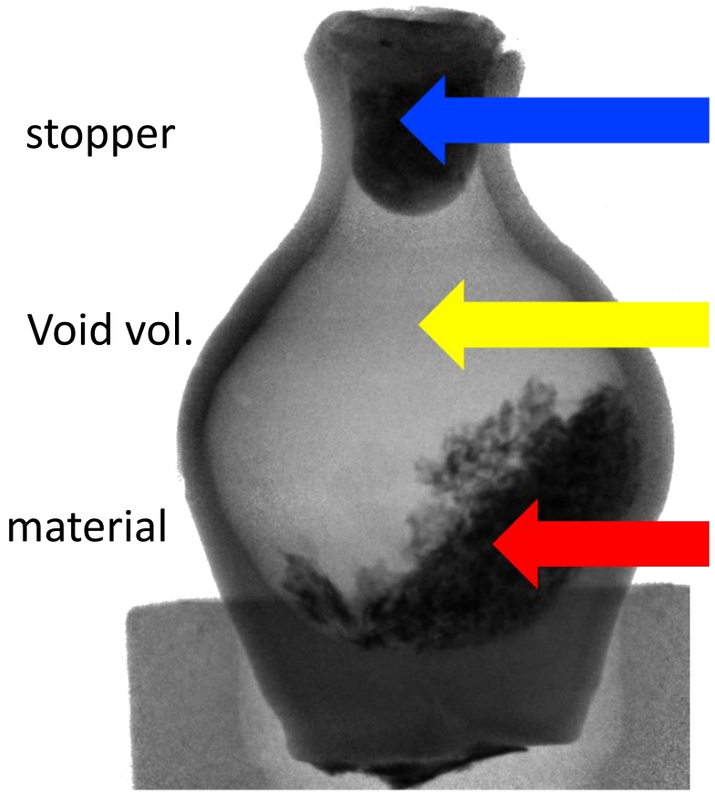

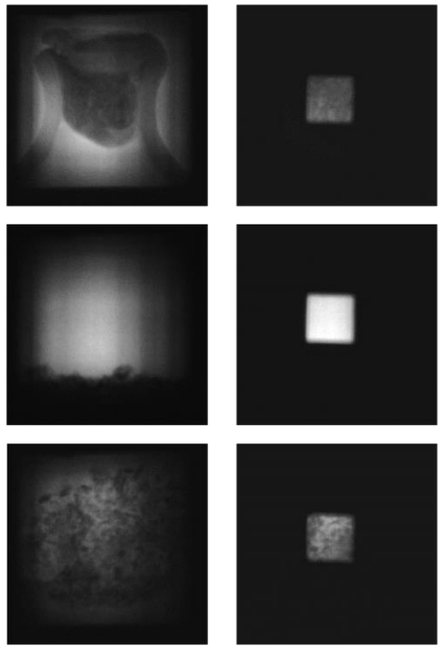

Full beam

10×10 mm² beam for PGAI

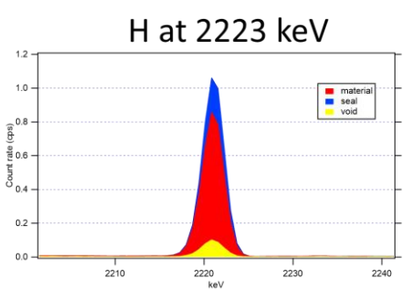

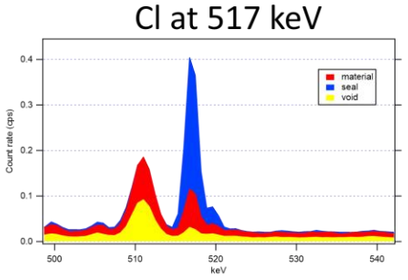

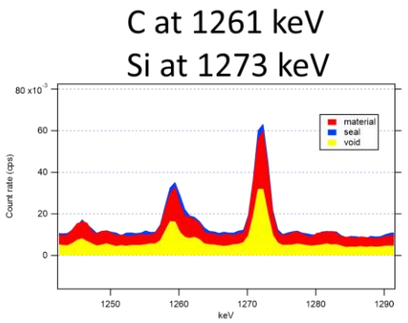

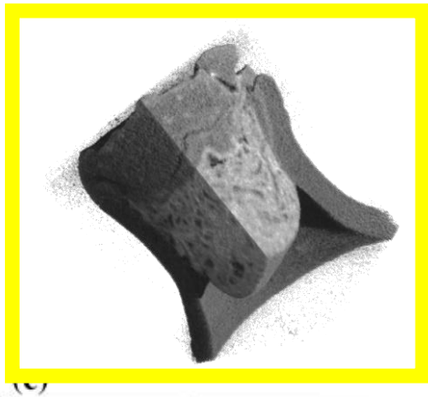

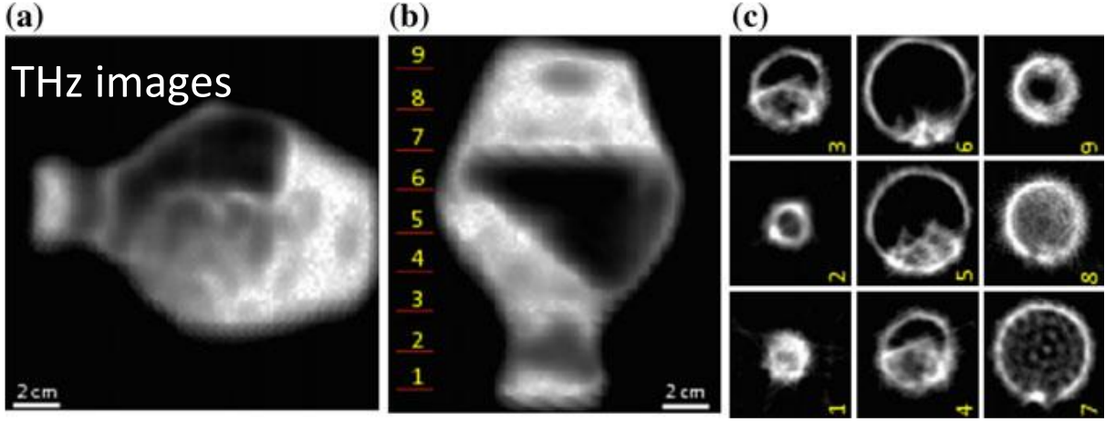

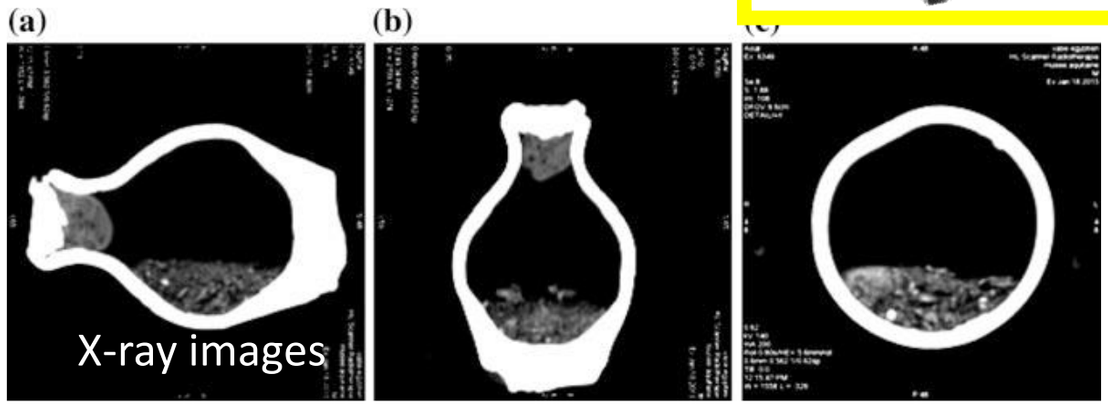

Setup for in-situ PGAA

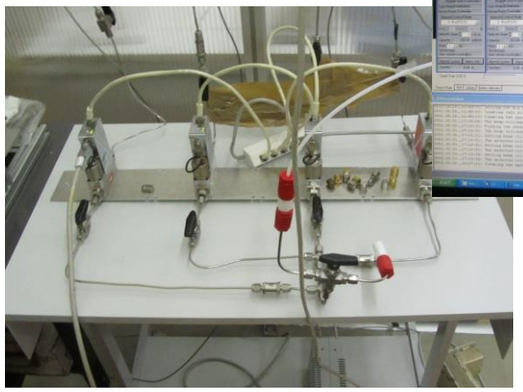

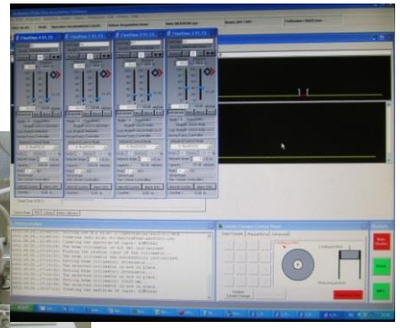

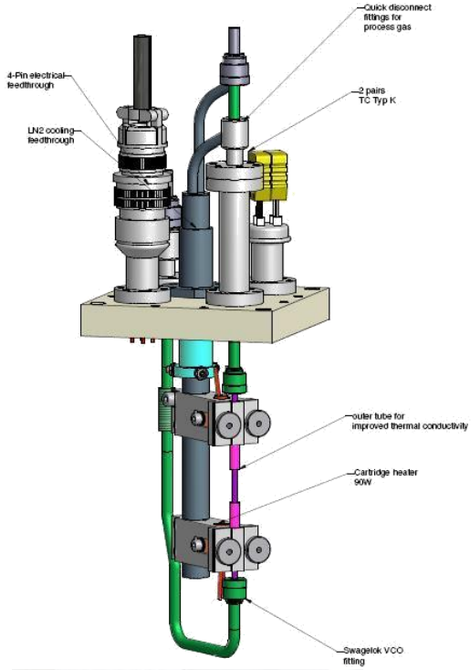

Zs. Révay et al., *Anal. Chem.* 2008, *80*, 6066.

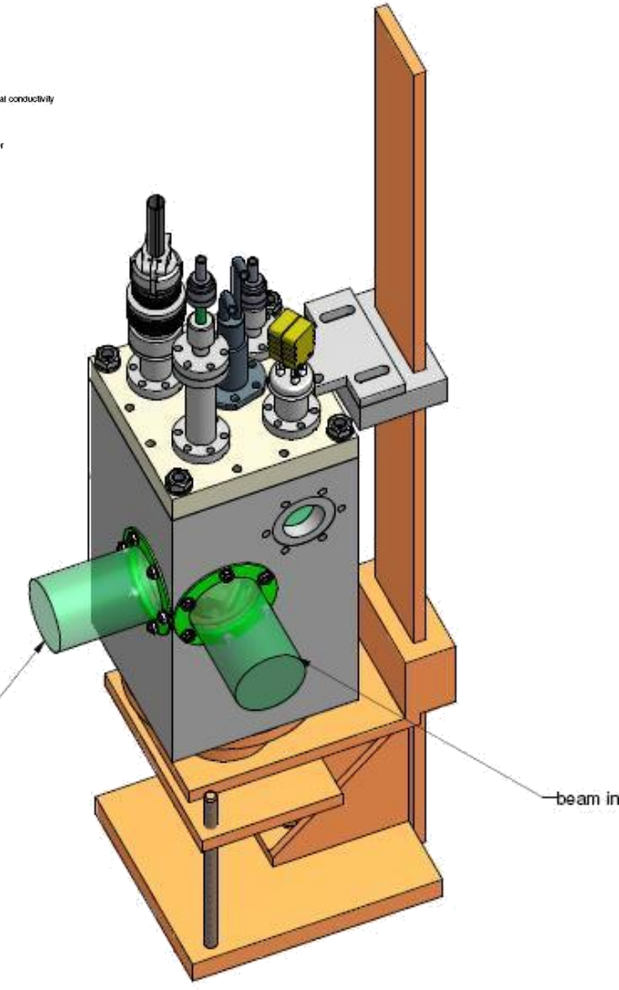

PGAA spectrum of the catalytic reactor

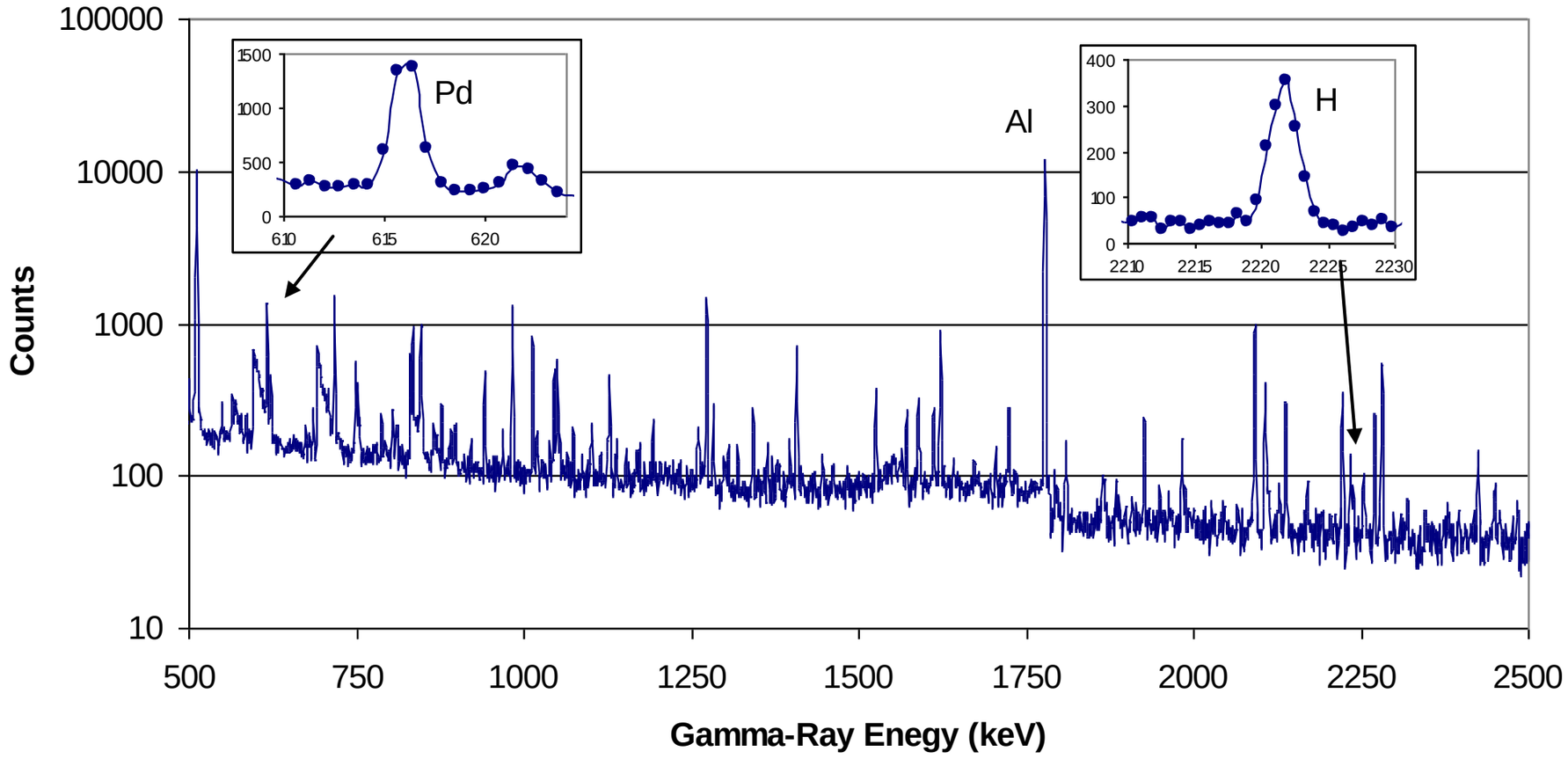

To reveal reaction mechanisms

Selective hydrogenation on Pd

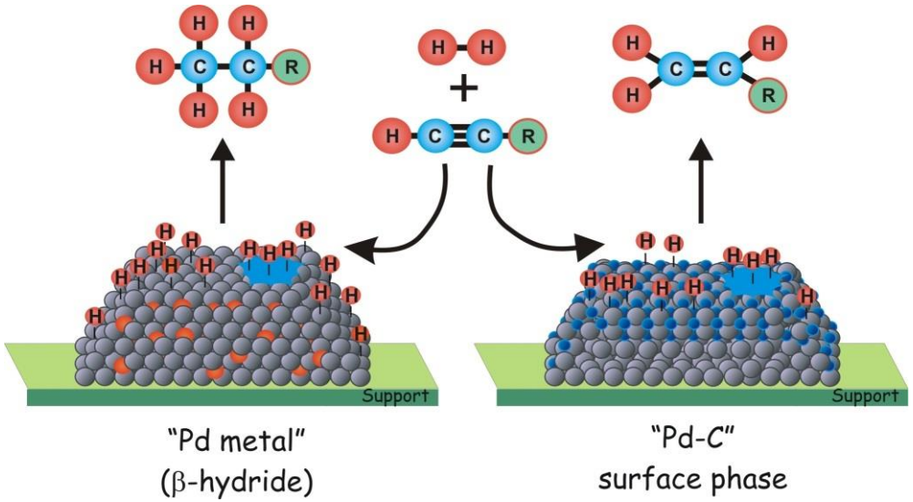

Deacon-reaction (recovery of waste HCl -> Cl_2)

$HCl+O^*+^* \leftrightarrow OH^*+Cl^*$ (1)

$OH^*+OH^* \leftrightarrow H_2O^*+O^*$ (2)

$H_2O^* \leftrightarrow H_2O+^*$ (3)

$Cl^*+Cl^* \leftrightarrow Cl_2+2^*$ (4)

$O_2+2^* \leftrightarrow O_2{}^{**}$ (5)

$O_2{}^{**} \leftrightarrow 2O^*$ (6)

On RuO_2 or CeO_2 catalyst

PGAA in space (orbit around planet Mars)

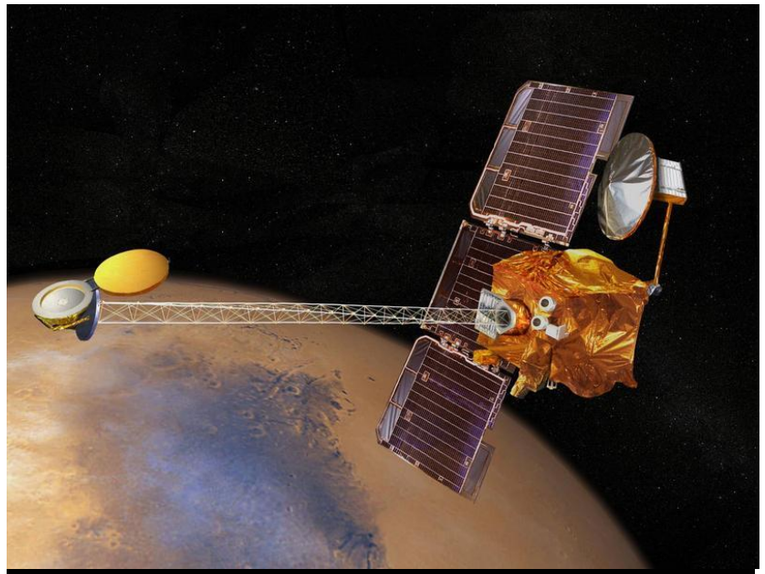

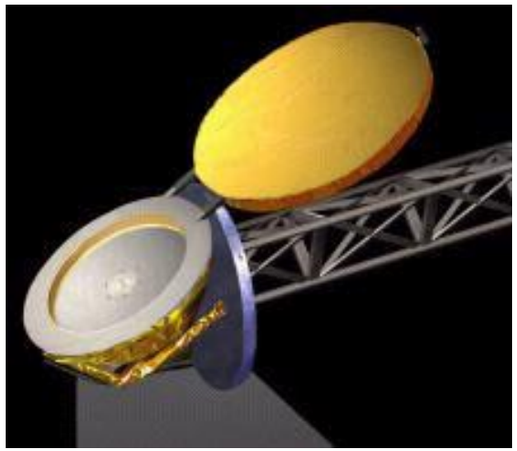

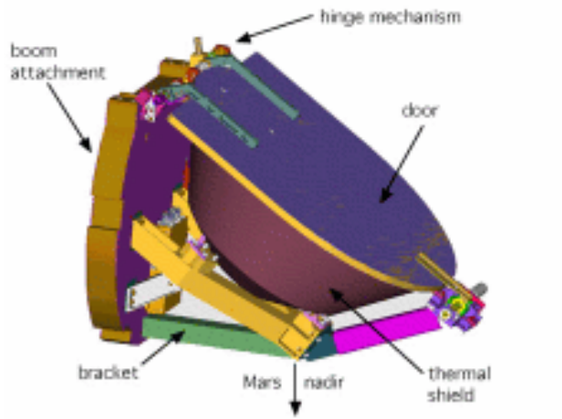

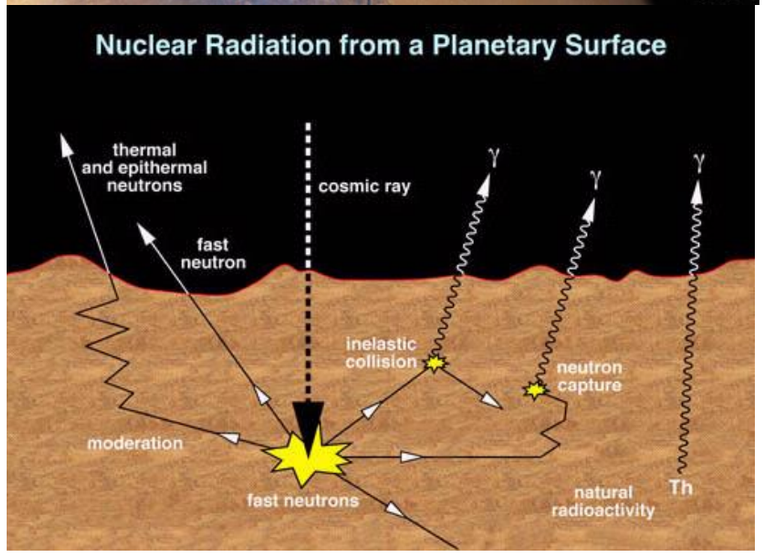

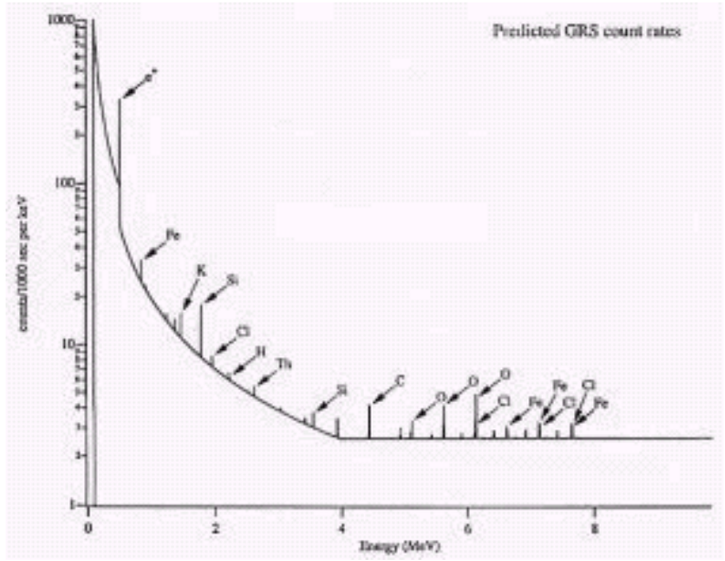

Budapest Neutron Centre
Centre for Energy Research

Monte-Carlo calculations

BNC
Budapest Neutron Centre

BUDAPEST
RESEARCH
REACTOR
1959
2019
60 YEARS
OF RESEARCH
& INNOVATION

Monte Carlo simulations – overview

Determination of quantities by computer simulation, using models of the physical processes and random numbers

Inputs:

- Geometry of the HPGe detector, BGO Compton suppressor, sample chamber neutron and gamma shielding
  - Engineering drawings, optimization of unspecified dimensions, e.g. the dead layer thickness
  - Szentmiklósi, L.; Berlizov, A. N. Characterization of the Budapest Prompt-Gamma Spectrometer by Monte Carlo Simulations. Nucl. Instruments Methods A 2009, 612 (1), 122–126. DOI 10.1016/j.nima.2009.09.127.
  - Szentmiklósi, L.; Kis, Z.; Belgya, T.; Berlizov, A. N. On the Design and Installation of a Compton–Suppressed HPGe Spectrometer at the Budapest Neutron-Induced Prompt Gamma Spectroscopy (NIPS) Facility. J. Radioanal. Nucl. Chem. 2013, 298 (3), 1605–1611. DOI 10.1007/s10967-013-2555-2.
- Detailed geometry of the sample
  - Analytic definition, assembled from elementary planes, objects using inside/outside, union/intersection operations
  - Complicated cases - surface optical scanning or volumetric imaging
  - Voxelization of the sample geometry, material assignation to unit voxels (inspired by dose simulations in medical physics, e.g. Zubal Phantom)
  - Reproduction of the experimental arrangement, sample placement
- Neutron beam properties
  - T. Belgya, Z. Kis and L. Szentmiklósi, Neutron Flux Characterization of the Cold Beam PGAA-NIPS Facility at the Budapest Research Reactor, Nucl. Data Sheets, 2014, 119, 419–421, DOI: 10.1016/j.nds.2014.08.118
- Nuclear Data
  - Lib80x25: J. Lloyd Conlin, W. Haeck, D. Neudecker, D. Kent Parsons and M. C. White, LA-UR-18–24034: Release of ENDF/B-VIII.0-Based ACE Data Files, Los Alamos, 2018.

Outputs:

- Neutron beam intensity map
- Neutron capture rate map -> Conversion to gamma emission rates
- Gamma self absorption and neutron self shielding factors -> To correct the masses and concentrations

Implementation of the PGAA and NIPS-NORMA detector geometry in MCNP6.2

Engineering drawing -> MCNP input file -> sample -> simulation -> visualization of the results

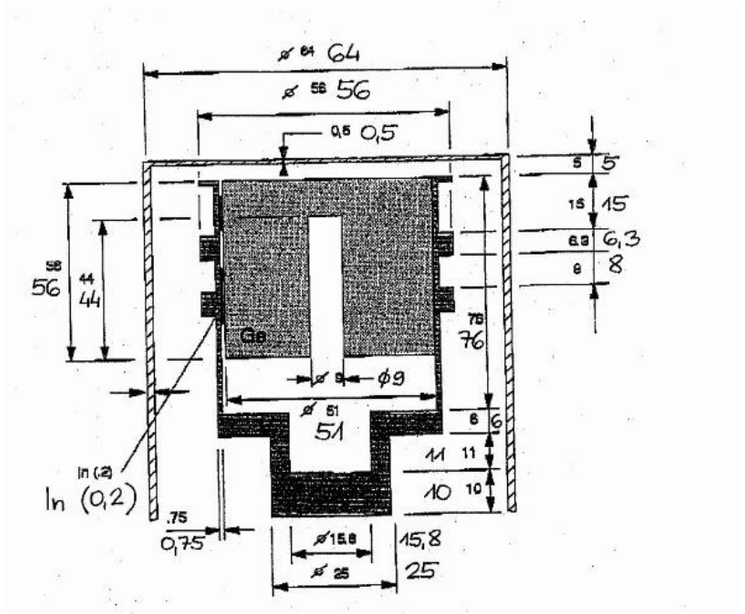

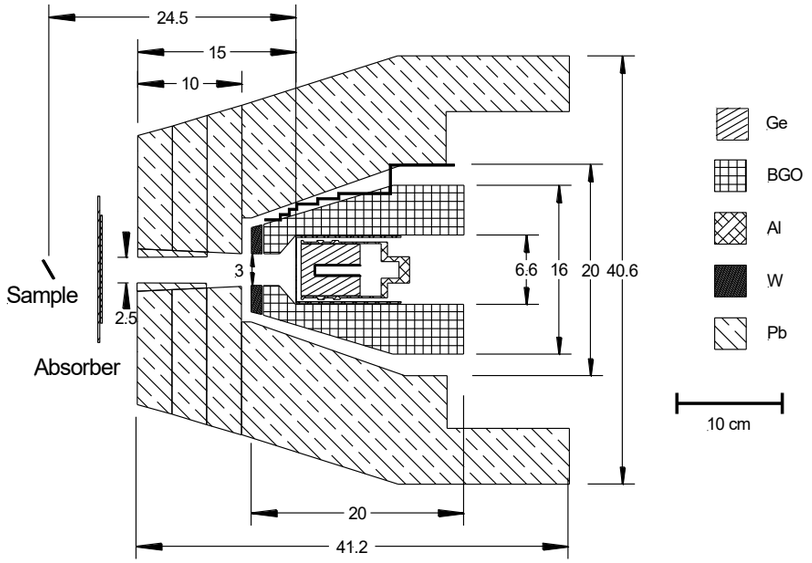

Lister - [d:\MCNPWork\NORMA_metal_sandwich\Rot0\CuZnSn_00.inp]

Fájl Szerkesztés Beállítások Kikódolás Súgó 9 %

```
c ISOCENTER in measurements = (0 -27.3 0)
c ISOCENTER in simulations = (0 -27.3 0)
c detector in measurements: Canberra GR2318/S HPGe + Scionix BGO
c detector in simulations: Canberra GR2318/S HPGe + Scionix BGO
c
c THIS INPUT FILE IS TO CALCULATE:
c the number of the activated XX or YY atoms in the sample irradiated in a
c position shifted and/or rotated around ISOC.
c We need only the number of gammas with specific energies reaching the
c entrance surface of the HPGe detector. Moreover, we need a ratio between
c the number of gammas in the different positions.
c
c
c
c !!!!  TO ACTUALIZE THE SETUP ONE SHOULD CHANGE ONLY THE FOLLOWING CELLS  !!!!
c !!!!      FOR THE SAMPLE ITSELF: CELL NUMBERS STARTING WITH 5XX          !!!!
c !!!!       FOR THE AIR AROUND THE SAMPLE: CELL WITH NUMBER 900           !!!!
c
c !!!!                  IRRADIATED OBJECTS SHOULD BE SET                   !!!!
c !!!!                      USING SAMPLE POSTIONING                        !!!!
c
c
c ===========================================================================
c ====================== CELLS ==============================================
c ===========================================================================
c HPGe DETECTOR, always three characters beginning with "1"
100  1 -5.32  (-9 1 -3 ):(9 -2 10 -3 ) &   $ Ge detector; 1  -5.32
              imp:n=1 imp:p=1 $
102  0         (7 -2 -8 )      imp:n=1 imp:p=1  $ empty core of detector
103  1 -5.32 (9 -7 -10 ): &           $ Ge dead layer around core
              (-10 8 7 -2 )   imp:n=1 imp:p=1
110  5  -2.702 15 -16 -17      imp:n=1 imp:p=1  $ front Al cap
111  5  -2.702 (16 -17 18 -5 ) imp:n=1 imp:p=1  $ side Al cap
114  0         16 -1 -18 #998  imp:n=1 imp:p=1  $ vacuum in Al (front)
998  0         -998 imp:n=1 imp:p=1        $ to tally photons through det entrance
115  0         (1 -27 -18 32 )#((1 -36 32 -35 ): &   $ vacuum in Al (outside)
              (37 -38 32 -35 ):(39 -40 32 -35 )) imp:n=1 imp:p=1
c
116  0         (27 -34 -18 31 ): &      $ vacuum in Al (outside back)
              (29 -34 33 -18 ) imp:n=1 imp:p=1
120  5  -2.702 (26 -27 30 -32 ):(27 -28 30 -31 ): &  $ Catcher holder
              (28 -29 -31 33 ) imp:n=1 imp:p=1
121  5  -2.702 (1 -26 3 -32 )   imp:n=1 imp:p=1  $ detector holder Al
122  0         (2 -26 -3 ): &            $ vacuum in Al (inside back)
              (26 -28 -30 )    imp:n=1 imp:p=1
123  8  -8.933 (28 -99 -33 )    imp:n=1 imp:p=1  $ cold-finger
124  5  -2.702 (34 -5 -18 33 )  imp:n=1 imp:p=1  $ back Al cap
125  5  -2.702 (1 -36 32 -35 )  imp:n=1 imp:p=1  $ mounting bands
126  5  -2.702 (37 -38 32 -35 ) imp:n=1 imp:p=1
127  5  -2.702 (39 -40 32 -35 ) imp:n=1 imp:p=1
c
c  BGO DETECTOR, always three characters beginning with "2"
213  6  -7.130 (44 -45 -42 41 -43 -52): & $ cylindrical part of BGO
              (-42 -45 52)     imp:n=1 imp:p=1   $ LLD=0.12
219  6  -7.130 (-25 59 20 -43 ): &        $ BGO
              (-15 25 54 -43 ) imp:n=1 imp:p=1   $ LLD=0.12
228  5  -2.702 (-43 -45 42 -47 ) imp:n=1 imp:p=1  $ BGO out cover triang
229  6  -7.130 (15 -44 41 -43 ) imp:n=1 imp:p=1   $ LLD=0.12  $ BGO front block
```

PGAA

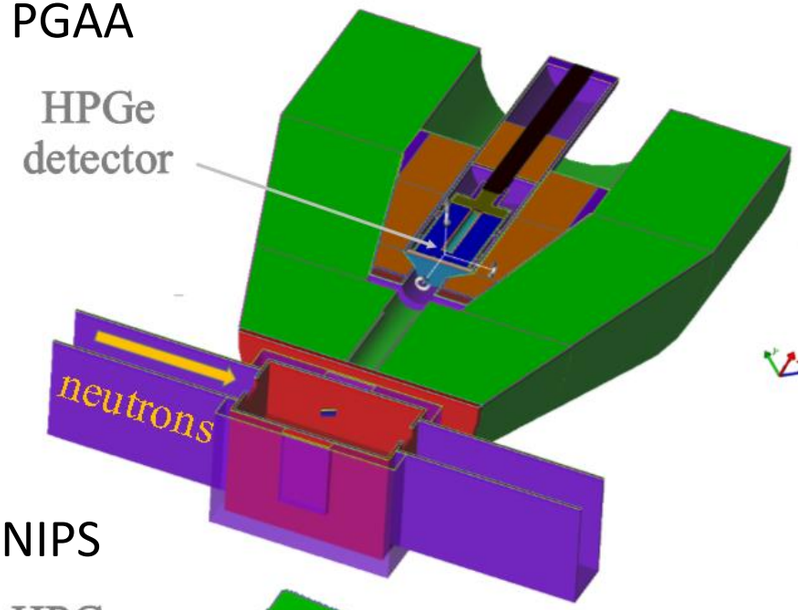

NIPS

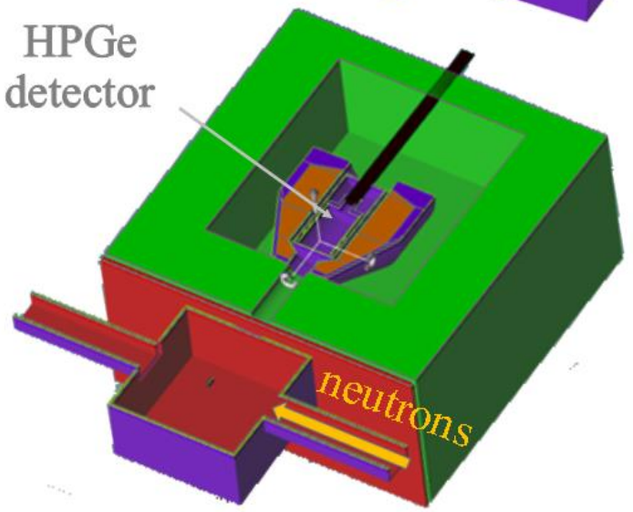

L. Szentmiklósi, B. Maróti and Z. Kis, Prompt-gamma activation analysis and neutron imaging of layered metal structures, *Nucl. Instruments Methods A.*, 2021, **1011**, 165589.

Centre for Energy Research

PGAA – incremental rotation of layered samples

Budapest Neutron Centre

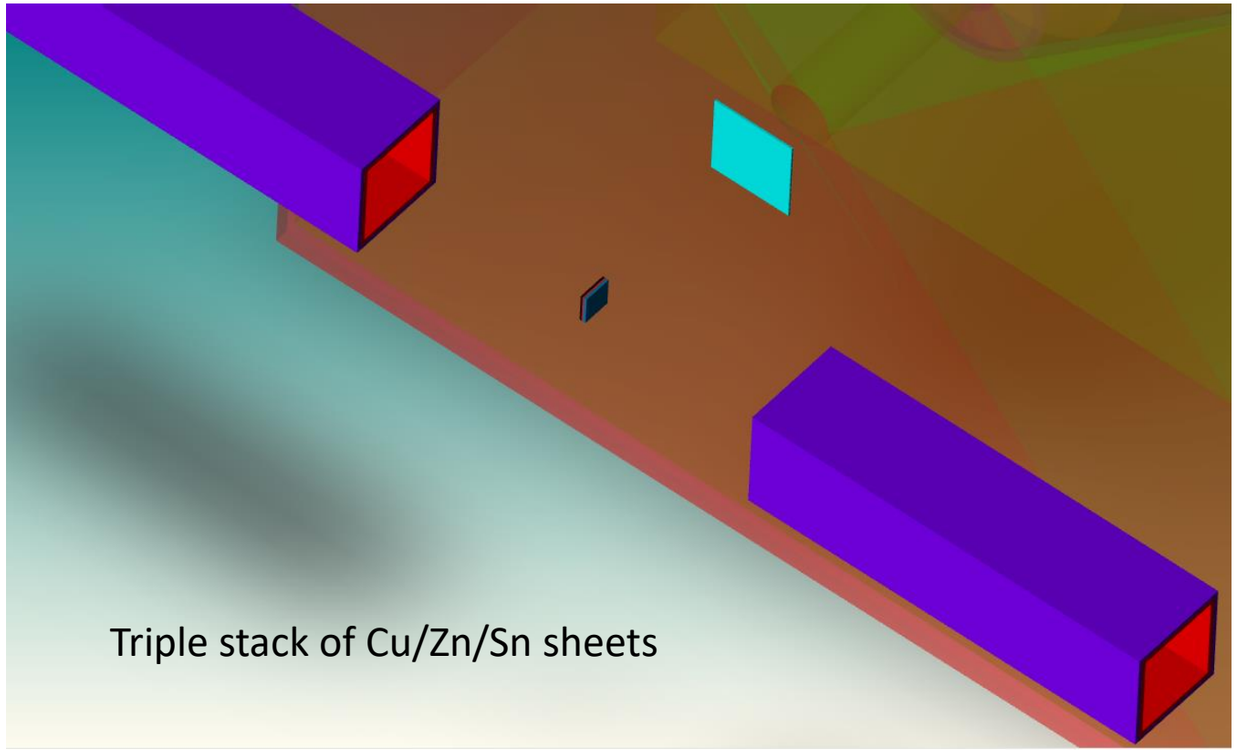

Experimental vs simulated prompt gamma count rates of elements at different angles

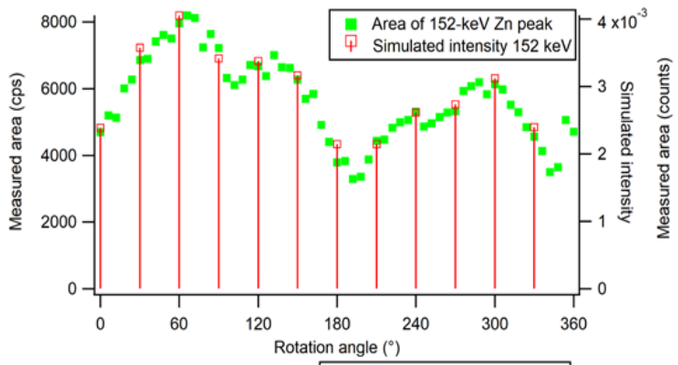

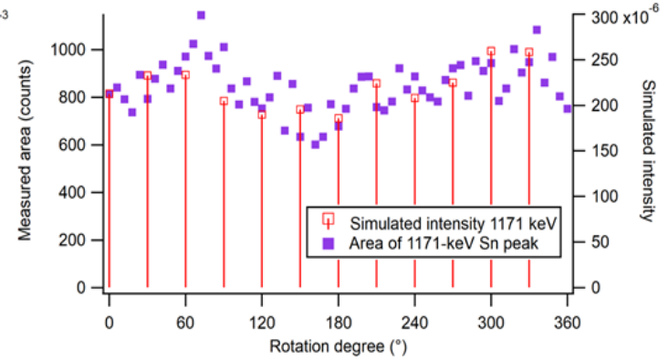

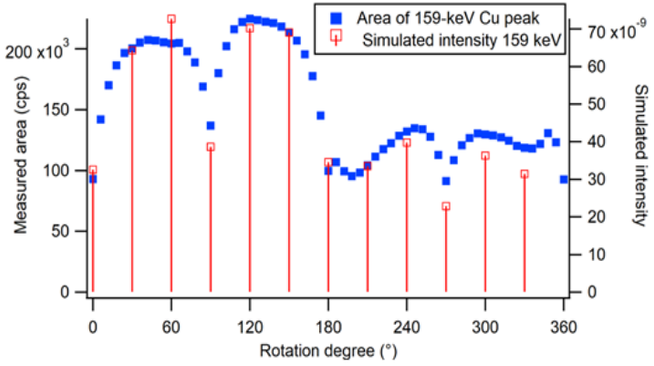

Maximum count rates of thin slab samples: 30-45 degrees rel. to the beam axis

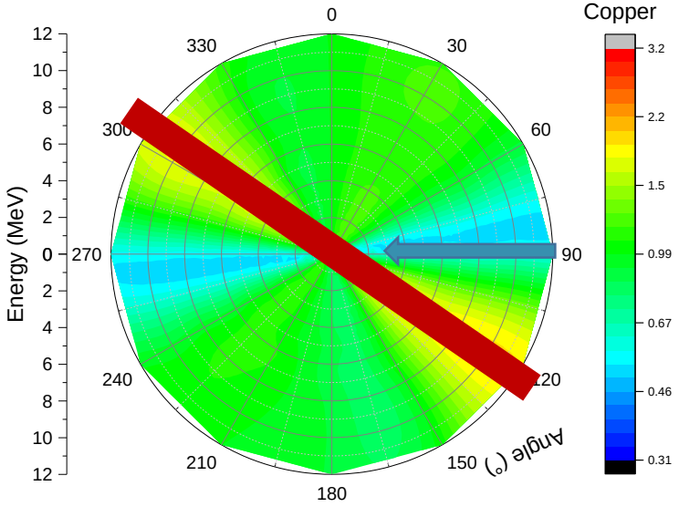

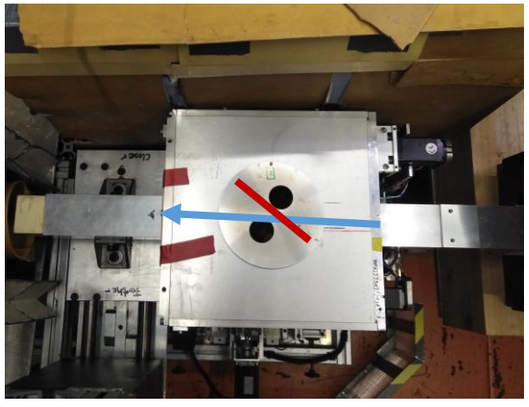

Cu neutron absorption (0.023)

Zn neutron absorption (0.0023)

Sn neutron absorption (0.00026)

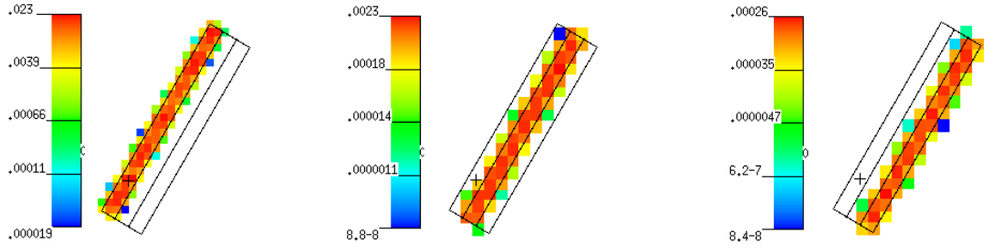

neutron beam

Centre for Energy Research

Bulky, regularly-shaped homogeneous object

Budapest Neutron Centre

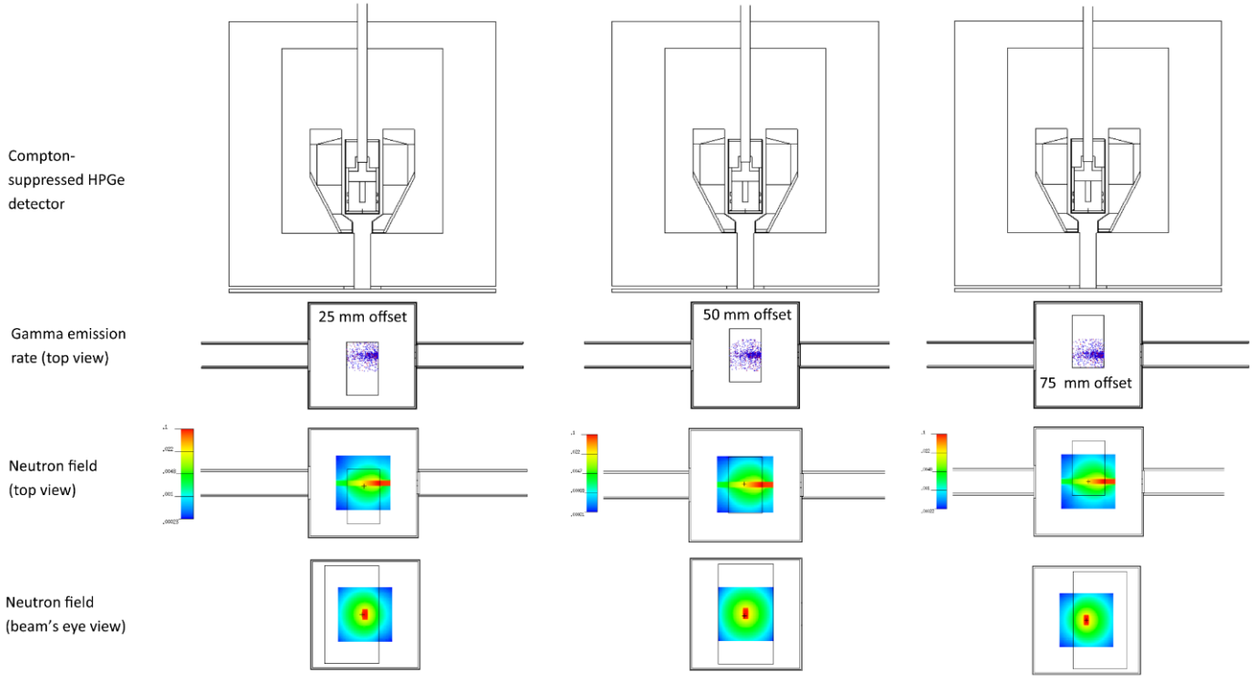

3D scan

Pavement stone sample

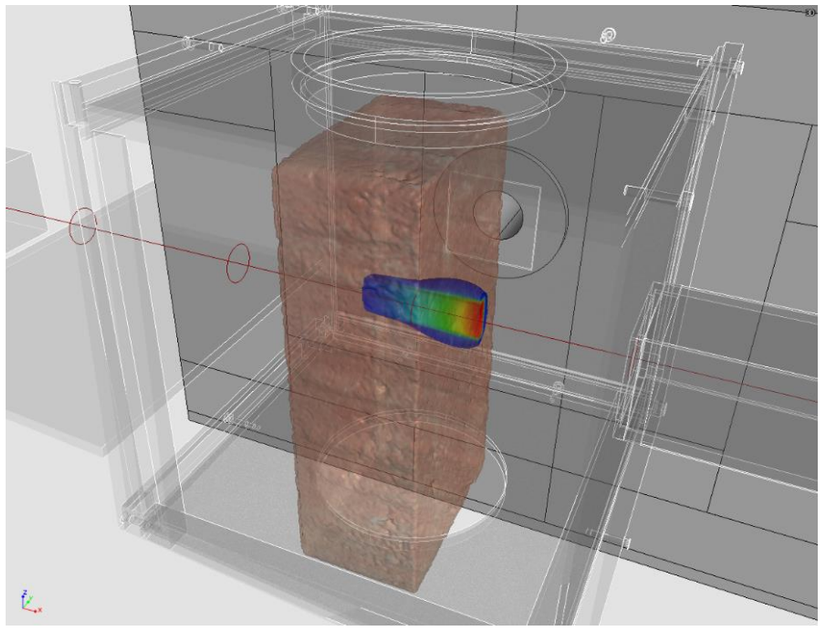

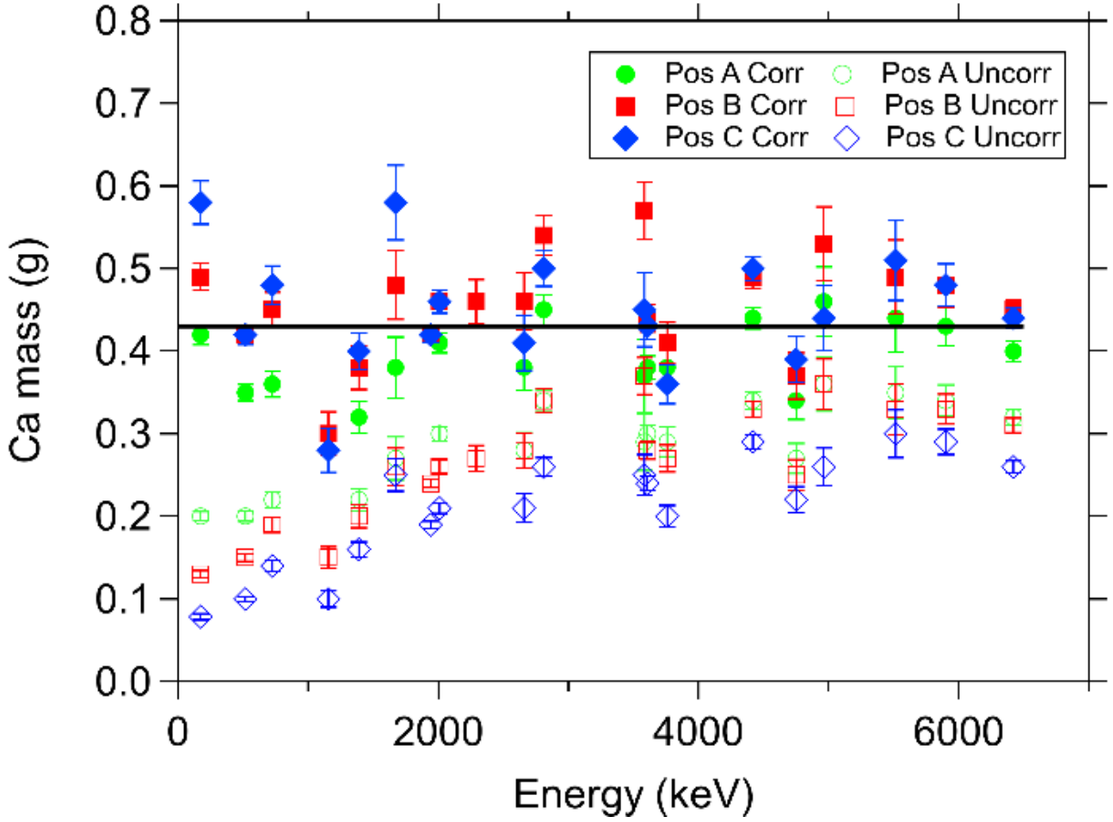

László Szentmiklósi, Zoltán Kis, Boglárka Maróti and László Zoltán Horváth: Correction for neutron self-shielding and gamma-ray self-absorption in prompt-gamma activation analysis for large and irregularly shaped samples, J. Anal. Atomic Spectrom., 2021 DOI: 10.1039/d0ja00364f

3D visualization of the results

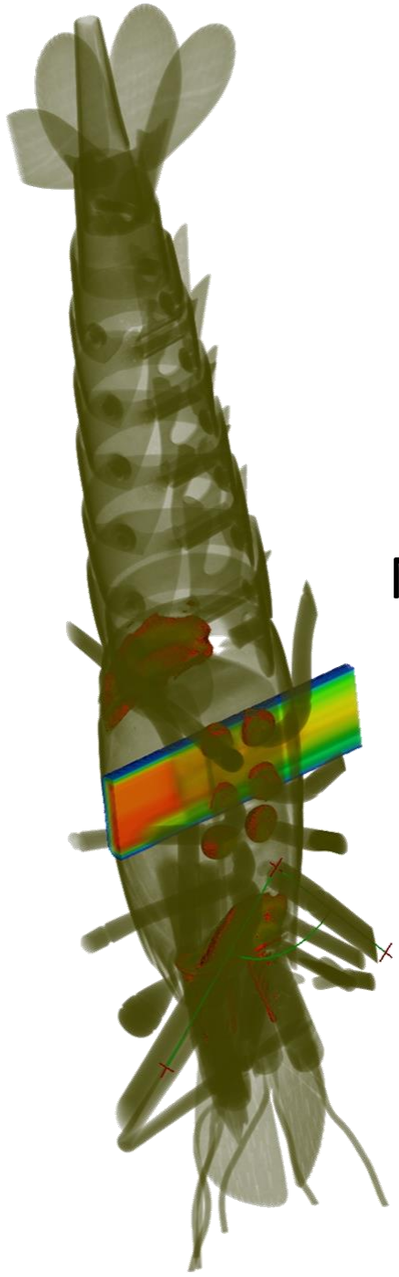

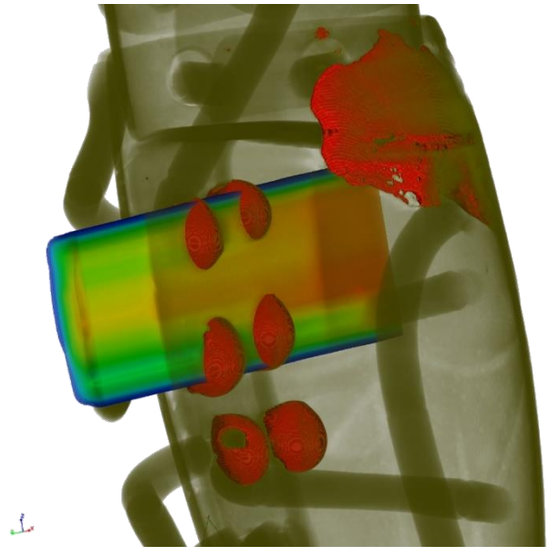

Neutron beam intensity

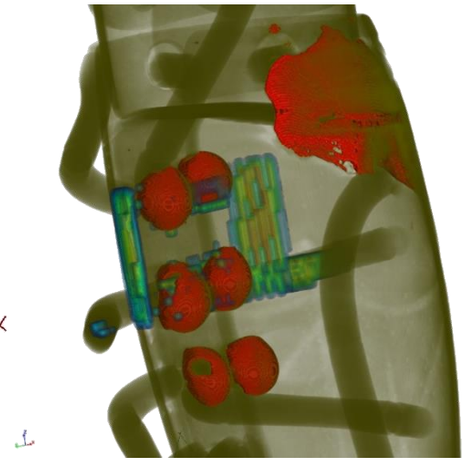

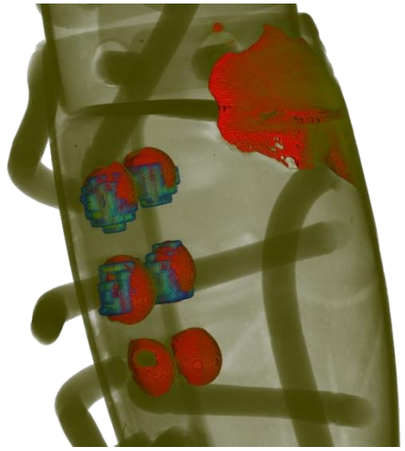

Emission map elements

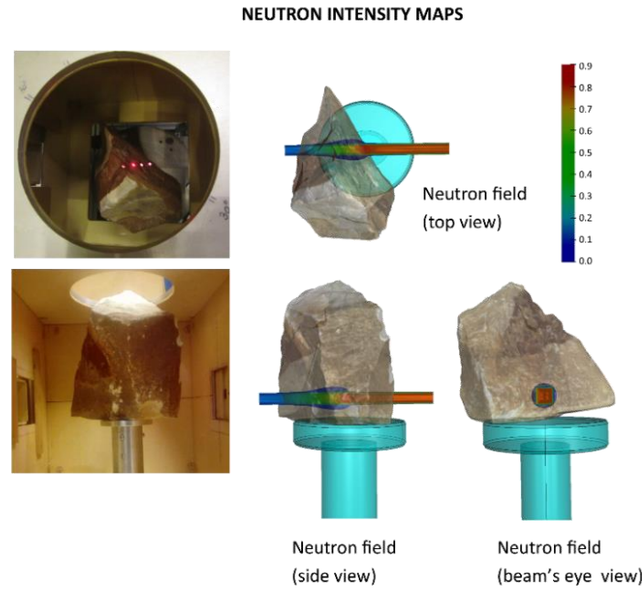

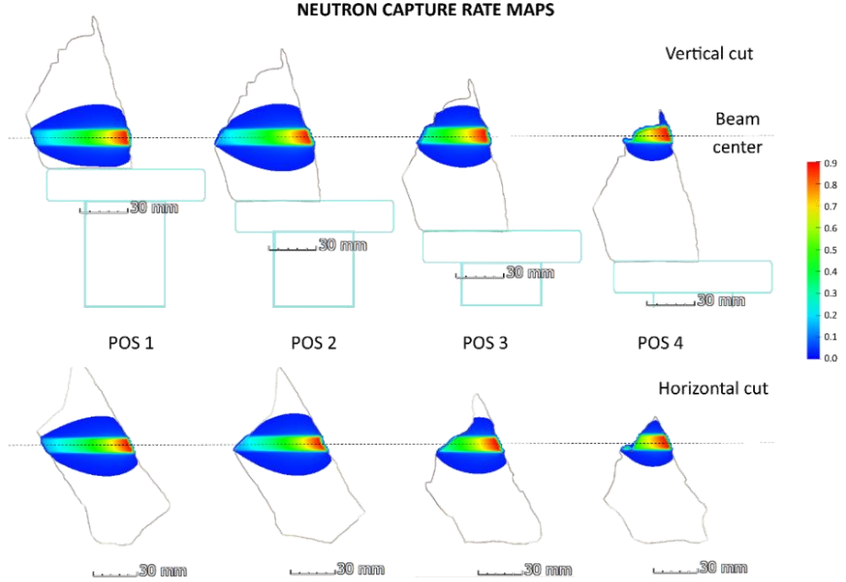

L. Szentmiklósi, Z. Kis, B. Maróti and L.Z. Horváth: Correction for neutron self-shielding and gamma-ray self-absorption in prompt-gamma activation analysis for large and irregularly shaped samples, J. Anal. Atomic Spectrom., 2021,36, 103-110

Centre for Energy Research

Comparison to results of destructive sampling

Budapest Neutron Centre

	Pos 1		Powder Pos 1		Pos 2		Powder Pos 2		Pos 3		Powder Pos3		Pos 4		Powder Pos4	
	m%	rel unc %	m%	rel unc %	m%	rel unc %	m%	rel unc %	m%	rel unc %	m%	rel unc %	m%	rel unc %	m%	rel unc %
H	0.124	0.9	0.161	1.4	0.125	1.8	0.144	1.3	0.141	0.9	0.138	1.2	0.137	1.2	0.134	1.2
B	18.0 ppm	0.8	22.6 ppm	1.4	19.5 ppm	0.9	23.8 ppm	1.3	36.7 ppm	0.9	37.1 ppm	1.2	38.6 ppm	1.1	38.4 ppm	1.6
C	5.8	5.3	6	16	5.4	6.0	6	12	< 3.5 (DL)		< 3.5 (DL)		< 3.5 (DL)		< 3.5 (DL)	
O	49.9	5	50	5	49.5	5	51	5	48.2	5	53	5	47	5	53	5
Al	2.13	1.8	0.8	7.8	0.85	2.0	0.69	4	0.67	2.1	0.49	2.4	0.56	2.3	0.49	2.3
Si	21.2	1.6	21.4	2.05	22.4	1.8	21.8	1.9	43	1.1	45	1.3	44	1.3	45	1.4
Cl	< 30 ppm (DL)		28 ppm	15	< 30 ppm (DL)		25 ppm	16	30 ppm	5.	40 ppm	5.	32 ppm	5.	43 ppm	4
K	0.243	2.2	0.26	2.6	0.25	2.2	0.24	2.6	0.232	1.9	0.18	2.2	0.207	2.2	0.192	1.9
Ca	20	2.4	21	2.4	20	2.7	19	2.4	3.8	3.1	0.27	3.1	1.46	2.6	0.57	2.6
Ti	280 ppm	2.9	350 ppm	3.5	290 ppm	3.0	310 ppm	3.2	260 ppm	2.9	210 ppm	3.1	220 ppm	3.1	220 ppm	2.6
Mn	0.055	2.4	0.053	2.3	0.051	3.9	0.049	2.2	90 ppm	10.	20 ppm	5	180 ppm	3.1	24 ppm	9.2
Fe	0.31	2.2	0.44	6.1	0.36	2.9	0.39	6	0.32	2.6	0.27	2.9	0.30	2.6	0.33	3.3
Sm	0.96 ppm	2.2	1.14 ppm	2.9	0.99 ppm	2.0	1.10 ppm	2.2	0.62 ppm	2.4	0.54 ppm	2.1	0.55 ppm	2.8	0.38 ppm	2.3
Gd	1.5 ppm	7.1	1.5 ppm	5.9	1.5 ppm	9	1.4 ppm	7.1	0.8 ppm	7	0.6 ppm	6	0.7 ppm	5	0.5 ppm	18

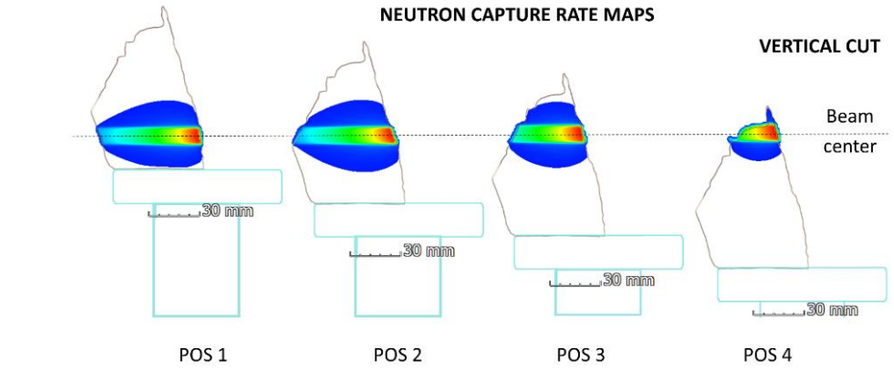

László Szentmiklósi, Zoltán Kis, Boglárka Maróti and László Zoltán Horváth: Correction for neutron self-shielding and gamma-ray self-absorption in prompt-gamma activation analysis for large and irregularly shaped samples, J. Anal. Atomic Spectrom., 2021 DOI: 10.1039/d0ja00364f

Budapest Neutron Centre
Centre for Energy Research

Applications

Rocks and minerals (Geology, Archaeometry)
Metals (Materials Research, Archaeometry)
Nuclear Materials (Safeguards, Transmutation)
Ceramics (Archaeometry)
Glasses (Archaeometry, Industry)

BNC
Budapest Neutron Centre

BUDAPEST RESEARCH REACTOR
1959 2019
60 YEARS OF RESEARCH & INNOVATION

Cultural Heritage applications

Applicable:

- Bulk composition of any (solid, liquid) sample
- Minimum sample mass ~ 0,1 g
- In principle all chemical elements
  Very sensitive: H, B, Cl, Cd, Nd, Sm, Eu, Gd
- Detection Limits 0,1 ppm – 1000 ppm

Advantages:

- Non-destructive
- Minimal sample preparation
- Average for the total irradiated volume
- Parts of large objects can be studied
  (beam size: 5 mm^2 – 2x2 cm^2)

Classification of stone tools made of various

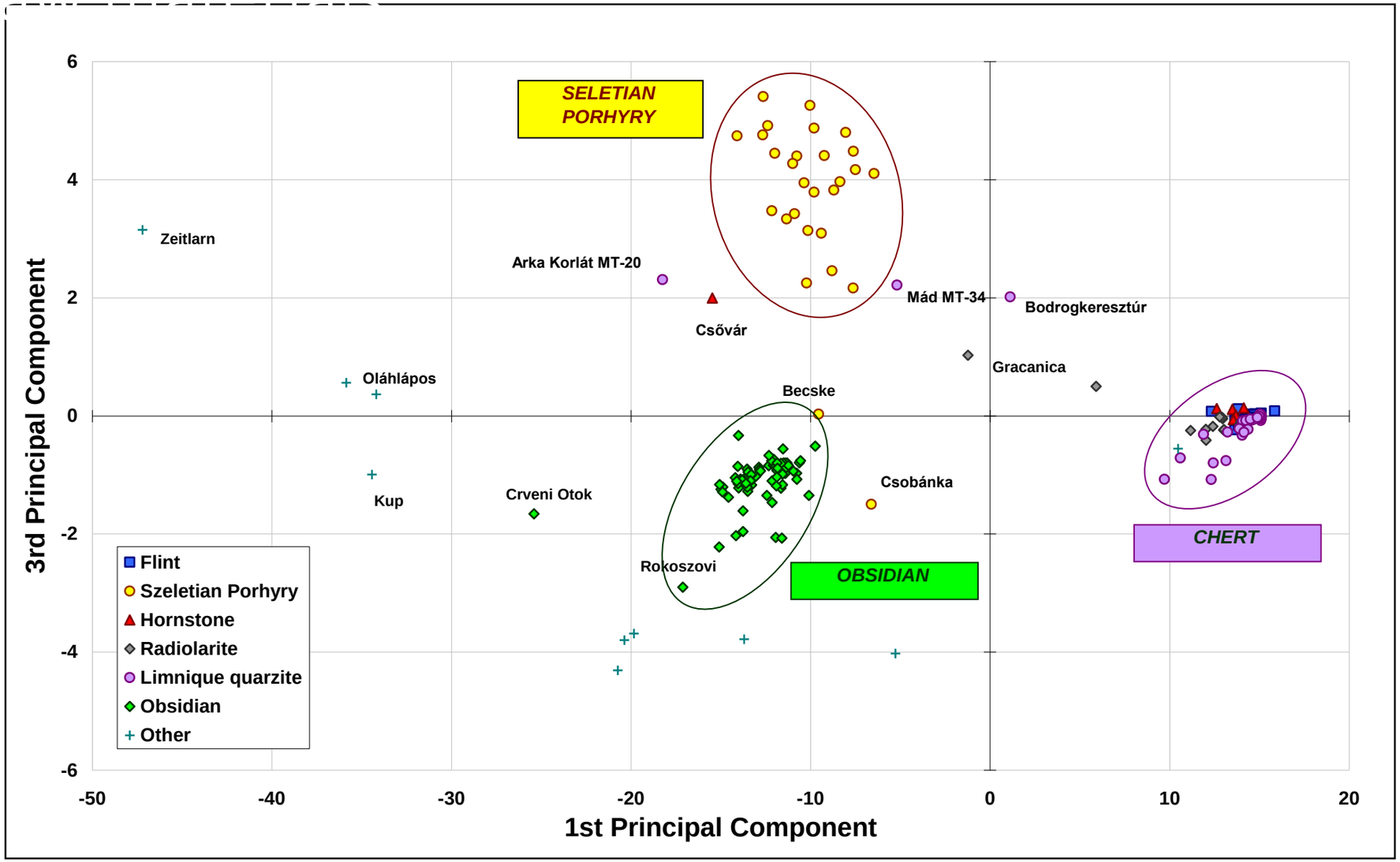

Zs. Kasztovszky, Archaeometry 50, 1 (2008) 12–29

Provenance of Venezuelan pottery

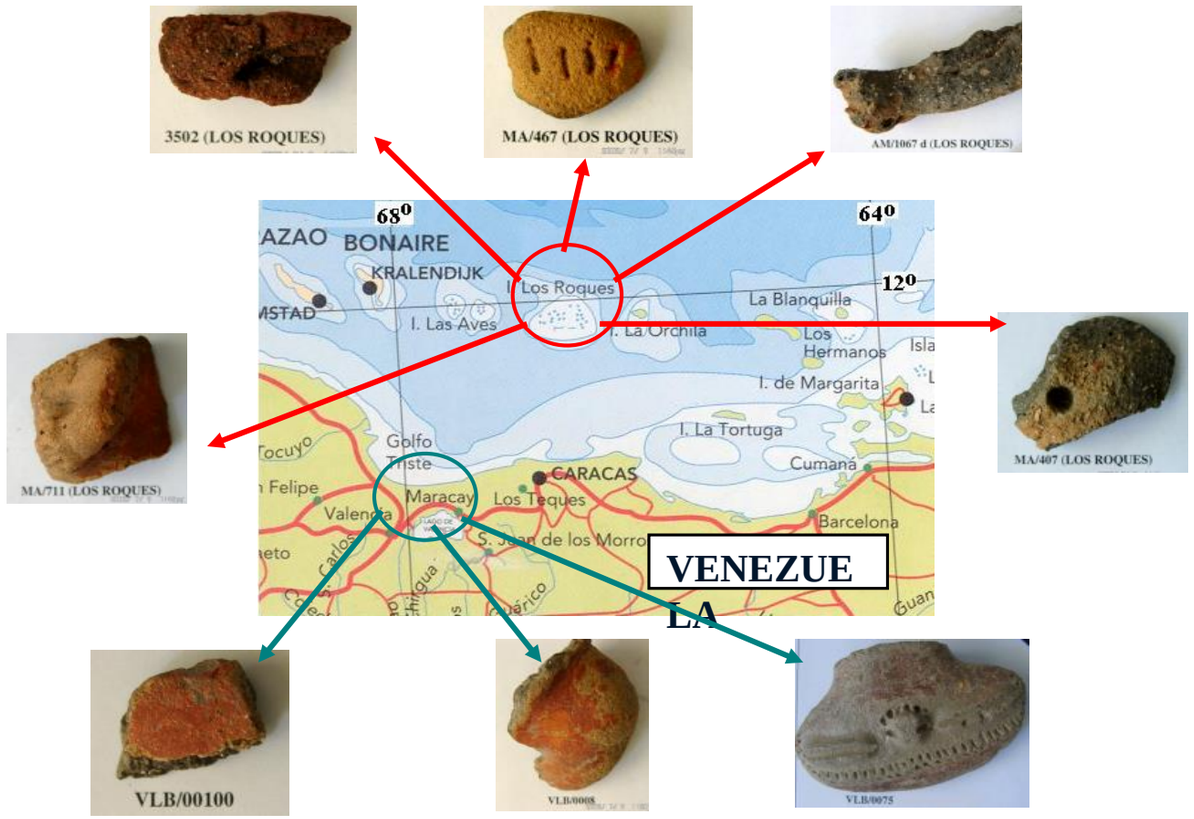

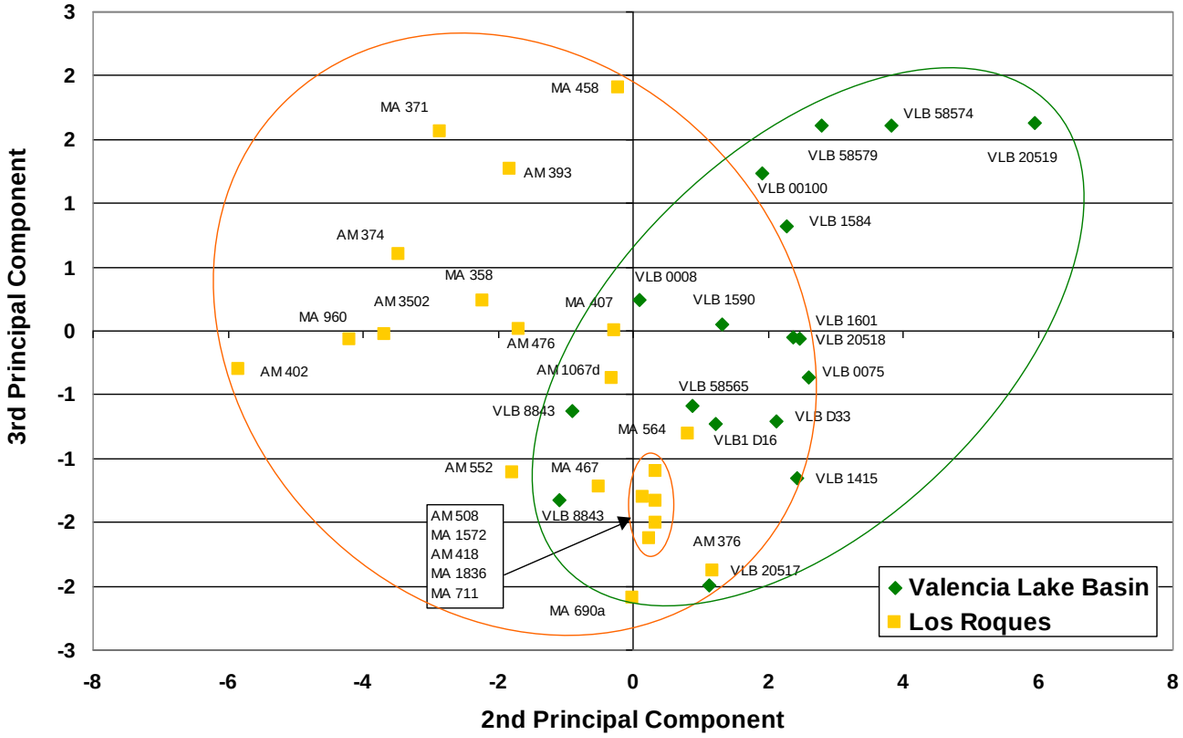

Zs. Kasztovszky et al, Nukleonika 49 (3), 107-113 (2004)

Classification of Glassware

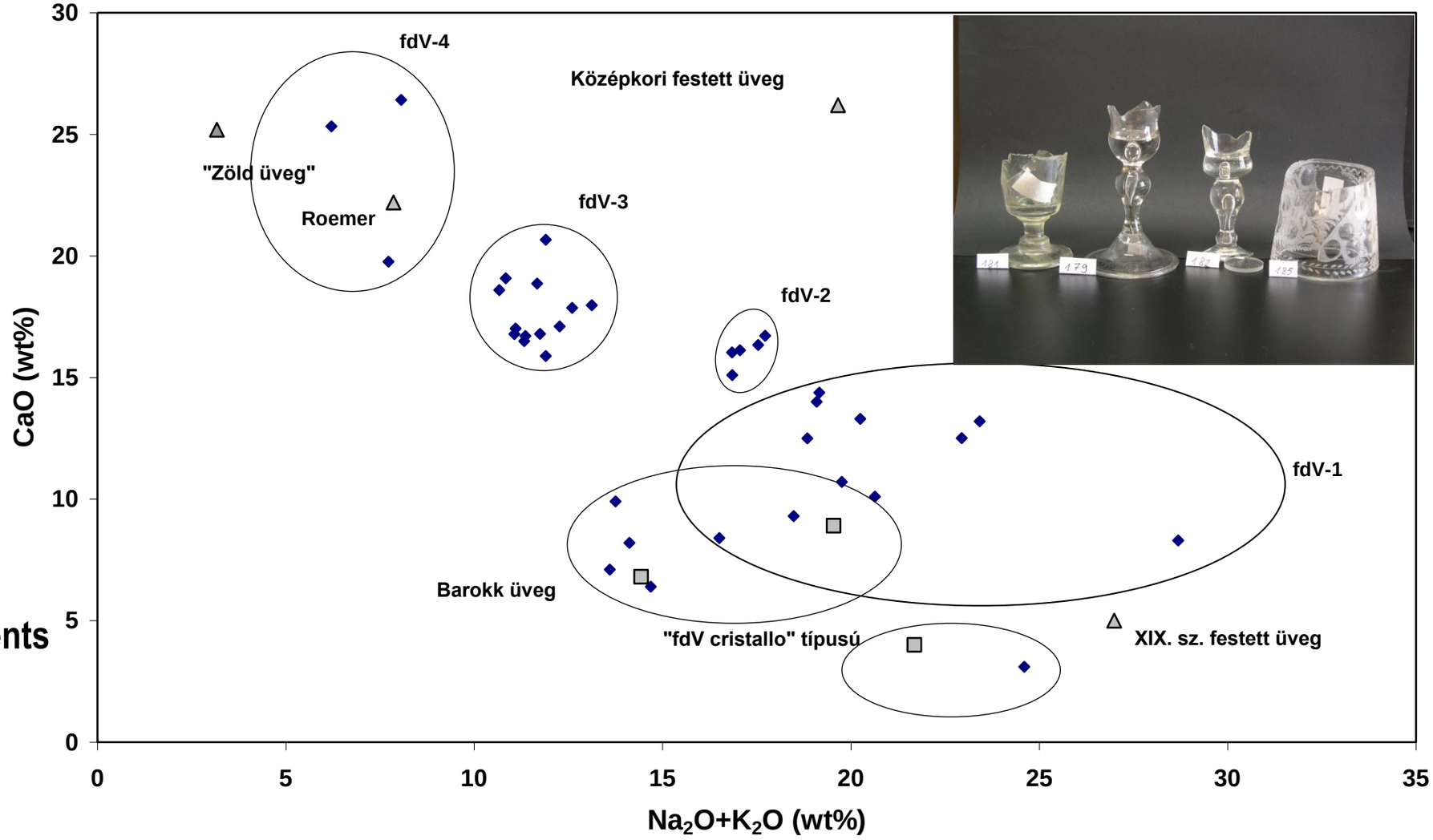

45 medieval and baroque glass fragments analysed

AIM: Workshop identification,
special regard to B
Comparison with EPMA

Jerzy Kunicki-Goldfinger - Inst. Nuclear Chemistry and Technology, Warsaw

Metals

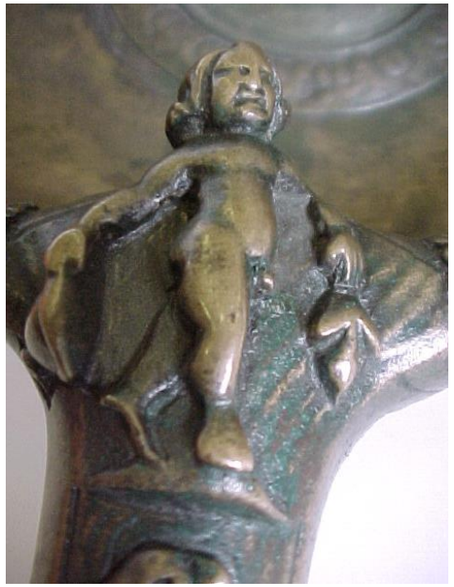

Roman silver coins

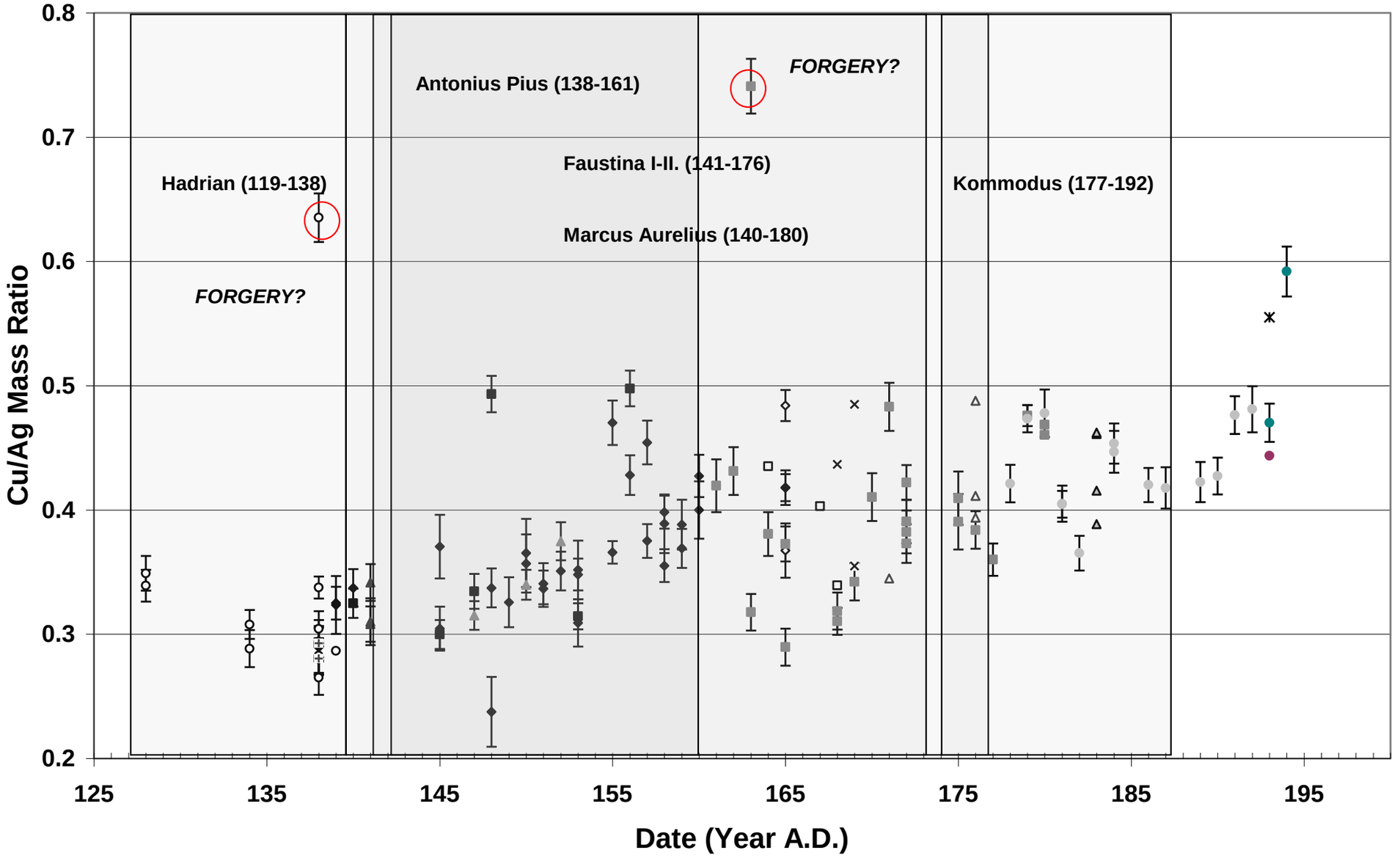

Ewa Panczyk – Inst. of Nuclear Chemistry and Technology, Warsaw

Local elemental composition via radiography-

- Measurement positions overlaid on the radiogram
- Real-time feedback using radiography and xyzω sample stage
- At one position multiple materials may present
- Decomposition and correction of signals via Monte Carlo calculations

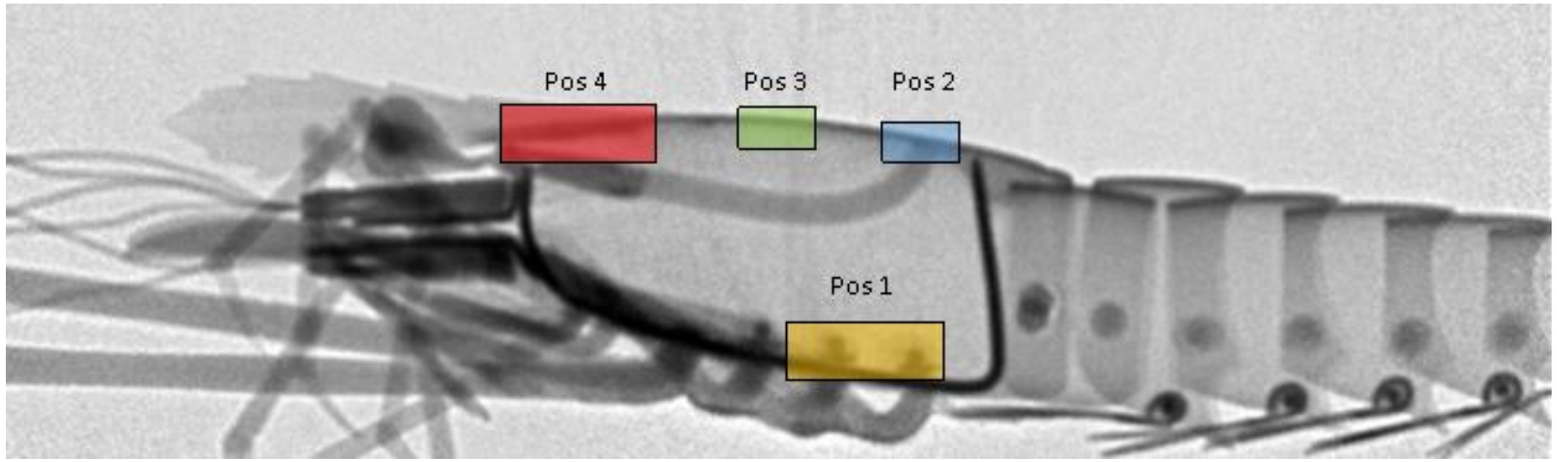

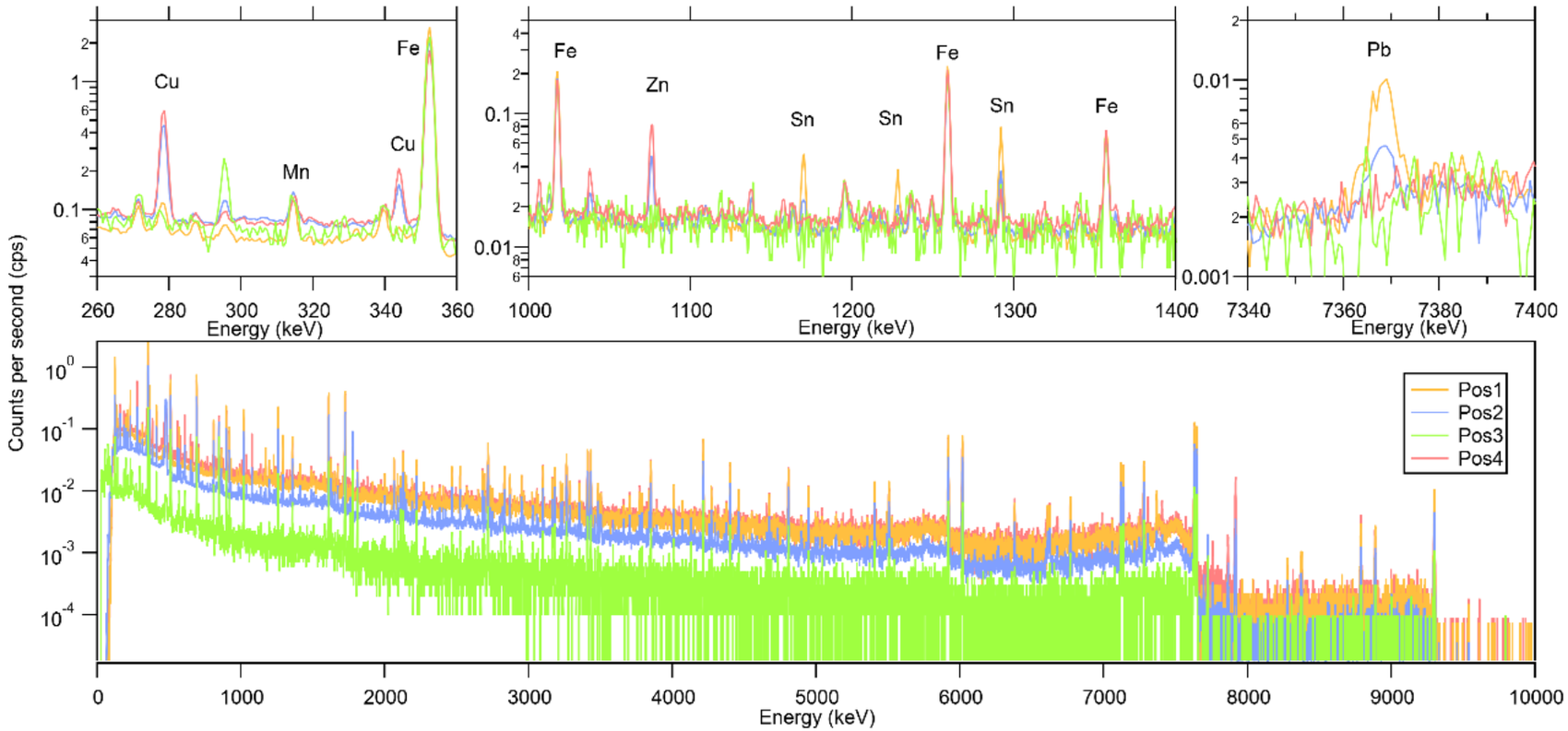

L. Szentmiklósi, Z. Kis, M. Tanaka, B. Maróti, M. Hoshino, K. Bajnok: Revealing hidden features of a Japanese articulated iron lobster via non-destructive local elemental analysis and 3D imaging, J. Anal. Atomic Spectrom. DOI 10.1039/d1ja00261a

Rocks and minerals

Flints, chipped stones, marbles, gemstones, lapis lazuli, …

Geology

Nondestructive feature is not so important
Unnecessary sample preparation makes it attractive
Objects:

- Volcanic rooks or rock powders
- Fast determination of main components
- Unique: B, H content, Cl, Sm, Gd
- Helps to understand tectonic plate collisions, vulcanism

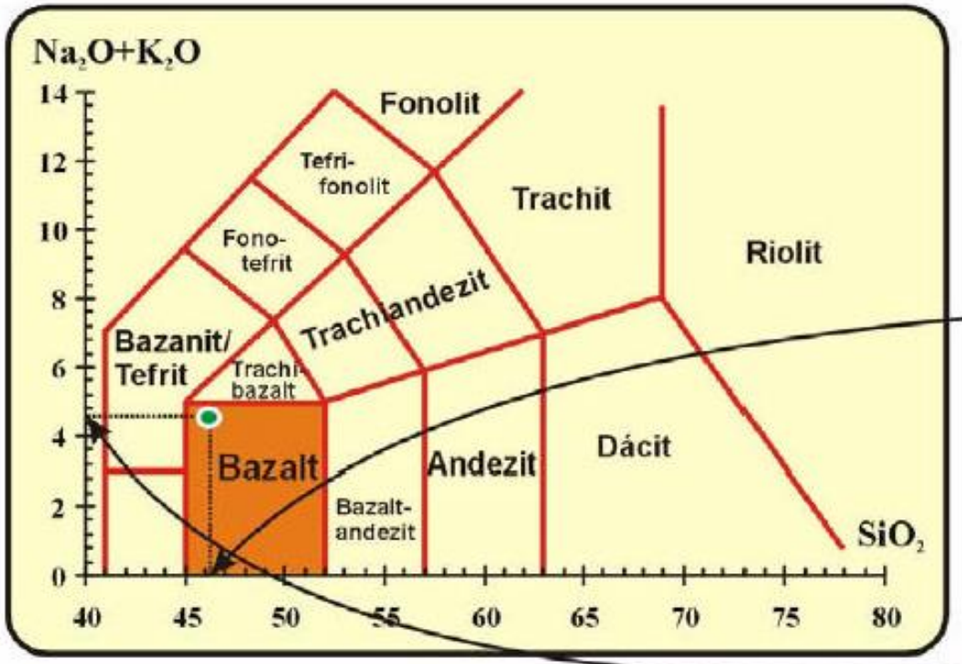

Chemical composition

Kémiai összetétel

SiO_2	46,22
TiO_2	2,51
Al_2O_3	15,24
Fe_2O_3	11,03
MnO	0,21
MgO	7,65
CaO	10,46
Na_2O	2,45
K_2O	2,11
P_2O_5	0,73

Na2O+K2O=4,56

Geological applications

Advantages in geochemistry:

- BULK analysis without sample preparation! No contamination!
- Non-destructive, same sample can be measured with other methodes!
- Major element oxides are well measurable.
- Rear and rearly measured trace elements are easy to measure, like H, B, Cl and Gd!

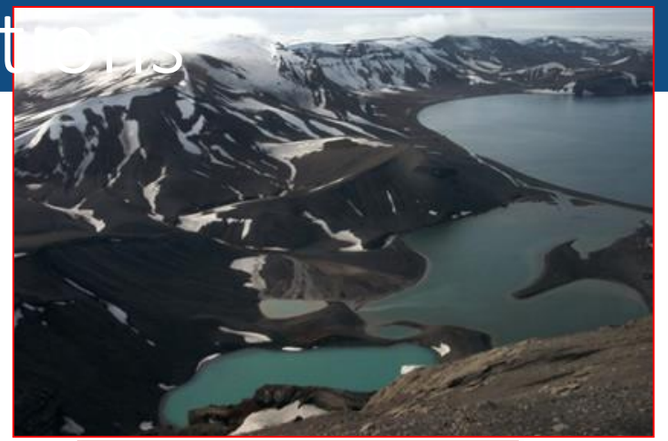

B and bulk rock composition of Arc volcanic rocks

B content of metamorphic rocks

Dehydration reactions and light element transport

Subduction geometry and magma generation informations

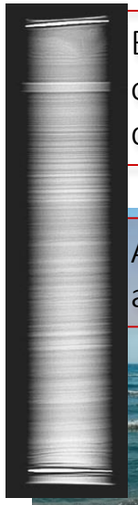

B and Cl content changes of sea sediments with dept

Absorption from sea water and disturbance

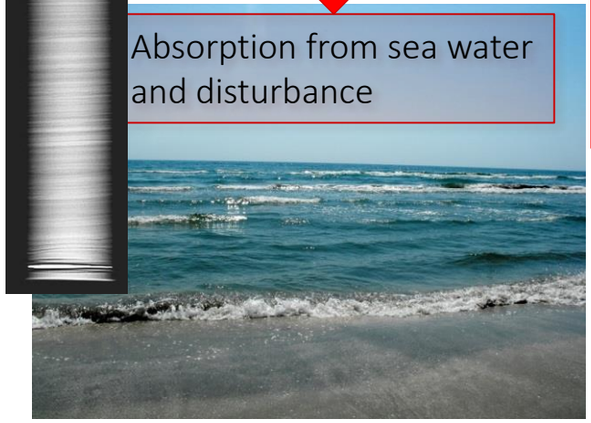

Geological standard measurements

for validation

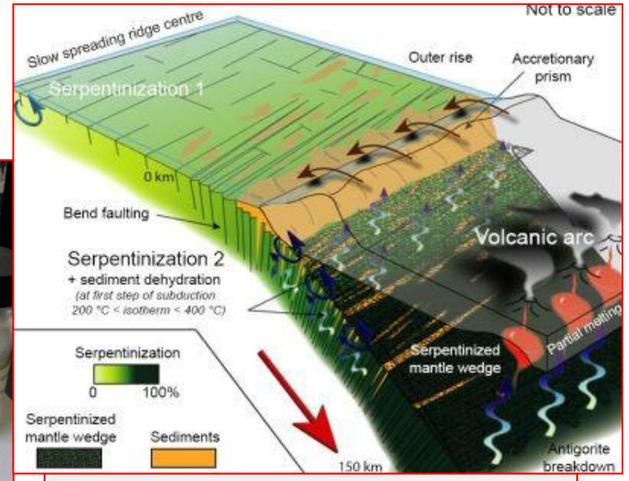

B and Cl content of ocean base serpentinies

Subduction recycle of materials

Provenance study of lapis lazuli

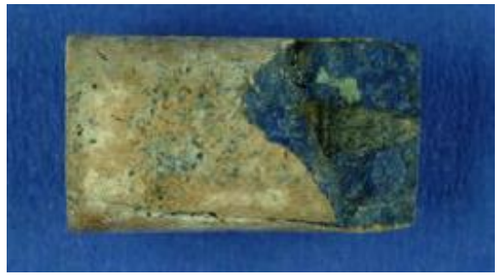

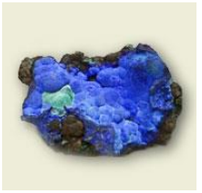

- A few geological occurances in the World (Ural, Chile, Afghanistan, Lake Bajkal)
- **Main mineral**: Lazurit / $(Na,Ca)_{7-8}(Al,Si)_{12}O_{24}[(SO_4)Cl_2(OH)_2]$
- **AIM**: Identification of raw materials, provenance of art objects
- **PGAA**: H, Na, Mg, Al, Si, K, Ca, Ti, Mn, Fe, S, Cl

Project leader: Judit Zöldföldi

Deep see vents on the Pacific ocean floor

Deep see vents have been found on the ocean floor near faults

The overheated water dissolves different minerals

The investigated samples contain sulfates of Cu and Fe

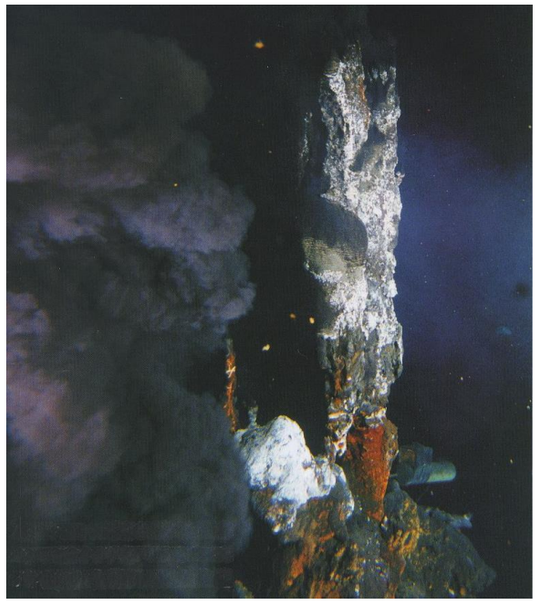

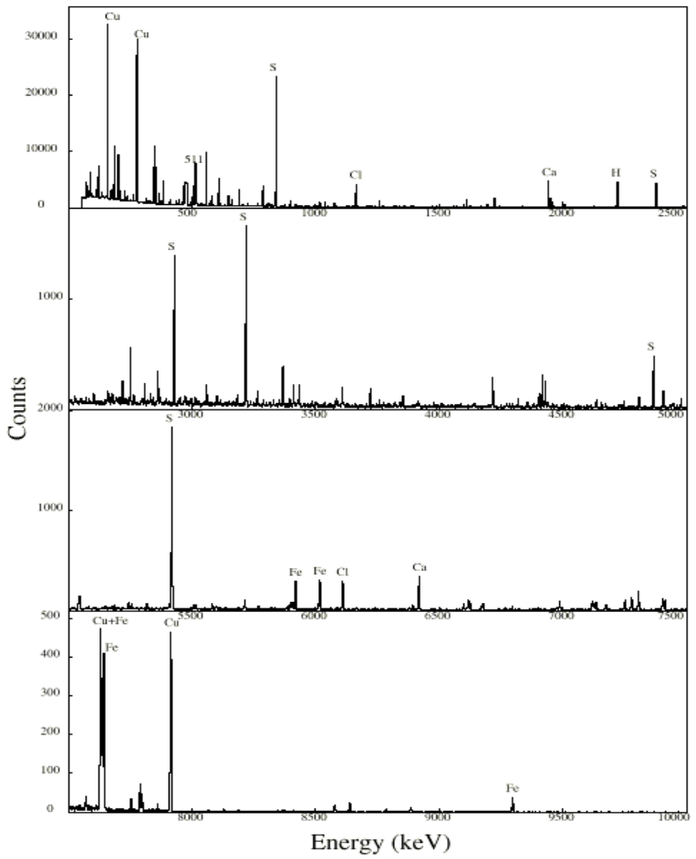

	ALVIN 917-R4	ALVIN 1457-1R-C	ALVIN 1461-2R
O	45.9*	41(6), 44.9*	45.1*
S	20.0 (0.2)	0.151 (0.005)	0.16 (0.01)
Ca	11.3 (0.2)	7.22 (0.11)	7.25 (0.13)
Fe	9.28 (0.11)	9.65 (0.08)	9.37 (0.09)
Cu	7.67 (0.07)	---	---
Al	---	7.10 (0.07)	7.06 (0.12)
Mg	1.8 (0.2)	3.98 (0.11)	3.6 (0.2)
Zn	1.36 (0.05)	---	---
P	---	0.85 (0.18)	1.6 (0.2)
Ni	1.17 (0.003)	0.022 (0.002)	---
Ti	---	1.097 (0.008)	1.060 (0.010)
Si	0.55 (0.05)	22.6 (0.3)	22.3 (0.3)
H	0.368 (0.004)	0.0290 (0.0005)	0.027 (0.001)
K	0.27 (0.06)	0.138 (0.004)	0.16 (0.01)
Cl	0.194 (0.002)	0.0566 (0.0005)	0.0188 (0.0005)
Mn	---	0.154 (0.002)	0.161 (0.004)
Na	0.140 (0.014)	1.97 (0.04)	1.96 (0.05)
V	---	0.042 (0.002)	0.046 (0.003)
Co	0.0066 (0.0011)	0.0045 (0.0003)	0.0058 (0.0009)
Sc	---	0.0039 (0.0002)	0.0058 (0.0005)
Cd	0.00352 (0.00005)	---	0.00024 (0.00003)
B	0.00220 (0.00002)	0.000659 (0.000007)	0.000658 (0.000008)
Dy	---	0.00099 (0.00008)	0.00111 (0.00014)
Gd	0.000050 (0.000006)	0.000524 (0.000007)	0.000556 (0.000010)
Sm	0.00033 (0.00003)	0.000330 (0.000005)	0.000340 (0.000007)

(Lawrence Berkeley National Laboratory)

Inactive tracing of a glass-melting furnace

- Homogenization and flow properties of an industrial melting furnace were investigated
- To avoid high level radioactivity, inactive tracers of Gd_2O_3 and H_3BO_3 were added in 10 ppm concentration
- Samples were taken regularly at the outlet and measured with PGAA
- Properties were found to be close to ideal case

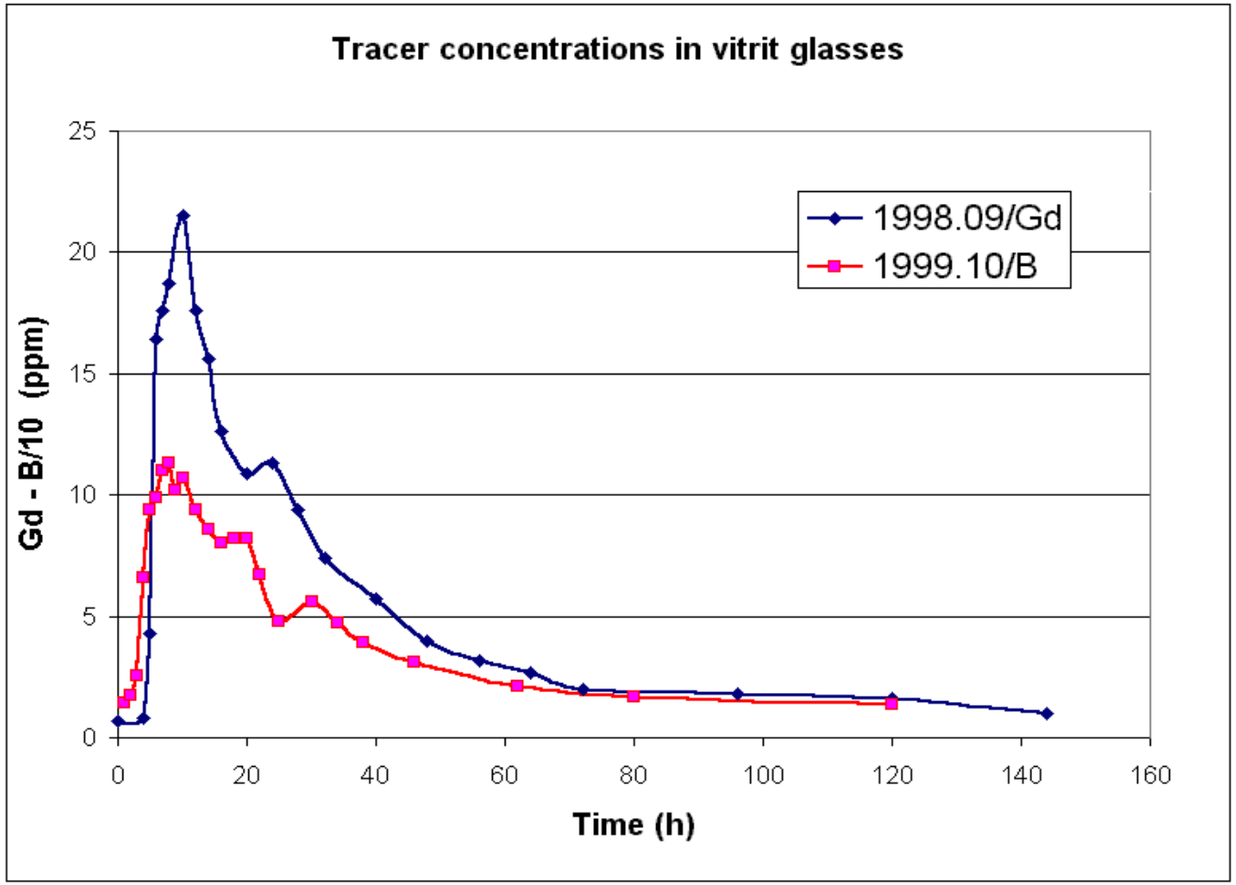

Facility access programs

BNC
Budapest Neutron Centre

IPERION HS

E-RIHS
EUROPEAN RESEARCH INFRASTRUCTURE FOR HERITAGE SCIENCE

eric
Central European Research Infrastructure Consortium

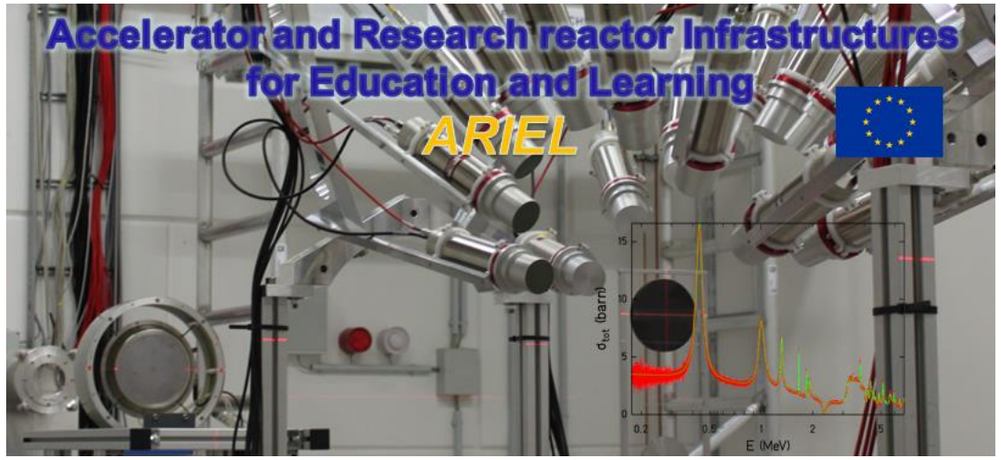

ReMade @ARI
a hub for materials research

Feel free to contact us and submit your proposal!

Conclusions

- PGAA is a versatile method for non-destructive element analysis
- Major and minor components, some trace elements (even more with NAA)
- Best with guided cold neutron beam
- On-line detection of gammas: shielding is crucial
- Gamma spectroscopy in the 11 MeV energy range

- Bulk or local composition, also in combination with radiography/tomography
- In situ observation of time-dependent processes

- Widespread applications in material science, archaeometry, geology and industry

Conclusions

Main benefits of PGAA

- Non-destructive
- Bulk (average composition)

PGAA is the method of choice for

- Expensive and valuable objects

(material science, circular economy & heritage science)

- In-depth composition needs to be measured

(complementary to XRF, PIXE, LIBS, LA-ICP-MS)

- Samples that are difficult to dissolve or sample preparation would be time consuming

(chemical analysis of geological samples)

- In-situ monitoring of dynamic processes

(catalysis experiments)

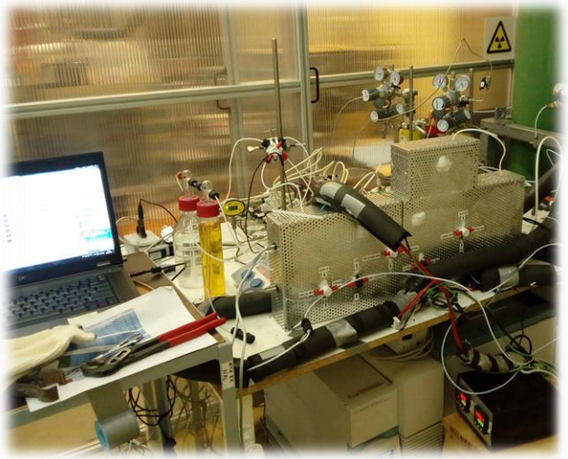

Thank you for your attention!

BNC
Budapest Neutron Centre

BUDAPEST RESEARCH REACTOR
60 YEARS OF RESEARCH & INNOVATION